



D4.2

Floating Wind O&M Strategies Assessment

RAMBOLL / COBRA / EQUINOR / ESTEYCO / FIHAC

August 2021

Disclaimer:



This project has received funding from the European Union's Horizon 2020 Research and Innovation programme under grant agreement No 815083.

Project details:

Duration:
1 Sep 2019 - 28 Feb 2023
Grant agreement:
No: 815083

Document information

Deliverable number	D4.2
Deliverable name	Floating Wind O&M Strategies Assessment
Dissemination Level	Public
Reviewed by	José Luis Dominguez (IREC), Qi Pan (USTUTT), Raúl Guancho Garcia (FIHAC)
Date	31.08.2021
Work Package and Task	WP4, Task 4.2
Lead Beneficiary for this Deliverable	RAMBOLL

Authors

Name	Organisation
Marie-Antoinette Schwarzkopf	RAMBOLL
Friedemann Borisade	RAMBOLL
Jannis Espelage	RAMBOLL
Eve Johnston	RAMBOLL
Rubén Durán Vicente	COBRA
Sara Muñoz	COBRA
Pål Hylland	EQUINOR
Wei He	EQUINOR
Joaquín Urbano	ESTEYCO
Francisco Javier Comas	ESTEYCO
Andrea Arribas	ESTEYCO
Miguel Somoano Rodriguez	FIHAC
Sergio Fernandez Ruano	FIHAC
Lucía Meneses Aja	FIHAC
Raul Guancho García	FIHAC
Álvaro Rodríguez Luis	FIHAC

Version control

Version	Date	Author	Description of Changes
1	2021-08-31	RAMBOLL	Final version for submission

Table of Content

1	Nomenclature.....	5
2	Executive Summary	7
3	Introduction.....	8
4	Life-Time OPEX Analysis	9
4.1	Overview of the Simulation Study	10
4.2	Simulation Scenario Description.....	11
4.2.1	Sensitivity Study	11
4.2.2	Impact Study	11
4.3	Inputs to O&M Cost Model	13
4.3.1	Scheduled Maintenance for Floating Wind Farms	13
4.3.2	Corrective Maintenance for Floating Wind Turbines	14
4.3.3	Vessels.....	17
4.3.4	Personnel	18
5	Operational Limits for Scenarios	19
5.1	Floating-to-Floating Major Component Exchange.....	20
5.1.1	Background of Study	20
5.1.2	Goals and Assumptions	21
5.1.3	Generic Heavy Lift Crane Vessels	23
5.1.4	OrcaFlex Model Setup and Load Cases	29
5.1.5	Operational Limits for Heavy Lift Maintenance	32
5.2	Tow-In Operation	43
5.2.1	Acceptance Criteria for Tow-In Operation	43
5.2.2	Methodology and Model Description	43
5.2.3	Sensitivity Analysis	54
5.2.4	Preliminary Analysis in Frequency Domain	63
5.2.5	Detailed Analysis in Time Domain	68
5.2.6	Tow Line Tension Demand	70
5.2.7	Operational Limits for Tow-In	71
5.3	Workability and Transportability.....	74
5.3.1	Standards and Motion Limit Criteria	74
5.3.2	Workability Method	75

5.3.3	Workability Limits for Offshore Maintenance Works	77
5.3.4	Transportability Method	80
5.3.5	Transportability Limits for Crew Transfer	80
5.4	Accessibility for CTV and SOV	81
5.4.1	Accessibility Method	81
5.4.2	Accessibility Limits for CTV and SOV	83
6	Results and Interpretation	88
6.1	Parameter Analysis	88
6.1.1	Monte Carlo Convergence Behaviour	88
6.1.2	Sensitivity Analyses	89
6.2	Influence of Major Component Exchange Strategy on Lifetime OPEX	94
6.2.1	Simulation Results	94
6.2.2	Outlook and Conclusion	96
6.3	Influence of Vessel Type on Lifetime OPEX	96
6.3.1	Simulation Results	97
6.3.2	Outlook and Conclusions	98
6.4	Optimised Scenario for Each Floater Type at Each Site	99
7	Validation with Real O&M Data and Experience	100
7.1	O&M Experience in Real Floating Wind Farms	100
7.2	Validation of Results	101
8	Conclusions	102
9	References	104

1 Nomenclature

Abbreviation	Description
ADCP	Acoustic Doppler Current Profilers
AHC	Active Heave Compensation
AUV	Autonomous Underwater Vehicle
BEM	Boundary Element Method
CBM	Condition Based Maintenance
CM	Condition Monitoring
COG	Centre of Gravity
CTV	Crew Transfer Vessel
DCI	Decompression Illness
DP	Dynamic Positioning
FOWF	Floating Offshore Wind Farm
FOWT	Floating Offshore Wind Turbine
HLM	Heavy Lift Maintenance
HLCV	Heavy Lift Crane Vessel
HLV	Heavy Lift Vessel
HSE	Health, Safety and Environment
JUV	Jack-Up Vessel
LCE	Large Component Exchange
LCOE	Levelised Cost of Energy
LCT	Load Case Table
LSW	Lightship Weight
LWC	Light weight crane
MCE	Major Component Exchange
MSL	Mean Sea Level
NTM	Normal Turbulence Model
O&M	Operations and Maintenance
OPEX	Operational Expenditures
OSS	Offshore Substation
OSV	Offshore Service (or Support) Vessel
PBA	Production-Based Availability
PPE	Personal Protective Equipment

RAO	Response Amplitude Operator
RNA	Rotor-Nacelle-Assembly
ROV	Remotely Operated Vehicle
SHM	Structural Health Monitoring
SOV	Service Operation Vessel
SRB	Spherical Roller Bearing
SSCV	Semi-Submersible Crane Vessel
TBA	Time-Based Availability
TBM	Time Based Maintenance
TDO	Two-row Double-Outer Race
USV	Unmanned Surface Vessel
VSP	Voith-Schneider Propeller
W2W	Walk-to-Work
WTG	Wind Turbine Generator

2 Executive Summary

This study investigates the effect of different O&M strategies and new requirements on the OPEX in the prospect of future floating offshore wind farms by providing a comprehensive O&M cost model analysis. A commercial-scale reference floating wind farm, consisting of 80 units at 15 MW rating, is modelled with reference site conditions (West of Barra, Scotland; Gran Canaria, Spain; Morro Bay, USA). Further, the wind farms are modelled for two different floater designs, i.e. Windcrete (spar) and ActiveFloat (semi-submersible). The OPEX simulations are carried-out for scenarios with a lifetime of 25 years.

To generate representative operational limits for different maintenance activities, and to allow reliable O&M cost model simulations, preliminary studies are conducted. These studies investigate, first, the offshore major component exchange, and discuss on the relative motions and on motion compensation requirements. Second, the tow-in operation of both floater types is analysed, applying limiting criteria to the wind turbine motions. Third, the effects of the floater motion during maintenance work (i.e. workability) and the influence of the vessel motions on the human comfort of the exposed technicians during transit (i.e. transportability) are assessed. Eventually, an analysis of the accessibility methods and limitations of a generic SOV and CTV is performed.

The operational limitations resulting from these studies have been included into the O&M cost model. The sensitivity analysis of various input parameters showed that especially the vessel costs have a strong impact on the total operational costs of the floating wind farm.

The OPEX and the wind farm availability of a baseline O&M scenario are further benchmarked against alternative scenarios with different O&M strategies for major component exchange and access. The findings showed that the tow-in solution is the most economically effective solution. For the offshore major component exchange strategy, a clear trend was observed for the semi-submersible crane vessel, which is more cost effective over the lifetime than the monohull crane vessel. The workability and transportability assessment showed that, the larger the floater or the vessel, the smaller the impact of the motions on the human comfort of the passengers. The vessel selection for the daily maintenance activities is mainly driven by the weather conditions at site. In the calm weather conditions at Gran Canaria, access via bow-transfer using a CTV was the most cost-effective solution. At Morro Bay, where the average wave heights are higher, a clear trend towards the SOV solution by using a motion compensated gangway was observed.

Finally, the most promising scenarios with the most favourable strategy for major component exchange and crew transfer are summarised for each reference floater design and reference site. Due to the very harsh weather conditions, no cost-effective maintenance strategy was deduced for the site at West of Barra, Scotland. The results were validated based on experience of the COREWIND partners operating floating offshore wind farms.

Table 2-1: Summary of the results on OPEX, availability, and lost production of the optimised scenarios.

Optimised Scenario				Availability		OPEX	Lost Production
Site	Floater Type	Major Exchange Strategy	Access Vessel	TBA [%]	PBA [%]	Per MW and Year [€/MW/yr]	Per MW and Year [MWh/MW/yr]
Gran Canaria	ActiveFloat	Tow-in	CTV	98.70	98.95	77,214	63.67
	Windcrete	Tow-in*	CTV	98.70	98.96	77,305	63.10
Morro Bay	ActiveFloat	Tow-in	SOV	98.66	98.95	73,712	43.11
	Windcrete	Tow-in*	SOV	98.67	98.97	73,518	42.32

*Theoretical scenario due to draft of Windcrete spar and potential port restrictions.

3 Introduction

The COREWIND project investigates the influence of different O&M strategies and new requirements on the OPEX in the prospect of future floating offshore wind farms. The O&M of floating wind farms being a major cost driver motivates the assessment of new strategic opportunities and developments to reduce the O&M costs. A comprehensive overview of the floating wind specific O&M requirements, as well as a review of state-of-the-art inspection and maintenance strategies and monitoring techniques, have already been published in deliverable D4.1 of August 2020. Deliverable D4.1 concludes with general recommendations on O&M strategies for floating wind farms and a reflection on required studies to be performed for a detailed OPEX assessment.

This deliverable D4.2 continues on the previous considerations, and it summarises the activities undertaken to assess O&M strategies specific to floating wind. The lifetime OPEX and availability of a commercial-scale floating wind farm are evaluated in this report for several O&M scenarios. COREWIND's reference wind farm consisting of 80 units at 15 MW rating per unit is modelled using a combination of the reference floater designs – i.e. Windcrete (spar) and ActiveFloat (semi-submersible) – and the reference site conditions – i.e. West of Barra, Scotland (site A), Gran Canaria, Spain (site B) and Morro Bay, USA (site C).

In Chapter 4, an overview of the required inputs and delivered outputs of the simulation studies is given. Details on each simulated scenario are further described. The input parameters to the O&M cost model, for example, the component failure rates, their repair times, the amount and type of O&M resources (i.e. vessels and personnel) and their costs are reported. The OPEX simulations are performed for full 25-year lifetime scenarios of floating offshore wind farms. In Chapter 5, a particular focus is on defining representative operational limits required for setting-up reliable O&M cost model simulations. Preliminary studies are conducted regarding the:

- offshore major component exchange, with a discussion on the relative motions between a floating crane vessel and the FOWT, and on motion compensation requirements;
- major component exchange inshore with tow-in operation of both floaters applying limiting criteria to the wind turbine motions;
- effects of the floater motion during maintenance work (i.e. workability) and the influence of the vessel motions on the human comfort of the exposed technicians during transit (i.e. transportability);
- accessibility methods and limitations of a generic SOV and CTV.

In Section 6.1, the sensitivity of OPEX and wind farm availability to the following input parameters is assessed:

- vessel dayrate, vessel mobilisation cost, cost of technicians and failure rate;
- weather limitations of CTV, SOV, tug boat and floating crane vessel.

In Sections 6.2 and 6.3, the OPEX and the wind farm availability of a baseline O&M scenario are further benchmarked against alternative scenarios with different O&M strategies for major component exchange and access, based on the preliminary studies of Chapter 5. Finally, the most promising scenarios with the most favourable strategy for major component exchange and crew transfer are summarised for each reference floater design and reference site in Section 6.4.

This study concludes in Chapter 7 with a validation of the assumptions and findings based on experience of the COREWIND partners operating floating offshore wind farms. Lessons learnt from the O&M are provided.

The costs taken as input in this study have been aligned with the required assumptions for work package 6 of COREWIND, which focuses on the LCOE analysis and life cycle assessment. This deliverable D4.2 contributes significantly to the objectives, expected impact and identified exploitable results of the COREWIND project regarding the development of an O&M planning and strategy tool landscape. This includes pre- and postprocessing tools around an O&M cost model.

4 Life-Time OPEX Analysis

The aim of this deliverable is to assess the operational expenditures (OPEX) and availability in the lifetime of a commercial-sized floating wind farm, comprised of 80 wind turbines with 15 MW each, and 2 offshore substations, and thus resulting into a 1.2 GW wind farm. The layout of the wind farm is based on the optimized layouts of the different sites from the COREWIND deliverable D6.1 [1]. Site C (Morro Bay) is taken as baseline scenario. The weather conditions of this site are moderate and they lie between the conditions of the other two sites (A: West of Barra; B: Gran Canaria) [2]. This allows drawing more reliable conclusions for the more severe (Site A) and milder (Site B) weather conditions (see Section 5).

The layouts include two offshore substations (OSS) which have also been modelled in the O&M tool. However, maintenance at the OSS was only considered from a high level perspective. The historic weather time series of the three sites used in the modelling have been provided by the COREWIND partner FIHAC (IHDATA metocean data base).

The analyses are performed with Shoreline’s simulation engine, [3], for full life-cycle scenario modelling of offshore wind farms. The commercial tool allows for flexible web-based user input and probabilistic cost assessments and supports a Monte Carlo based simulation. Multiple simulation scenarios and sensitivity studies can be run simultaneously. To enhance the simulation with project specific boundary conditions, different preliminary studies have been performed (see Chapter 5 for details). These include weather limitations for access, offshore operations and workability. The outputs have been included into the Shoreline simulation model. The following subchapters introduce the reader to the modelling approach for the life-time OPEX analysis. Section 4.1 gives an overview of the workflow of the analysis, the interfaces between the several steps of the investigation, and the outcomes of each one of these. Section 4.2 describes the several scenarios examined in this study. Finally, in Section 4.3, the input parameters to the OPEX simulation model are listed.

The O&M cost model requires the definition of a O&M port location for the underlying calculations of the transfer times. Therefore, a simplified assumption has been made by defining potential O&M ports in proximity of the wind farms for all three reference sites. Port capacities or draft restrictions have, however, not been verified. Further no vessel routing optimization has been made.

A lifetime of 25 years is chosen for the simulations, which is a typical lifetime of a wind farm. To benchmark the results for the different scenarios, the KPIs of the operational expenditures (OPEX), the time-based availability (TBA) and production-based availability (PBA) are chosen. The KPIs are calculated by the Shoreline Design tool and are briefly described in the following. For more details, the reader can refer to the online support manual, [4], of the tool, from which the following definitions have been taken:

Production-Based Availability (PBA)

According to [4], “the Production-based availability is a measure of how much of the potential production is actually produced.”

$$PBA [\%] = \frac{\text{Actual production [MWh]}}{\text{Potential production [MWh]}} \quad (\text{eq. 4.1})$$

The **potential production** is defined as “the amount of energy an asset can produce if it was always operational (never fails or shuts down). Found by calculating energy production using the power curve of the asset and the wind speed at hub height.”

The **actual production** is “the amount of energy an asset produces when operational. Found by calculating energy production using the power curve of the asset and the wind speed at hub height.”

The **lost production** is “the energy not produced when an asset is non-operational but would be produced if it was operational. Calculated as the difference between potential production and lost production.”

Time-Based Availability (TBA)

According to [4], “the time-based availability is a measurement of an asset's availability or the fraction of time the asset is operational. It is calculated as the ratio of hours available as a fraction of the full period.”

$$TBA [\%] = \frac{\text{Possible uptime [h]} - \text{Downtime [h]}}{\text{Possible uptime [h]}} \cdot 100 = \frac{\text{Time available [h]}}{\text{Total time in consideration [h]}} \cdot 100 \quad (\text{eq. 4.2})$$

“**Downtime** is measured per asset in hours. Working on the asset and critical component failures is an example of the downtime period among other causes.”

The **possible uptime** is defined as “the total time being considered regardless of asset availability. It is the number of hours from the start until the end of the simulation multiplied by the number of assets (simulated years * 8,760[h] * the number of assets).”

Operational Expenditures (OPEX)

The operational expenditures, short OPEX calculated in Shoreline as the sum of the calculated general costs and the maintenance costs. These are defined in [4], as follows:

- “The general costs include all ports, transportation and personnel costs.”
- “The maintenance costs include costs related to all scheduled and corrective maintenance tasks.”

4.1 Overview of the Simulation Study

The aim of this deliverable is to provide realistic cost and availability figures for an optimized O&M strategy at all three sites and for both floater types (Windcrete spar and ActiveFloat semi-submersible). To achieve this, the focus of pre-analyses has been on enhancing the results of the Shoreline cost model by identifying representative the input data for the operational weather limits:

- A first study investigates the **offshore major component exchange**. For the offshore lifting operation the relative motions between the floating crane vessel and the floater are highly dependent on the wave period of the prevailing sea state. Project-specific weather windows are therefore essential for a realistic estimate of the OPEX and to enhance the outcomes of the study.
- In a second study the **tow-in operation** of both floaters is investigated. Operational weather windows are calculated by applying limiting criteria to the wind turbine motions during tow-in.
- A third study investigates the effect of the floater motion during maintenance work (**workability**) and the influence of the vessel motions during transit on the human comfort of the exposed technicians (**transportability**). Low frequency motions in a specific frequency range are known to induce motion sickness, which poses an HSE risk and reduces the performance of the person concerned. Operational weather windows for each floater type are calculated for which workability and transportability are guaranteed.
- Eventually, the **accessibility** of a generic SOV and CTV is calculated. The resulting availability matrices serve as input to the respective vessels of the Shoreline model.

The scatter tables, output of these analyses, serve as input to the Shoreline simulation tool. The cost model study will run sensitivity studies on the various input parameters and different scenarios to assess the impact of alternative strategies on the selected KPIs (i.e. TBA, PBA, and OPEX). Next to the operational limits, a large number of other input parameters need to be defined a basis for the simulations. These variables and their

assumed value are listed in Section 4.3. The chart in Figure 4-1 illustrates the interfaces between the preliminary studies, the Shoreline simulations as well as the input parameters and the outputs.

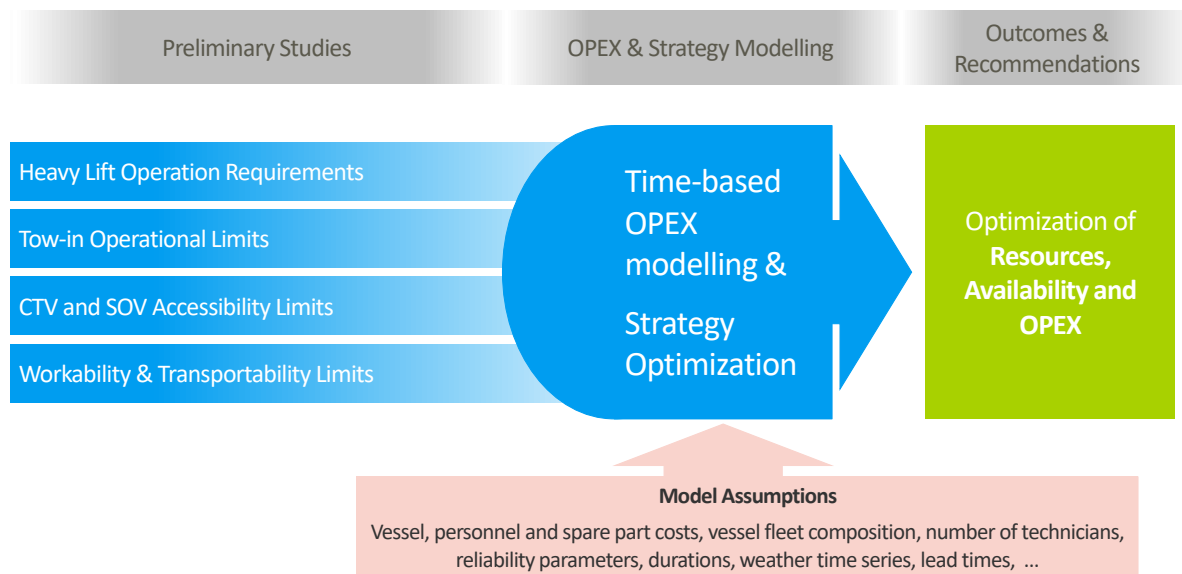


Figure 4-1: Overview illustrating the interfaces between the preliminary studies, the O&M simulations as well as the input parameters and the outputs [Source: Ramboll].

4.2 Simulation Scenario Description

4.2.1 Sensitivity Study

The results of sensitivity analyses are reported in Section 6.1. The variations of the overall OPEX and the farm availability are measured when the input values (e.g. the vessel dayrates, the mobilization costs, the personnel costs, and the failure rates) of the optimized scenario are increased and decreased by 10%. A further sensitivity of the results on the weather limitations for the CTVs, SOVs, tug boats, and the floating crane vessel is then conducted.

4.2.2 Impact Study

For the impact study a baseline scenario is defined and benchmarked against alternative scenarios. The impact on the principle wind farm key performance indicators (KPIs), the OPEX and the wind farm availability is studied.

The **baseline scenario** includes access with crew transfer vessels (CTV) for the scheduled and unscheduled maintenance activities, by accessing the turbine via bow-transfer method. The component replacement is executed inshore, requiring the tow-in of the wind turbine to port and the subsequent tow-out at concluded repair. A baseline scenario is calculated for each of all three sites and either one of the floater designs. In the subsequently described scenarios **only one aspect of the baseline scenario** will be changed.

- F2F Scenario:** This scenario alters the strategy with which the major component exchange is performed. A floating crane vessel is used for a floating-to-floating (F2F) solution to perform the major component exchanges offshore. The F2F scenario is compared to the baseline scenario, in Section 6.2, with the aim to benchmark the two alternative solutions for major component exchange: F2F versus tow-in. It shall be noted that, according to UPC, the Windcrete floater is not meant for maintenance tow-in. Nevertheless, the environmental towing limitations have been studied and documented in Section 5.2, and they are used for a theoretical assessment in this scenario.

- **SOV Access Scenario:** In this scenario the maintenance activities are performed with an SOV accessing the wind turbine using a motion compensated gangway instead of a CTV. Scenario 2 is compared to the baseline scenario, in Section 6.3., with the aim to benchmark the impact of a access method allowing for bigger weather windows.
- **Workability and Transportability Scenario:** It was planned to analyse the impact of the workability and transportability restrictions, as defined in Section 5.3, on the KPIs. However, the results of Section 5.3 have shown that the workability and transportability restrictions on the weather windows are lower than the accessibility limits of the vessels used in the simulations. Therefore, an impact study is not conducted for this scenario.

Table 4-1 provides an overview of the several scenarios described above. An optimized scenario, corresponding to the most favourable strategy for major component exchange and crew transfer, is identified and simulated in Section 6.4 for each one of the sites and floater types in analysis. It shall be noted that Windcrete cannot be installed at site A (West of Barra), due to the higher water depth required for the deployment of the spar-type substructure. Therefore, no OPEX analyses was performed for this scenario.

Table 4-1: Overview of the simulations studied in the O&M tool.

Scenario Name	Access Strategy	Major Component Exchange Strategy	Site	Floater Type
Baseline (Tow-in)	Bow-transfer (CTV)	Inshore (tow-in)	A	ActiveFloat
			B	both
			C	both
Floating-to-floating (F2F)	Bow-transfer (CTV)	Offshore (F2F)	A	ActiveFloat
			B	both
			C	both
SOV Access	Motion compensated gangway (SOV)	Inshore (tow-in)	A	ActiveFloat
			B	both
			C	both
Optimized Scenarios for each site	Defined individually	Defined individually	A	ActiveFloat
			B	both
			C	both

The resources applied in the different scenarios are listed in Table 4-2. In the SOV-access scenario the same SOVs are used for the corrective and scheduled maintenance of the WTG and floating platform, as for the subsea inspections. Here the SOV enables personnel transfer via a motion compensated gangway. In the CTV-access case the 2 SOVs are only used for scheduled and corrective subsea inspections where ROVs are required. The maintenance activities on the WTG and floating platform are performed with CTVs. Personnel transfers to the platform over the boat landing.

Table 4-2: Resources applied in different O&M scenarios.

Resources	Tow-in Scenario With CTV Access (Baseline)	F2F Scenario With CTV Access	Tow-in Scenario With SOV Access
Crew set up	1 service technician group + 2 SOV groups	1 service technician group + 2 SOV groups	2 SOV groups
Number of Personnel	60 service technicians + 20 SOV members (10 per group)	60 service technicians + 20 SOV members (10 per group)	60 SOV members (30 per group)
Shift set up	Staggered shift per group	Staggered shift per group	Staggered shift per group
AHV	1	1	1
Assisting CTV for AHV	1	1	1
SOV incl. ROV garage	2	2	2
CTV (owned)	7	7	0
CTV (chartered)	1	1	0
Offshore Tug	2	0	2
Onshore Crawler Crane	1	0	1
Floating Crane Vessel	0	1	0

4.3 Inputs to O&M Cost Model

In this section, all simulation inputs for the O&M simulation tool are listed. Cost inputs made in this study have been aligned with required assumptions for work package 6 of COREWIND on the LCOE analysis and Life Cycle Assessment.

4.3.1 Scheduled Maintenance for Floating Wind Farms

Table 4-3 reports the input parameters to the OPEX model calculation for the scheduled inspections. These cover the planned inspections for the floating wind turbines, for the export cable, and for the offshore substations (OSS). Two OSS are part of the reference wind farm layout. Although they are not the focus of this study, their scheduled inspection and two corrective maintenance actions are included into the simulations to draw more realistic figures from this O&M cost analysis.

Table 4-3: Scheduled maintenance inspection intervals and key parameters.

Inspection	Frequency	Vessel Type	Duration [h]	No. of Technicians	Material Cost [€]	Vessel
Sub-Sea Inspections of Cables, Mooring Lines and Floater Hull	2-yearly	ROV support vessel (SOV)	12	5	500	SOV with ROV
Sub Sea Inspection of Export cable	2-yearly	ROV support vessel (SOV)	12	5	500	SOV with ROV
Inspection of structural elements above water (e.g., Visual deck check,	yearly	CTV / SOV	24	4	600	CTV (or SOV in certain scenarios)

Inspection	Frequency	Vessel Type	Duration [h]	No. of Technicians	Material Cost [€]	Vessel
transition piece, floater compartments)						
Inspection of Wind Turbine components	yearly	CTV / SOV	24	3	1500	CTV (or SOV in certain scenarios)
Inspection of the OSS	yearly	CTV / SOV	24	4	500	CTV (or SOV in certain scenarios)

4.3.2 Corrective Maintenance for Floating Wind Turbines

Carroll et al., [5] grouped the wind turbine failures into three maintenance categories, which are originally based on the classification defined by the RELIAWIND project in [6]. These categories are: minor repair, major repair, and major replacement.

The exponential failure distributions used in this study are also defined for the three failure categories, according to the INNWIND.EU project [7]. The failure rates of the turbine components are based on the annual failure rates given for the DTU 10 MW wind turbine of the INNWIND project [7], and they are listed in Table 4-4.

Table 4-4: Annual failure rates Wind Turbine according to [7], [5] and [8]

Component	Minor Failure [failures/year]	Major Failure [failures/year]	Replacement [failures/year]	Vessel
Direct Drive Generator	0.546	0.030	0.009	CTV (or SOV in certain scenarios)
Power Converter	0.538	0.338	0.077	
Main shaft	0.231	0.026	0.009	
Power electrical system	0.358	0.016	0.002	
Yaw system	0.162	0.006	0.001	
Pitch system	0.824	0.179	0.001	
Blades	0.456	0.010	0.001	

Table 4-5: Annual failure rates Floating Substructure and OSS based on interviews and inhouse expertise

Component	Minor Failure [failures/year]	Major Failure [failures/year]	Replacement [failures/year]	Vessel
Fix broken / blocked pumps of active ballast system (where applicable)	0.010	-	-	CTV (or SOV in certain scenarios)
Mooring Line	-	0.015	0.0125	AHV with assisting CTV
Anchor	-	0.015	0.0125	AHV with assisting CTV
Subsea Marine Growth Removal	0.120	-	-	SOV with ROV

Component	Minor Failure [failures/year]	Major Failure [failures/year]	Replacement [failures/year]	Vessel
IA / Dynamic Cable	-	0.025	0.016	SOV with ROV
Buoyancy modules (dislocation/ replacement)	-	-	0.033	SOV with ROV
Export cable inspection after incident	-	0.020	-	SOV with ROV
OSS Corrective maintenance	0.200	0.010	-	CTV (or SOV in certain scenarios)

The repair times required for each corrective maintenance action are listed in Table 4-6.

Table 4-6: Repair Times according to [5] and [8], adapted and upscaled by [9] & inhouse expertise

Component	Minor Failure [h]	Major Failure [h]	Replacement [h]
Direct Drive Generator	13	49	244
Power Converter	14	28	170
Main shaft	10	36	144
Power electrical system	10	28	54
Yaw system	10	40	147
Pitch system	18	38	75
Blades	18	42	864
Fix broken / blocked pumps of active ballast system (where applicable)	8	-	-
Mooring Line	-	240	360
Anchor	-	240	360
Subsea Marine Growth Removal	-	40	-
IA / Dynamic Cable	-	240	360
Buoyancy modules (dislocation/ replacement)	-	-	40
Export cable inspection after incident	-	60	-
OSS Corrective maintenance	12	60	-

Upscaling factors were used, as suggested by Walgern in [9], to calibrate the repair times due to bigger turbine size; a factor 2 is used to scale minor and major repairs, while a factor 3 is employed for major replacements.

Table 4-7: Lead Time according to [5] and [8], adapted and upscaled by [9] & inhouse expertise

Component	Minor Failure [hrs]	Major Failure [hrs]	Replacement [hrs]
Direct Drive Generator	0	48	336
Power Converter	0	48	168
Main shaft	0	48	168

Component	Minor Failure [hrs]	Major Failure [hrs]	Replacement [hrs]
Power electrical system	0	48	168
Yaw system	0	48	168
Pitch system	0	48	168
Blades	0	48	336
Fix broken / blocked pumps of active ballast system (where applicable)	0	-	-
Mooring Line	-	336	336
Anchor	-	336	336
Subsea Marine Growth Removal	-	48	-
IA / Dynamic Cable	-	336	336
Buoyancy modules (dislocation/ replacement)	-	-	168
Export cable inspection after incident	-	48	-
OSS Corrective maintenance	0	48	-

Table 4-8: Number of technicians according to [5] and [9] & inhouse expertise

Component	Minor Failure [-]	Major Failure [-]	Replacement [-]
Direct Drive Generator	2	3	8
Power Converter	2	3	4
Main shaft	2	3	5
Power electrical system	2	3	4
Yaw system	2	3	5
Pitch system	2	3	4
Blades	2	3	21
Fix broken / blocked pumps of active ballast system (where applicable)	2	-	-
Mooring Line	-	10	10
Anchor	-	10	10
Subsea Marine Growth Removal	-	5	-
IA / Dynamic Cable	-	10	10
Buoyancy modules (dislocation/ replacement)	-	-	5
Export cable inspection after incident	-	5	-
OSS Corrective maintenance	2	5	-

Table 4-9: Repair Costs according to [5] and [9] & inhouse expertise

Component	Minor Failure [€]	Major Failure [€]	Replacement [€]
Direct Drive Generator	1,000	14,340	236,500
Power Converter	1,000	7,000	55,000
Main shaft	1,000	14,000	232,000
Power electrical system	1,000	5,000	50,000
Yaw system	500	3,000	12,500
Pitch system	500	1,900	14,000
Blades	5,000	43,110	445,000
Fix broken / blocked pumps of active ballast system (where applicable)	1,000	-	-
Mooring Line	-	20,000	135,000
Anchor	-	75,000	512,000
Subsea Marine Growth Removal	-	1,500	-
IA / Dynamic Cable	-	30,000	220,000
Buoyancy modules (dislocation/ replacement)	-	-	100,000
Export cable inspection after incident	-	30,000	-
OSS Corrective maintenance	2000	100,000	-

4.3.3 Vessels

The vessels are needed to perform the inspections and corrective actions. The dayrates, mobilisation and demobilisation costs are listed in Table 4-10.

It shall be noted that the same costs are assumed for the floating crane vessels (either monohull or semi-submersible). An internal market screening has shown that as per today no floating crane vessel is available in the market that has the required capacity for a floating 15 MW offshore wind turbine (combination of required lifting height and weight, see Section 5.1.3). Therefore, the assumptions on the vessel costs are highly speculative. The same is true for jack-up vessels, as reported by [10].

Table 4-10: Vessel costs, purpose and weather limits, according to inhouse databases

Vessel	Purpose	Dayrate [€]	Mob- and Demobilisation Cost [€]	CAPEX [€]	Significant Wave Height Limit ($H_{s,max}$)
SOV + ROV garage with ROV	Subsea inspections and repairs + Access to Asset (in certain scenarios)	75,000	225,000	-	See matrices in Section 5.4.2
Crew Transfer Vessel (CTV) - owned	Access to Asset	3,500	-	3,000,000	See matrices in Section 5.4.2
Crew Transfer Vessel (CTV) - chartered	Access to Asset + Assisting AHV	11,000	30,000	-	See matrices in Section 5.4.2
Anchor Handling Vessel (AHV)	Mooring Line and anchor repair	55,000	500,000	-	2.50 m
Offshore Tug	Floater tow-in and tow-out	30,000	200,000	-	See matrices in Section 5.2.7
Monohull Crane Vessel (HLCV)	Major component exchange offshore	290,000	325,000	-	See matrices in Section 5.1.5
Semi-Submersible Crane Vessel (SSCV)	Major component exchange offshore	290,000	325,000	-	See matrices in Section 5.1.5
Onshore Crawler Crane	Major component exchange inshore	25,000	185,000	-	N/A

4.3.4 Personnel

In the scenarios in which the CTV is used for accessing to the wind turbines, two personnel groups are chosen. The first group comprises the service technicians, which perform the day-to-day maintenance tasks for the scheduled and the corrective activities, for either the wind turbine or the floater, above the water level. The second group includes SOV technicians, who are in charge of the subsea inspections, and corrective maintenance tasks involving the use of an ROV.

In the case in which the SOV replaces the CTV for regular inspections, the SOV technicians are in charge of all maintenance works in the wind farm. The annual salary of the technicians of both groups is assumed to be 80,000 €.

5 Operational Limits for Scenarios

The following subsection describe the assessment of operational limits for four representative scenarios as introduced in Section 4.2. The results of the preliminary studies feed into the O&M cost model in Section 6. The approach, the simulation models and the processing of in- and output data are described.

The COREWIND project provides three reference sites A (West of Barra, Scotland), B (Gran Canaria, Spain) and C (Morro Bay, West Coast of USA). For this study, **site C was selected as the reference site** due to the moderate metocean conditions (with respect to the magnitude of 50-year extreme wave height and extreme wind speed) and medium size of floating substructure (only ActiveFloat semi-submersible) compared to the other sites (site A: harsh, site B: benign). Site C is considered as a reasonable starting point for extrapolation of results towards more benign and harsh conditions. The water depth may become a key driver of the O&M cost when major replacements of mooring system components or power output cables are needed. Nevertheless, for the sake of simplicity the impact of water depth over OPEX has been neglected in this study. Only a water depth of 870 m at site C as site specific value from the design basis [11] has been considered. Variations of metocean condition – i.e. different combinations of significant wave height, wave period and wave direction – are considered so that the results can be considered dependent on the specific substructure concept, but independent of the site. A combined wave-scatter diagram is shown in Figure 5-1 for all three COREWIND reference sites. Only a few combinations for the range of $0 \leq T_p \leq 4$ are more benign (in terms of H_s for site A and B) than site C, while other H_s - T_p combinations occur at site A with higher waves. Based on common weather limits for typical O&M operations, it is assumed that higher wave heights, present at site A, are unfeasible for operation and excluded.

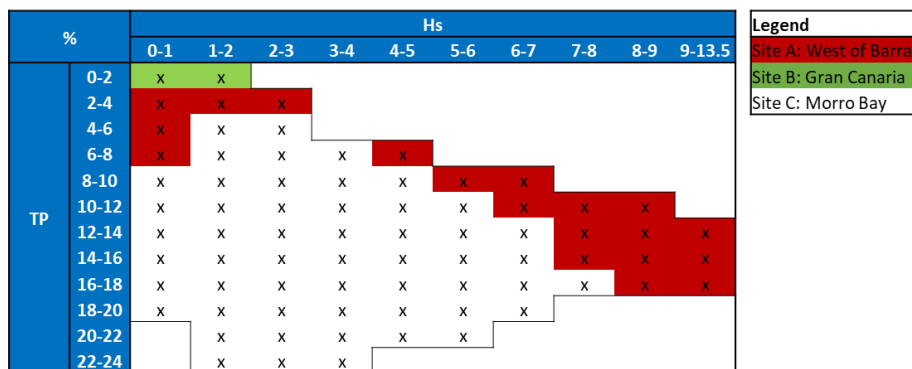


Figure 5-1: Illustration of a combined wave-scatter diagram for the three COREWIND sites. The coloured cells represent H_s - T_p combinations which are specific to site A and B only [Source: Ramboll].

5.1 Floating-to-Floating Major Component Exchange

Major component exchange operations are addressed in the following section with detail provided on the background, goals and assumptions, as well as model setup and the load cases considered in the simulation study. The results are presented and discussed in Section 5.1.5.

5.1.1 Background of Study

Major Component Exchange (MCE) describes a marine operation conducted during the operational life of a FOWF. It typically involves special equipment, cranes and vessels for lifting operations. Heavy Lift Maintenance (HLM) is an analogous term used frequently in the public domain. The lifting operation can be categorized according to whether the crane support and/or the structure that will support the payload after lifting/mating are either fixed or floating (airborne lifting operations using drones or aircrafts is not considered relevant here):

- **Fixed-to-fixed** lifting operation from onshore crane to onshore asset (such as onshore wind turbine), or from a Jack-Up Vessel (JUV) that is fixed to the seabed to a fixed offshore asset (such as bottom fixed offshore wind turbine)
- **Fixed-to-floating** lifting operation from a JUV to a floating offshore asset (such as FOWT), or from a heavy lift crane at quayside to a floating offshore asset (such as FOWT during turbine installation, or vessel for transportation of WTG components)
- **Floating-to-fixed** lifting operation from a floating offshore asset (such as Heavy Lift Vessel (HLV)) to a fixed offshore asset (such as bottom fixed offshore wind turbine)
- **Floating-to-floating** lifting operation from a floating offshore asset (such as HLV) to a floating offshore asset (such as FOWT), also referred to as ship-to-ship




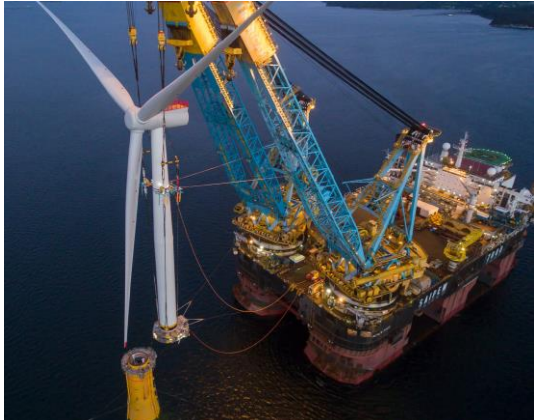
Below Table 5-1 shows an overview of lifting operations using fixed and floating assets. While fixed-to-fixed and fixed-to-floating lifting operations are common practice in offshore wind, floating-to-fixed lifting operations are more frequently used in O&G. The installation of the DOT wind turbine on a preinstalled monopile substructure at Eneco Princess Amalia Wind Park off the coast of the Netherlands using Heerema Marine Contractors' DP3 vessel Aegir¹ in 2018 is an example of floating-to-fixed heavy lifting in offshore wind. Another example is the planned floating-to-fixed WTG installation on monopile substructures for Parkwind's Arcadis Ost 1 offshore wind farm in the German Baltic Sea². Turbine integration using floating-to-floating lifting operations was performed for Equinor's Hywind Scotland spar substructure using the semi-submersible crane vessel (SSCV) Saipem 7000 in 2017. The described examples relate to turbine integration and installation works. The categorisation of lifting operations can also be applied to the O&M phase such as for the exchange of major components.

This study focuses on the **scenario of a floating-to-floating lifting operation for major component exchange offshore**. During a marine operation a HLV approaches a FOWT on site (offshore) for O&M works such as exchange of rotor blades. A major component of a wind turbine in this context refers to **large or heavy components** such as rotor blade, blade bearing, hub, generator, HV equipment, etc. which require external lifting equipment. Floating wind specific requirements for major component exchange are discussed in more detail in COREWIND's Deliverable D4.1 [12].

¹ Source: <https://hmc.heerema.com/news-media/news/heeremas-dp3-vessel-aegir-installs-first-offshore-wind-turbine>

² Source: <https://hmc.heerema.com/news-media/news/parkwind-heerema-and-mhi-vestas-announce-a-revolutionary-construction-methodology-for-arcadis-ost-1>

Table 5-1: Exemplary overview of lifting operations for fixed and floating assets.

From/ To	Fixed	Floating
Fixed	 <p>Figure 5-2: Installation of bottom fixed offshore wind turbine using JUV [Source: DEME].</p>	 <p>Figure 5-3: Turbine integration of WindFloat Atlantic at outer harbour of Ferrol, Spain [Source: Vestas].</p>
Floating	 <p>Figure 5-4: Turbine integration of DOT wind turbine on monopile using HLV [Source: Heerema].</p>	 <p>Figure 5-5: Turbine integration with Hywind Scotland spar using HLV [Source: Saipem].</p>

5.1.2 Goals and Assumptions

The simulation study on floating-to-floating major component exchange has two main goals summarized in Table 5-2. Two different types of generical crane vessels are evaluated, a semi-submersible crane vessel (SSCV) and a monohull heavy lift crane vessel (HLCV). The ActiveFloat and Windcrete concept designs for site C are considered. COREWIND Deliverable D1.3 [13] includes the models for site B³. Hence, four combinations of vessel and FOWT are simulated in this study:

- ActiveFloat concept and SSCV or HLCV
- Windcrete concept with SSCV or HLCV

³ Optimised models for ActiveFloat and Windcrete for the reference sites A and C have been developed within the COREWIND project. However, at the time this report was submitted, the models had not yet been published, so reference can only be made to the models for Site B.

Table 5-2: Overview of goals of study on floating-to-floating major component exchange with required inputs and provided outputs.

Number	Goal Description	Required Input	Provided Output
1	Assess weather limits for OPEX calculation of floating specific O&M scenarios	<ul style="list-style-type: none"> - Design basis with metocean conditions (water depth, wave-scatter diagram, ...) - FOWT concept design from WP1 (ActiveFloat semi-submersible and Windcrete spar concept designs) and mooring system from WP2 (optimised mooring systems: semi-taut polyester mooring) - Generic crane vessel design for calculation of motion RAOs - Scenario definition (reference points for evaluation of relative motion, parameter variations for load cases, ...) 	<ul style="list-style-type: none"> - Weather limits for OPEX calculation of T4.2 (see Section 5.1.5)
2	Identify compensation requirements from relative motion between the vessel and the FOWT during O&M works	<ul style="list-style-type: none"> - Relative motions between the vessel and FOWT - Input and specifications from technology providers - Internal and external expert knowledge 	<ul style="list-style-type: none"> - Indicative compensation requirements for horizontal and vertical direction based on evaluation of displacements, velocities and accelerations

A summary of the main assumptions of the study on floating-to-floating major component exchange is given below:

- The **software OrcaFlex** is used in combination with scalable **cloud computing** capabilities to perform simulation studies in the time-domain. **Relative motions between a nacelle and crane reference location** are used to evaluate the relative horizontal and vertical displacement, velocity and acceleration.
- **Wind and current loads** on FOWT and crane vessel are **neglected. Only wave loads are considered.** It is assumed that the wind turbine is parked during the maintenance operation. Rotor blades are pitched to parked position resulting mainly in wind-induced drag loads on the tower and RNA. Neglecting wind loads results in a more simplified and computationally less demanding simulation model as aerodynamics are not considered for either a full representation of the RNA (and tower) or a simplified rotor disk approach. However, this assumption could have some impact on the results, and it is not clarified in this study whether neglecting wind loads is less or more conservative. Hence, it is recommended to include wind loads in future and more comprehensive studies.
- The hydrodynamic, **multi-body interaction** between the floating substructure and the crane vessel is **neglected.** This assumption could have an impact on the results depending on wave directionality with potential sheltering effects and hydrodynamic coupling between FOWT and crane vessel. For future and more comprehensive studies the impact of multi-body interaction should be evaluated.

- The **ActiveFloat semi-submersible** and **Windcrete spar** concept designs for site C are analysed. The **optimised mooring system models** provided by WP2 (planned publication in Deliverable D2.2) are considered.
- A controller for the **DP system is not included** for the crane vessels in the OrcaFlex models. Only **motion RAOs** are calculated and used for simulating the motion behaviour of the crane vessels which might result in conservative results. For the FOWT, load RAOs are used as basis for the analysis. For future and more comprehensive studies the impact of a controlled DP system should be evaluated.
- **Active motion compensation** of the movement of the crane vessel (using a DP system), the FOWT or the offshore crane itself is **not considered in the OrcaFlex model directly**. Also, no auxiliary equipment such as an active heave compensator between crane hook and payload is modelled in OrcaFlex. During post-processing of the relative motions between FOWT and crane vessel for the heavy lift maintenance scenario, the sensitivity of the operational limits is evaluated by assuming limits for the relative vertical motion.

5.1.3 Generic Heavy Lift Crane Vessels

The floating major component exchange operation imposes high requirements on the crane vessel in terms of lifting capacity, lifting height and crane outreach. Two types of crane vessels have been identified that can fulfil the requirements: Semi-Submersible Crane Vessel (SSCV) and monohull Heavy Lift Crane Vessel (HLCV). Exemplary vessels are displayed in Figure 5-6 and Figure 5-7 for each vessel type. As both vessel types feature different motion behaviour, the floating-to-floating major component exchange operation shall be assessed individually. Generic vessel models are generated for each vessel type based on public data.



Figure 5-6: Exemplary selection of semi-submersible crane vessels; Left: Heerema Sleipnir [Source: Heerema], Middle: Heerema Thialf [Source: Heerema], Right: Saipem 7000 [Source: Saipem].



Figure 5-7: Exemplary selection of monohull heavy lift crane vessels; Left: Heerema Aegir [Source: Heerema], Middle: Deme Orion [Source: Deme], Right: Boskalis Boka Lift 2 [Source: Boskalis].

Main Parameters of Generic Vessels

The characteristic parameters for both generic vessels are compiled in Table 5-3. Figure 5-8 shows the hull models of the generic vessels. For each vessel, a mass model is set up to calculate the overall mass, centre of gravity and inertia of the vessel considering the main structural elements of the hull, cranes and bridges as well as seawater ballast. Additionally, a model of the buoyant force based on the external surfaces of the hull is generated for the calculation of hydrostatic properties, as well as for the hydrodynamic analysis of the body in ocean waves.

Table 5-3: Main dimension of generic crane vessels.

Parameter	Unit	Generic SSCV	Generic HLCV
Length	m	165.0	216.0
Breadth	m	88.0	49.0
Height (keel to working deck)	m	49.5	21.0
Operational draft	m	27.5	9.0
Lightship Weight (LSW)	t	71,500	40,900
Displacement at operational draft	t	186,800	71,900
Lifting capacity of main crane(s)	t	2x 7,000	1x 4,000

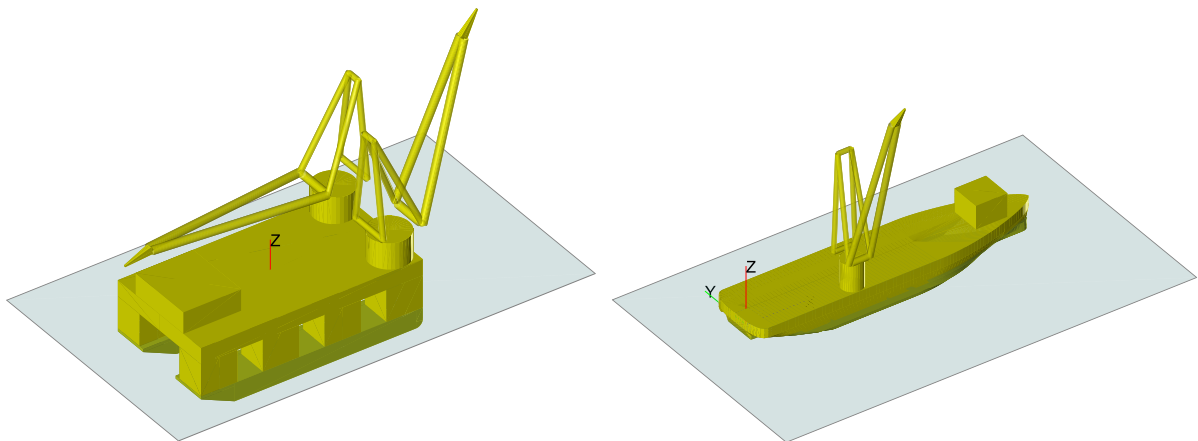


Figure 5-8: Models of the generic crane vessels showing the hull, cranes and bridge; Left: Generic SSCV [Source: Ramboll], Right: Generic HLCV [Source: Ramboll].

Approach for Calculation of RAOs

In order to represent the motion behaviour of the crane vessel within the OrcaFlex simulation environment, frequency-dependent response amplitude operators (RAO) for the motion of the vessels are required. The RAOs are a function of the hydrostatic and hydrodynamic properties as well as the mass and inertia of the vessels. The hydrostatic and hydrodynamic properties, such as hydrostatic stiffness matrix, added mass and damping as well as wave excitation forces are calculated using the software WAMIT. WAMIT solves the diffraction and radiation solution in the frequency domain based on representation of the geometrical body by boundary elements (panels) using the boundary integral equation method. This method utilizes the potential theory and thus neglects any viscous effects. In order to account for motion damping due to viscous effects, additional linear damping coefficients are applied to the roll, pitch and heave motion for the SSCV and to the roll motion for the HLCV. The sensitivity of additional viscous damping on the motion RAOs is discussed further below. The motion RAOs are calculated by solving the equation of motion considering the mass, centre of gravity and inertias of the vessel.

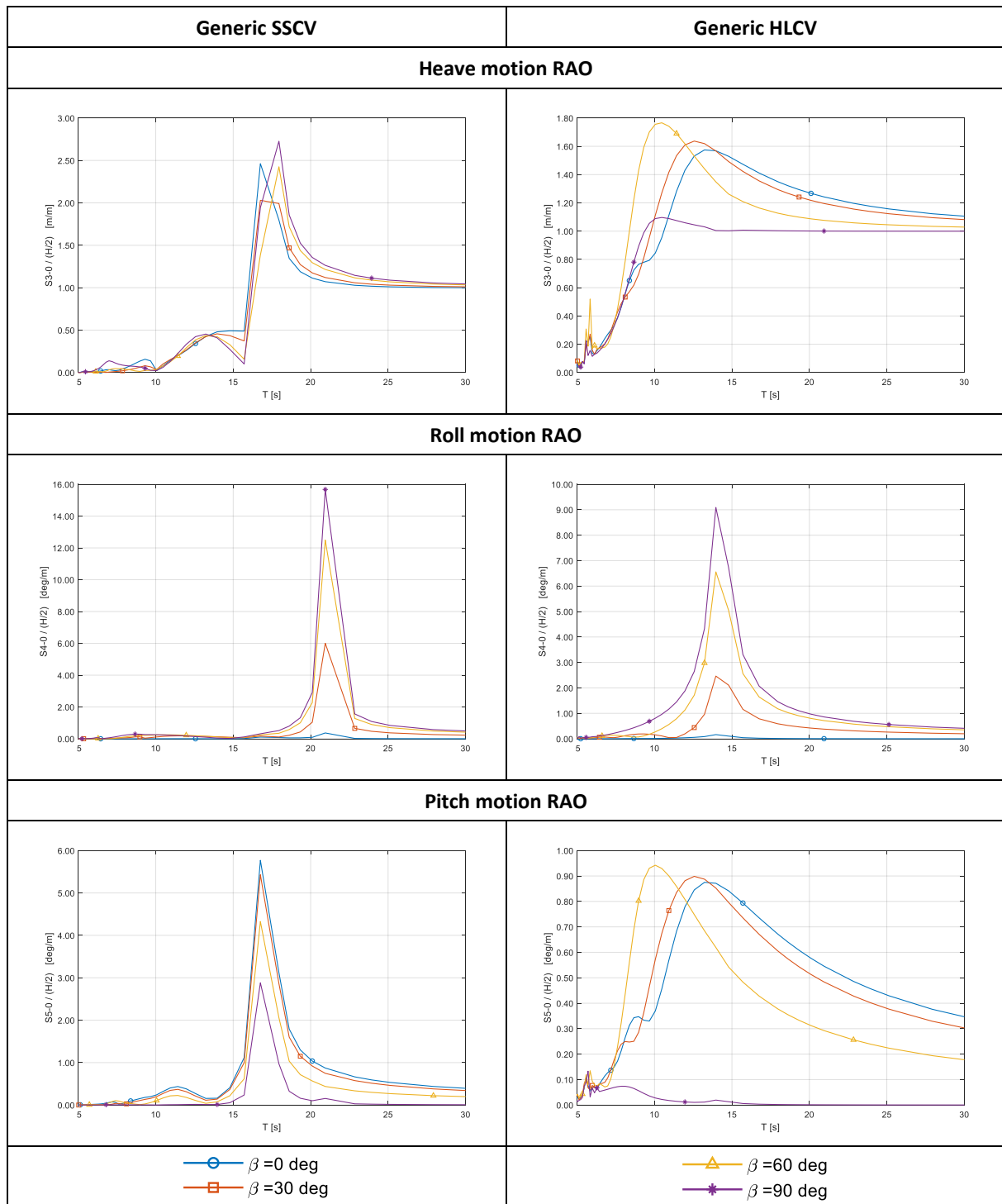


Figure 5-9: Motion RAOs of the generic crane vessels (vertical axis scales differently between generic SSCV and HLCV); Left: Generic SSCV, Right: Generic HLCV [Source: Ramboll].

The resulting natural periods of the rigid body modes are compiled in Table 5-4 and the RAOs for the heave, roll and pitch motion are displayed in Figure 5-9 for both generic vessels. The generic SSCV features larger natural periods compared to the generic HLCV due to the large inertia and reduced waterplane area. This is favourable regarding the wave induced motions of the crane vessel as the periods are above relevant wave excitation regions. Thus, the risk of excessive motions due to resonance with the wave periods is reduced for the SSCV.

Table 5-4: Natural periods of rigid body modes of generic crane vessels.

Rigid body mode	Unit	Generic SSCV	Generic HLCV
Heave	s	15.8	9.5
Roll	s	21.3	14.7
Pitch	s	15.9	9.4

Sensitivity of Additional Viscous Damping

As the additional viscous damping can significantly influence the motion behaviour and is generally subjected to large variations and uncertainties, the sensibility of the generic crane vessels regarding the considered linear damping coefficients has been investigated. In Figure 5-10, the calculated RAOs for the roll and pitch motion of the SSCV and the roll motion of the HLCV are displayed for 75%, 100% and 125% of the considered linear damping coefficients. Significant influence on the motion RAOs can only be observed around the natural periods. For the SSCV the influence of the damping on the motion behaviour is limited as the natural periods in roll and pitch are higher compared to the HLCV resulting in less influence by linear wave excitation on the SSCV. For the HLCV, however, the viscous damping can be critical for sea states that contain high wave energy around the natural roll period which is around 15 s. Additional linear damping in heave has also been considered for the SSCV but no sensitivity study was performed for this rigid body motion. Time-domain simulations with variations of the additional viscous damping are not performed for simplicity reasons.

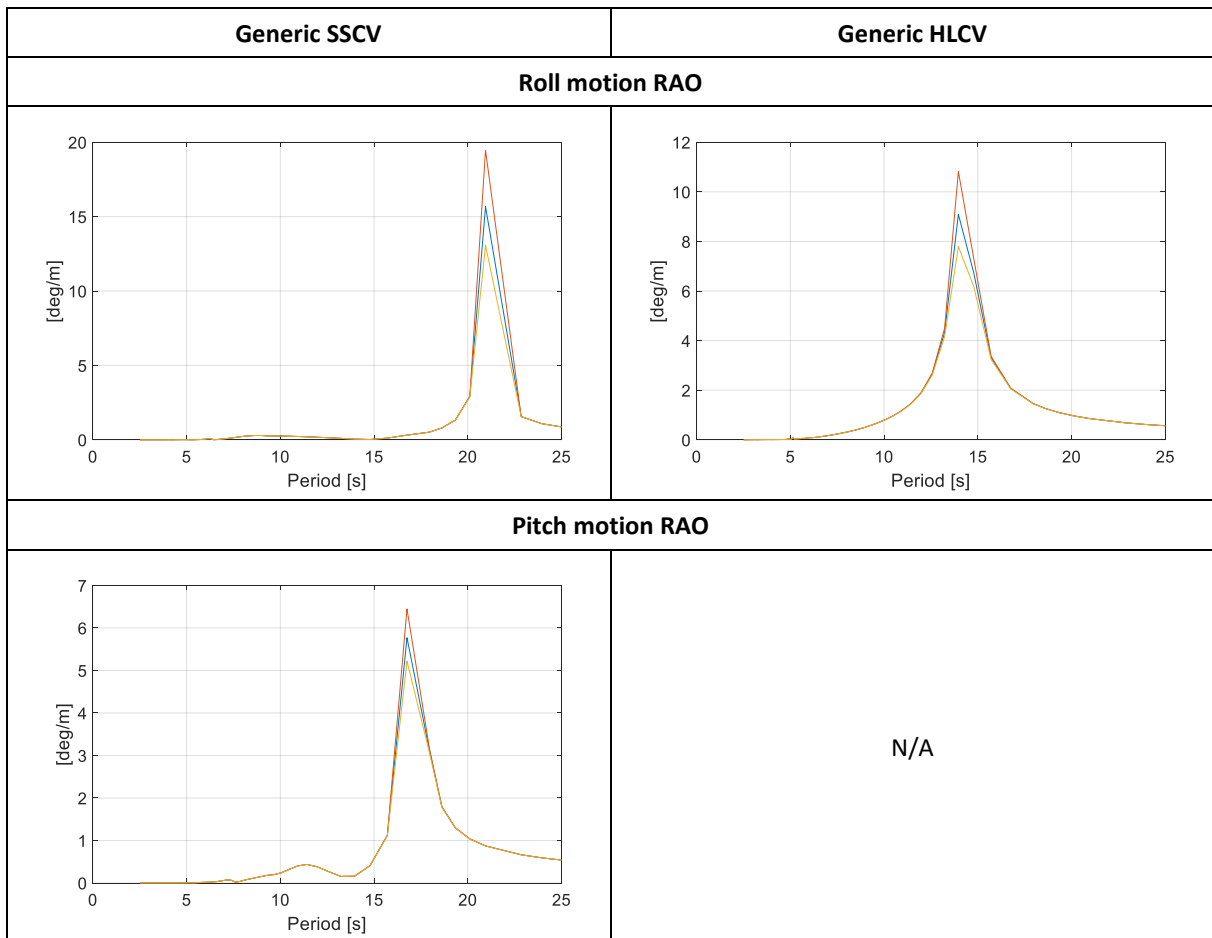


Figure 5-10: Influence of linear damping on motion RAOs; Left: Generic SSCV, Right: Generic HLCV [Source: Ramboll].

Lifting Height and Crane Outreach

The major component exchange imposes significant requirements on the operating crane vessel. Apart from motion limits and other requirements, the minimum lifting capacity, minimum lifting height and minimum crane outreach need to be taken into account. In general, these properties specific to a crane relate to one-another. The maximum lifting capacity decreases for increasing crane outreach when the crane boom is lowered. The maximum lifting height reduces with increased outreach of the crane as well. Thus, the following combinations are considered critical for the currently available crane vessels:

- high component mass (payload),
- large hub height and
- large horizontal distance from the outer edge of the floating substructure to the tower axis (e.g. the perpendicular distance from the outer column to the tower axis for the ActiveFloat concept as shown in Figure 5-11 on the right)

The calculation of the required lifting height and crane outreach is compiled in Table 5-5 and corresponds to both the SSCV and HLCV at site C. The hub height of ActiveFloat and Windcrete at site C are used as a boundary condition. Its difference is only marginal and can be compensated by adjusting the rigging. The same values for the minimum required lifting height of the crane h_{Crane} and the crane outreach R_{Crane} are used for ActiveFloat and Windcrete to avoid additional model variations of the SSCV and HLCV. Only one baseline model is generated for the SSCV and the HLCV. Hence, a higher distance between the crane vessel and the floating substructure d_{Margin} is resulting for Windcrete which relates to a higher safety margin when approaching the FOWT (see also Figure 5-13).

Table 5-5: Summary of required lifting height and crane outreach for major component exchange operation for ActiveFloat concept at site C using SSCV and HLCV.

Parameter	Symbol	Unit	ActiveFloat	Windcrete
Hub height above MSL	h_{Hub}	m	140.0	141.0
Height of lifting tool and rigging	$h_{Rigging}$	m	15.0	14.0
Height of hook	h_{Hook}	m	13.0	13.0
Minimum required lifting height of crane	h_{Crane}	m	168.0	168.0
Minimum distance between crane vessel and substructure to avoid collisions	d_{Margin}	m	10.0	31.0
Distance from outer column to tower axis for ActiveFloat substructure	d_{Sub}	m	30.7	N/A
Minimum required crane outreach (from outer edge of vessel hull to tower axis)	R_{Crane}	m	40.7	40.7

The symbols relating to Table 5-5 are shown schematically in Figure 5-11. In this report, only the combination of ActiveFloat and HLCV is displayed but the calculations are generally similar for the other vessel and substructure concept variations (ActiveFloat and SSCV, Windcrete and SSCV/HLCV). For the sake of this study, the properties of the crane(s), which is considered to be mounted on the generic crane vessels, have been adjusted to meet the requirements of Table 5-5 within reasonable ranges. However, currently no HLCV (and only a few SSCV) exists or is in service that would meet these requirements.

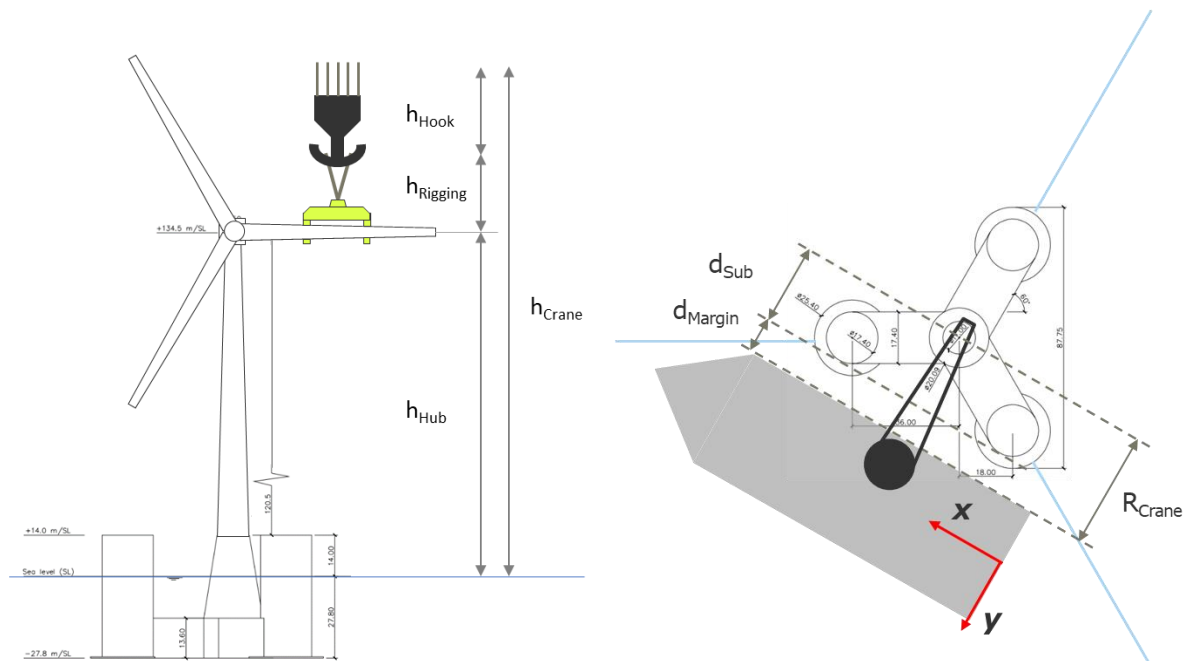


Figure 5-11: Left: Schematic view of the considered rigging setup with parameters defining the required lifting height of the crane. Blade lifting is displayed as exemplary major component exchange operation for the ActiveFloat substructure with maximum lifting height requirements that are assumed to be similar to requirements for exchange of the full nacelle.; Right: Schematic view of the required outreach of the crane for the HLCV. Lifting of the nacelle for the ActiveFloat concept is considered critical regarding crane outreach [Source: Ramboll with schematics from COREWIND].

Crane Reference Location

The lifting height and crane outreach is used to calculate the coordinates of the crane reference location with respect to the global coordinate system in OrcaFlex. In this study, the **crane reference location corresponds to the attachment point of the first auxiliary hook** as shown in Figure 5-12. The crane reference location is used to calculate the relative motion – i.e horizontal and vertical displacement, velocity and acceleration – between the crane vessel and nacelle of the FOWT.

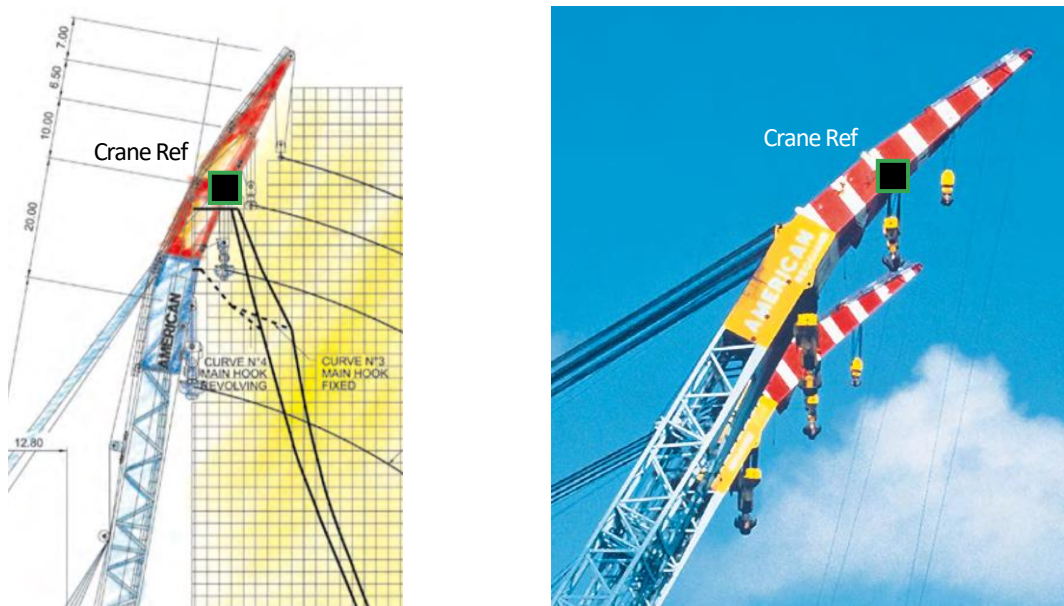


Figure 5-12: Illustration of the crane reference location “Crane Ref” at the attachment location of the first auxiliary hook highlighted as a square [Source: Modified from Saipem [14]].

5.1.4 OrcaFlex Model Setup and Load Cases

Parametric OrcaFlex models are setup for a baseline configuration of ActiveFloat or Windcrete and Generic SSCV or Generic HLCV resulting in four baseline models. The OrcaFlex models include the optimised mooring systems at site C developed and provided by WP2 (to be addressed in more detail in Deliverable D2.2). Figure 5-13 shows both substructure concepts with SSCV and also indicates the nacelle (Nacelle Ref) and crane reference location (Crane Ref), which are used for calculation of relative motions. The motion of Nacelle Ref and Crane Ref is tracked during the simulation to calculate and evaluate the relative horizontal and vertical displacement, velocity and acceleration. The **nacelle reference is located at the intersection of the horizontal plane (xy-plane) at hub height h_{Hub}** (see Table 5-5 and Figure 5-11) **and the tower centre axis (z-axis)** at the initial position (equilibrium). The crane reference is located directly above the nacelle reference and the distance between both points corresponds to height of the lifting tool and rigging $h_{Rigging}$ plus the height of the hook h_{Hook} (see Table 5-5 and Figure 5-11). Figure 5-13 also shows that the crane vessels are located sufficiently away from the floating substructure and mooring lines to avoid collisions. The safety margin for Windcrete is higher compared to ActiveFloat to avoid additional model variations of the SSCV and HLCV.

In the OrcaFlex simulation, the motion of the FOWT is calculated from the load RAOs while the motion of the crane vessel is based on the motion RAOs as described in Section 5.1.3. For ActiveFloat, the Centre of Gravity (COG) of the substructure body was corrected in the OrcaFlex model to compensate for the initial (pitch) offset originating from the rotor overhang and nacelle COG. It is assumed that the FOWT would be de-ballasted during an O&M operation using the active ballast system to a mean pitch of zero degree. A modification of the COG for the Windcrete substructure was not necessary.

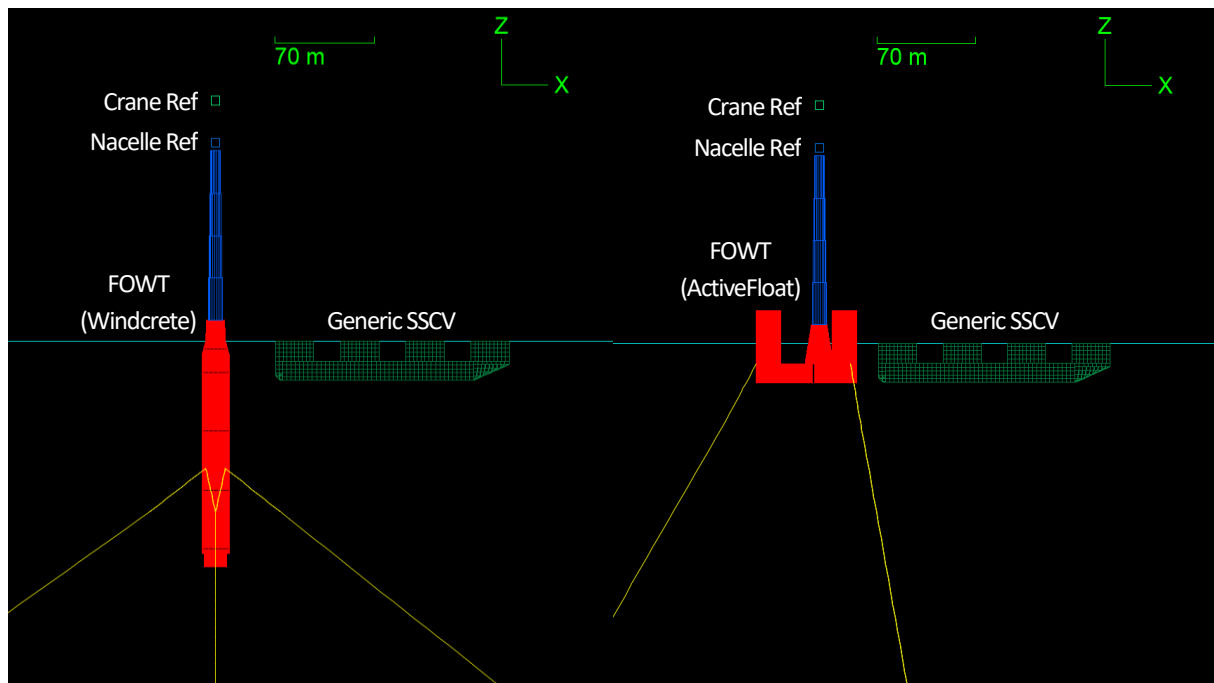


Figure 5-13: OrcaFlex model of Windcrete and Generic SSCV (left), and ActiveFloat and Generic SSCV (right) with nacelle (Nacelle Ref) and crane reference location (Crane Ref) at the initial position [Source: Ramboll].

The load cases considered in this simulation study for each combination of FOWT and crane vessel are summarised in Table 5-6. It shows the parameter variations for the orientation between the FOWT and crane vessel, the wave height, the wave period and the wave direction:

- **Orientation:** Different orientations between FOWT and crane vessel are simulated for the ActiveFloat concept depending on the crane vessel type and the considered wave directions. For Windcrete, only

one orientation is used because of the symmetric mooring system consisting of four mooring lines of same structural and geometric properties. For ActiveFloat, the mooring line at 270 deg in Figure 5-14 has a higher stiffness and different shape than the other two lines because the mooring system was optimised to the site C (Morro Bay, CA, USA) environmental conditions with dominant wind and wave direction.

- **Wave height:** The values of the wave height are chosen based on experience and common upper limits for O&M operations in offshore wind.
- **Wave period:** A screening study was performed for the wave period using a range of 0 s to 22 s with an increment of 4 s to evaluate a possible reduction of the parameter space before running the full set of load cases. It was found that a wave period of 2 s and 22 s is not needed in the full set. The vessel could be operated at 2 s, but the difference on the results from 4 s was reliable and therefore did not warrant specific simulation. A wave period of 22 s is close to the natural period of the roll rigid body mode of the SSCV (see Table 5-4) which would be excited, for example, for an orientation of 90 deg between FOWT and crane vessel and a wave direction of 180 deg.
- **Wave direction:** Waves coming from the north (not the magnetic north but a representative north based on the OrcaFlex model) correspond to a wave direction of zero degree, see the compass and block arrows in Figure 5-14 for ActiveFloat and Figure 5-15 for Windcrete.

In general, the symmetry of the FOWT and mooring system is used for simplifications of the Load Case Table (LCT). A full study would include wave directions from 0 to 360 deg and all orientations (90, 210 and 330 deg).

Table 5-6: Overview of parameter variations (load cases) considered for ActiveFloat and Windcrete with SSCV and HLCV for floating-to-floating major component exchange operation.

Parameter	Unit	ActiveFloat		Windcrete	
		Generic SSCV	Generic HLCV	Generic SSCV	Generic HLCV
Orientation between FOWT and crane vessel	deg	[90, 330]	[90, 210]	[90]	
Wave height	m	[0.5, 1.0, 1.5, 2.0, 2.5, 3.0]			
Wave period	s	[4, 6, 8, 10, 12, 14, 16, 18]			
Wave direction	deg	[90, 120, 150, 180, 210, 240, 270]	[0, 30, 60, 90, 120, 150, 180, 210, 240, 270, 300, 330]	[90, 120, 150, 180, 210, 240, 270]	[0, 30, 60, 90, 120, 150, 180, 210, 240, 270, 300, 330]
Number of load cases	-	672 = 2x6x8x7	1152 = 2x6x8x12	336 = 1x6x8x7	576 = 1x6x8x12

The full LCT entails 2736 simulations, each 1 hour of simulation time (not wall-clock time), with 1824 load cases for ActiveFloat and 912 load cases for Windcrete. Hence, the LCT can be reduced by taking advantage of the symmetry of the applied models for FOWT and mooring system. The large number of load cases required using a cloud computing setup to use CPU resources, RAM and disk storage efficiently. The results of the study are described in Section 5.1.5.

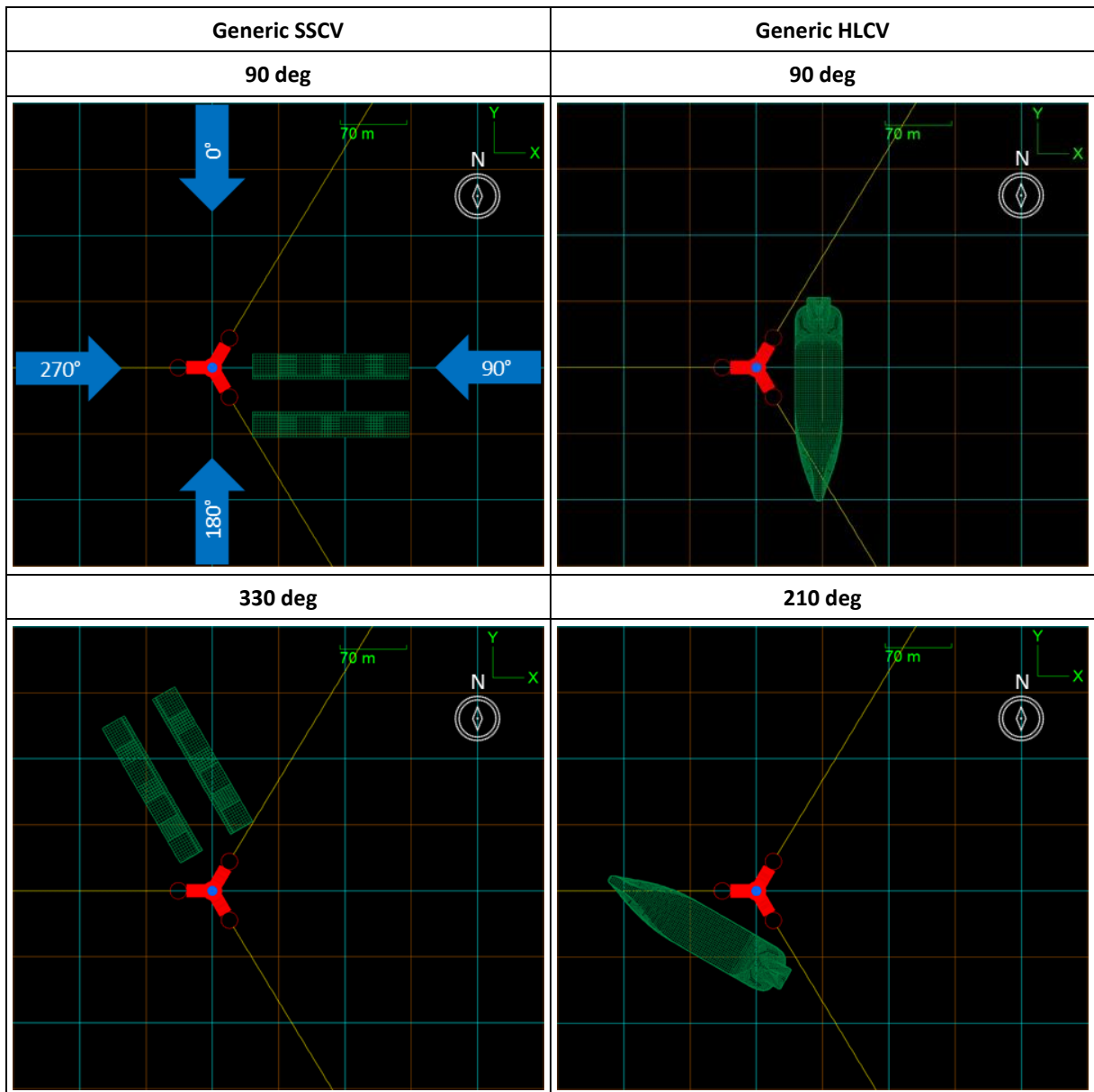


Figure 5-14: Orientations used for the OrcaFlex simulation study between FOWT using ActiveFloat concept and crane vessel. Blue arrows are indicating the wave direction; Left: Generic SSCV, Right: Generic HLCV [Source: Ramboll].

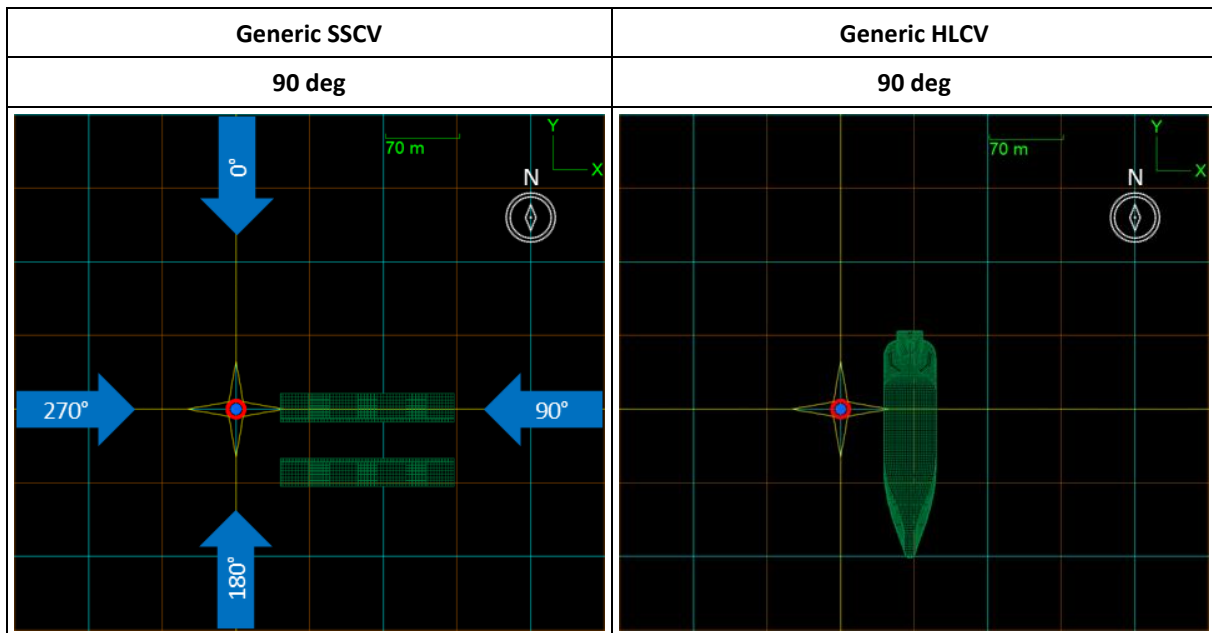


Figure 5-15: Orientations used for the OrcaFlex simulation study between FOWT using Windcrete concept and crane vessel. Blue arrows are indicating the wave direction; Left: Generic SSCV, Right: Generic HLCV [Source: Ramboll].

5.1.5 Operational Limits for Heavy Lift Maintenance

For each combination of floating substructure concept and crane vessel, the operational limits are assessed for different sea states as defined in Table 5-6. The maximum relative motions between the nacelle and the crane reference location occurring in each load case are obtained during post-processing of the results. Horizontal and vertical components for the maximum relative displacement, velocity and acceleration are presented in heatmaps for the maximum significant wave height H_s over the wave period T_p . A comparison of the data is given in the following subsections for the different combinations of floating substructure and crane vessel indicating general trends and peak values.

The data need to be further processed to be used as input for the O&M cost model described in Section 6. Operational limits for the different sea states need to be determined, meaning a maximum value of H_s for the T_p range to which the marine operation – i.e. the floating-to-floating major component exchange – can be conducted. However, it is challenging to define the acceptance criteria for each of the six motion components (horizontal and vertical displacement, velocity and acceleration). Considering a classical JUV based installation on bottom-fixed offshore wind substructures, both the vessel and the substructure are stable and the lifting operation is nearly acceleration free.

5.1.5.1 Discussion on Motion Compensation Technologies and Requirements

For floating-to-floating lifting operations some motion will be present and the question is to which extend it can either be allowed or if it needs to be compensated. For motion compensation in the context of this study (no subsea lifting operation), the following general considerations are relevant in principle.

1. Motion compensation could be achieved by either passive systems or active equipment.

Active systems can be advantageous in terms of certain motion criteria which could be reduced because the operation can be controlled more effectively using an actuator. However, active systems require real-time monitoring of the motion of the equipment or component itself (relevant for example for floating-to-fixed lifting, see Section 5.1.1) and, ideally, also tracking the movement of the target to which the lifting operation is to be performed (relevant for example for floating-to-floating lifting, see Section 5.1.1). This aspect of additional

sensor measurements and control make active systems more complex, also considering power supply by either batteries or power cable.

2. Either the motion of the floating substructure or the crane vessel could be compensated.

The motion of the floating substructure itself can be compensated in principle but it is unlikely due to additional, significant CAPEX and OPEX. For example, (active) propellers could be mounted to the floating substructure during the maintenance operation. Or additional vessels such as tugs could reduce the movement of the FOWT for a certain amount of time by pulling on taglines attached to a fairlead but involving high pulling forces.

SSCVs and HLCVs with large cranes usually are equipped with a dynamic DP system to compensate horizontal drift (longitudinal x- and lateral y- direction as in Figure 5-14) and keep the position of the vessel within a certain envelope depending on the sea state and DP capability. While a DP system can compensate for **surge**, **sway** and **yaw** motion of the crane vessel, it is not suited to limit **heave** motion. Rotational motion in roll and pitch affects the human comfort of workers onboard a vessel such as SOV or crane vessel. A propulsion and rudder system based on ducted azimuth thrusters, see Figure 5-16, cannot react as fast enough to compensate roll or pitch motion of a typical SOV or crane vessel. The azimuth propeller has to rotate completely to be able to generate reverse thrust, hence it cannot follow the roll period of the vessel.

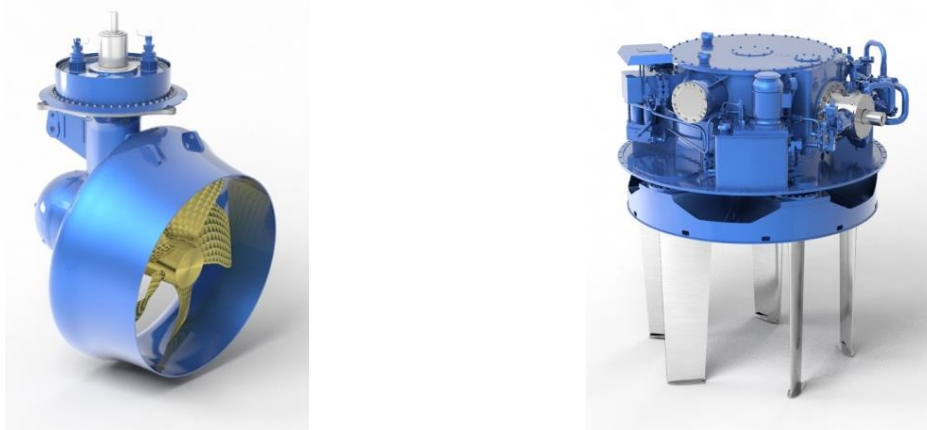


Figure 5-16: Illustration of ducted azimuth thruster (left) and Voith-Schneider propeller (right) [Source: Voith [15]].

However, a Voith-Schneider propeller (VSP), see Figure 5-16, can also provide active roll damping (or stabilisation) resulting in increased operational weather windows and working days, which benefits the OPEX. A VSP can adjust the amplitude and direction of the thrust force much faster than an azimuth propeller. The period from full to reverse thrust using a VSP is smaller than the natural roll period of the SOV or crane vessel. Hence, it can respond much more quickly to the vessel motion and can follow external forces more efficiently. For a large HLCV (monohull), a reduction of the roll motion can be achieved using VSPs, but the level of compensation decreases for larger vessels with higher length, breadth and displacement. For SSCV, roll stabilisation would involve a very large torque to be generated and it is still to be evaluated if VSPs would be strong enough and to what extent roll stability could be achieved, especially for floating-to-floating lifting operations. However, natural periods in roll increase for large vessels, see the comparison of generic SSCV and generic HLCV in Table 5-4, so that the roll motion is generally less excited for large vessels based on the metocean conditions. As the VSP reacts faster than an azimuth propeller and has a smaller footprint (more accurate manoeuvrability), relative motions in surge, sway and yaw potentially decrease if a SSCV would be upgraded with VSPs as DP system, but this would still need to be evaluated in detail. **Pitch** stabilisation for vessels follows the same principle as roll stabilisation, only the lever arm is much larger in pitch (higher length than breadth for monohull vessels). The

resulting torque during the pitch motion would be very large and cannot be compensated by propellers (either azimuth propeller or VSP).

In Summary for all six rigid body modes, heave and pitch motion of a vessel cannot be compensated efficiently. Surge, sway and yaw motion can be reduced using a DP system. Roll stabilisation can be achieved using active systems such as a VSP.

3. Besides compensating the motion of the full system such as the crane vessel, only the motion of a subsystem could be compensated to decouple the movement of the payload from the vessel motion.

Different technologies are on the market for active heave compensation during lifting operations. In O&G, standard subsea cranes use heave compensated winches to mitigate vertical movement of the vessel (in-water heave compensation). When the payload is fully submerged the damping from the surrounding water increases compared to when it is hanging on the crane hook above the water surface. In offshore wind, walk-to-work vessels use active motion compensated gangway systems for crew transfer from the vessel to an offshore asset. When loads need to be transferred between vessels (floating-to-floating) or between vessel and fixed structure (floating-to-fixed) motion compensated offshore cranes can be applied for accurate positioning. Cranes equipped with a gimbal foundation in the crane pedestal, telescoping crane boom and heave compensated winch can compensate for vessel motion in heave, roll and pitch, see for example Figure 5-17. However, available offshore crane capacity involving motion compensation is limit regarding the lifting height, the crane outreach and the maximum load, so that it cannot be applied in the context of this study, refer to requirements in Table 5-5 and Figure 5-11. Hence, the cranes mounted to the generic HLCV and SSCV models in Section 5.1.3 are considered as fixed to the vessel without the ability for motion compensation of the crane system itself. To meet the requirements for lifting height and load of this study using a three-dimensional motion compensated crane, the power demand and the resulting structural loads would be much higher compared to a typical use case for a motion compensated offshore crane for SOVs.

If the offshore crane itself cannot be equipped with a motion compensation system, auxiliary equipment such as passive or active heave compensators can be used during the offshore lifting operation. The additional tool is installed between the crane hook and the rigging and payload as illustrated in Figure 5-17, and different types of units are available on the market based on the specific purpose of the marine operation. Using an in-air heave compensation tool standard heavy lift cranes can be retrofitted and turned into an Active Heave Compensation (AHC) crane. The (crane) hook-based heave compensation can be a flexible and cost effective solution for large offshore cranes which do not offer crane-based heave compensation itself. Passive heave compensators have been used, for example, in offshore wind when installing a transition piece to compensate for heave movement of the vessel after the load is landed. Technologies are also available to prevent re-contact after the load is lifted. For active heave compensators, power supply is either delivered using power cables or batteries. However, active heave compensators can only control and compensate for vertical movement based on the tools specifications for the maximum stroke length – i.e. defining the maximum amplitude of the vertical displacement – and maximum speed – i.e. defining the (maximum) vertical velocity limit. For floating-to-floating lifting operations, real-time monitoring of the motion of the crane vessel and the FOWT reference location such as the nacelle is required to measure relative motions and apply control strategies. Hence, relative horizontal movement in surge, sway and yaw would need to be compensated using an efficient DP system of the vessel itself, while relative roll and pitch motion would remain non-compensated.



Figure 5-17: Top: SOV (vessel: Seaway Moxie) equipped with offshore crane allowing active compensation of the vessel's motion in heave, roll and pitch [Source: MacGregor]; Bottom: Illustration of auxiliary equipment for heave compensation positioned between crane hook and payload [Source: Cranemaster].

Approach Used for Consideration of Motion Compensation

Based on the above discussion on motion compensation requirements and technologies the following approach is used in this study to derive the operational limits for the floating-to-floating heavy lift maintenance scenario. Active motion compensation of the movement of the crane vessel (using a DP system), the FOWT or the offshore crane itself is not considered in the OrcaFlex model directly. Also, no auxiliary equipment such as an active heave compensator between crane hook and payload is modelled in the OrcaFlex time-domain simulation. **However, active heave compensation is included in the study during post-processing of the relative motions between FOWT (nacelle reference point) and crane vessel (crane reference point) by assuming limits for the maximum vertical velocity of an exemplary active heave compensator as auxiliary tool operated between crane hook and payload.** A value of $w_{AHC,max} = 1.5$ m/s for the relative vertical velocity limit is considered (“**medium**” scenario), which can be interpreted as common value based on industry feedback. In order to evaluate the sensitivity of the maximum relative vertical velocity on the operational limits of the heavy lift maintenance scenario, two additional variations are evaluated, in particular the values of $w_{AHC,max} = 1.0$ m/s (“**low**” scenario) and $w_{AHC,max} = 2.5$ m/s (“**high**” scenario). As a result six variations of operational weather limits are derived per floating substructure concept (three for the generic SSCV and three for the generic HLCV). The influence of the motion acceptance criteria on the OPEX is discussed and quantified in Section 6.1.2.2. Other motion limits, such as for the relative vertical displacement defined through the stroke capacity of the tool, or the relative vertical acceleration are not considered in addition because common values have not been found to be driving the operational limits.

In summary, although six H_s-T_p scatter diagrams are calculated for the relative horizontal and vertical displacement, velocity and acceleration for each combination of FOWT and crane vessel, the influence on the operational limits and OPEX is only considered through limits for the relative vertical velocity which can be compensated. An H_s-T_p combination (sea state) with a maximum relative vertical velocity below the defined compensation limit is considered to be operable (full heave compensation possible) and marked with a green

“1”, whereas non-operable sea states are indicated with a red “0”. As the parameter variation for wave period and wave height was limited (see Table 5-6), some assumptions are made for the OPEX model beyond available data points:

- $H_s > 3$ (for all T_p values): Non-operable sea state indicated with a red “0”
- $T_p < 4$ (for all H_s values): Result of sea state for $T_p = 4$ is copied
- $T_p > 18$ (for all H_s values): Result of sea state for $T_p = 18$ is copied

Further Considerations: Sea Transport, Mating Process, RNA Pre-Assembly

For the sea transport of WTG components, for example the rotor blade, nacelle or tower, acceleration limits are usually available. However, they cannot be used one to one for in the context of this study as the limits are usually not relevant for the structural integrity of the component itself, but indicate maximum motions up to which safe transport can be carried out considering the mounting in the transport frame.

Furthermore, guiding pins at the interfaces between components, for example at the blade root, hub, yaw bearing of the nacelle or tower sections facilitate the mating operation (for example shown in [16]). For floating-to-floating lifts, especially the mating process would need to be reviewed in detail as also the required forces and bending moments during the mating operation are very relevant from a practical perspective besides motion limits. Fast connectors, such as slip joint connections between the tower and nacelle, tower and transition piece, or even rotor blade and nacelle, have potential for reducing the required weather windows (timewise) during installation works. However, the technology is considered still in prototype status for bottom-fixed offshore wind⁴ and needs further qualification, maturity and large scale application for complete offshore wind farms until it can be transferred easily to floating wind.

Another strategy to reduce the required number of floating-to-floating lifts during offshore heavy lift maintenance (or installation works) is already presented in COREWIND deliverable D4.1 [12]. The RNA could be pre-assembled on the deck of a crane vessel using a dummy tower. This procedure would be considered similar to a fixed-to-fixed lifting operation as the crane and dummy tower share the same reference system. Weather windows would still be relevant for the lifting operations on deck as the crane vessel is moving and also wind speed can be a limiting factor. However, it is assumed that higher limits for the motion of the crane vessel itself would apply for pre-assembly of the RNA on deck which would allow better operational performance in principle. Floating-to-floating lifts would only be necessary for installation of the tower on the floating substructure and the pre-assembled RNA on the tower. This approach, which is also referred to as feeder concept, would need to be evaluated on a project-specific basis to quantify potential cost effectiveness versus a tow-in/tow-to-port scenario.

5.1.5.2 ActiveFloat and Generic SSCV and HLCV

Results of the relative motions between ActiveFloat and generic SSCV and HLCV are shown in Figure 5-18. The values included in the H_s - T_p diagrams represent the maximum values from all simulated combinations of orientation between FOWT and crane vessel and wave direction according to Table 5-6.

⁴ Reference projects: Slip Joint foundation at the Borssele Wind Farm Site V installed by Van Oord in April 2020 <https://www.vanoord.com/en/updates/van-oord-installs-worlds-first-submerged-slip-joint-successfully/>; Slip Joint Offshore Research project (SJOR) finished with offshore testing in September 2018 <https://grow-offshorewind.nl/project/sjor>

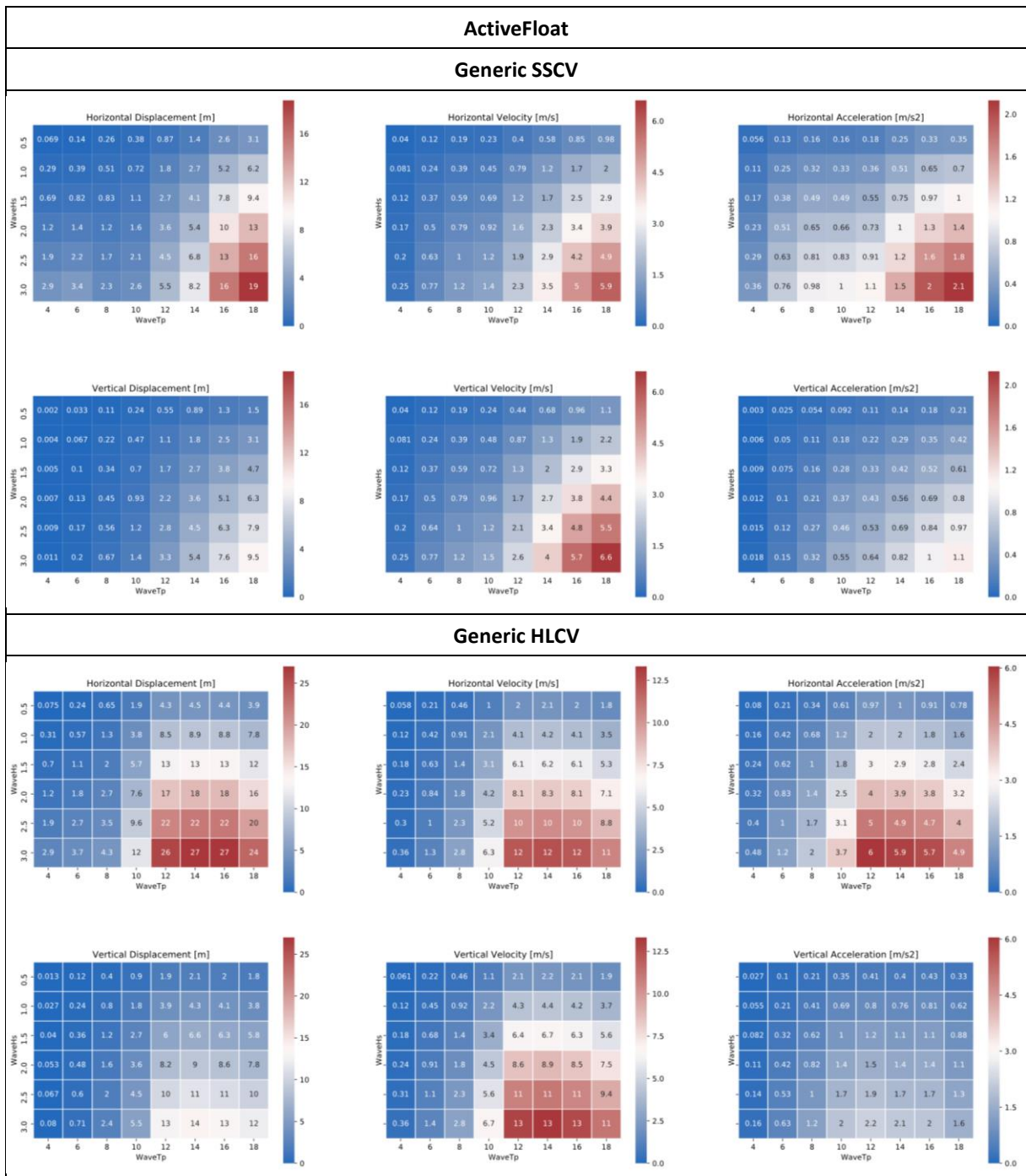


Figure 5-18: Maximum relative motions (first row: horizontal component, second row: vertical component, from left to right: displacement, velocity, acceleration) for floating-to-floating major component exchange of ActiveFloat; Top: Generic SSCV, Bottom: Generic HLCV [Source: Ramboll].

The motion of the crane vessel depends on the wave direction, especially seen in this study for the generic HLCV whose natural period in roll is smaller than for the generic SSCV, see Table 5-4, and lies within the linear wave excitation region. Hence, smaller relative motions between FOWT and crane vessel than shown in Figure 5-18 can be observed depended on the orientation and wave direction. But it was decided to use the maximum values as conservative assumption, also because it is not possible to account for different operational limits in the OPEX tool in Section 6 which depend on the wave direction. In practice, besides wave period and significant wave height of a sea state, also the wave direction would need to be considered to choose the orientation between

FOWT and crane vessel for the operation. A spar floating substructure concept offers more variety for the approach considering the required crane outreach than a semi-submersible with larger column spacing, compare Figure 5-14 and Figure 5-15. Hence, in a future study the most optimal orientation between FOWT and crane vessel could be used to minimise the relative motions and minimise the level of conservatism, for example the longitudinal x-axis of the generic HLCV would be aligned with the wave direction (90 deg orientation and 180 deg wave direction for the spar in Figure 5-15) to avoid excitation of roll motion. Some variation of the operational limits for the heavy lift maintenance operation is analysed and evaluated in Section 6.1.2.2.

In general, higher maximum relative motions can be observed in Figure 5-18 for the generic HLCV compared to the generic SSCV. For the relative vertical velocity which is used to derive the operational limits the values increase by a factor of two to four using the HLCV. As discussed in the previous paragraph lower motions can be observed depending on the orientation and wave direction, for example in Figure 5-19 for ActiveFloat and HLCV an orientation of 210 deg results in significantly lower maximum relative vertical velocities compared to the other possible orientation of 90 deg, see also Figure 5-14. For other wave directions, for example 240 deg, the relative motions of both orientations are in the same level of magnitude. That wave direction dependency is shown in Figure 5-20 using a wave rose plot of the maximum relative vertical velocities for different orientations.

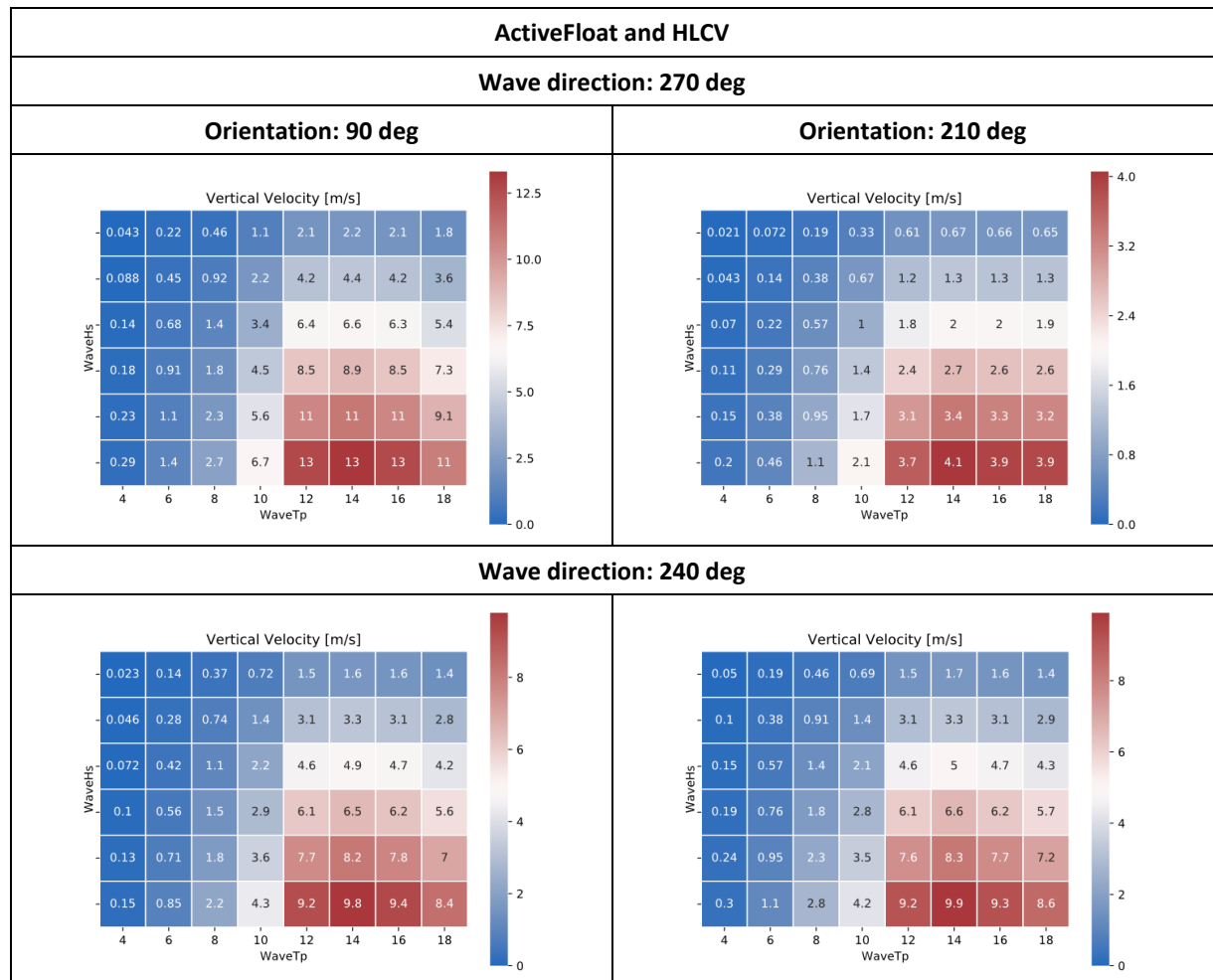


Figure 5-19: Maximum relative motions for floating-to-floating major component exchange of ActiveFloat and generic HLCV for different wave directions (top: 270 deg, bottom: 240 deg) and different orientations (left: 90 deg, right: 210 deg) [Source: RAMBOLL].

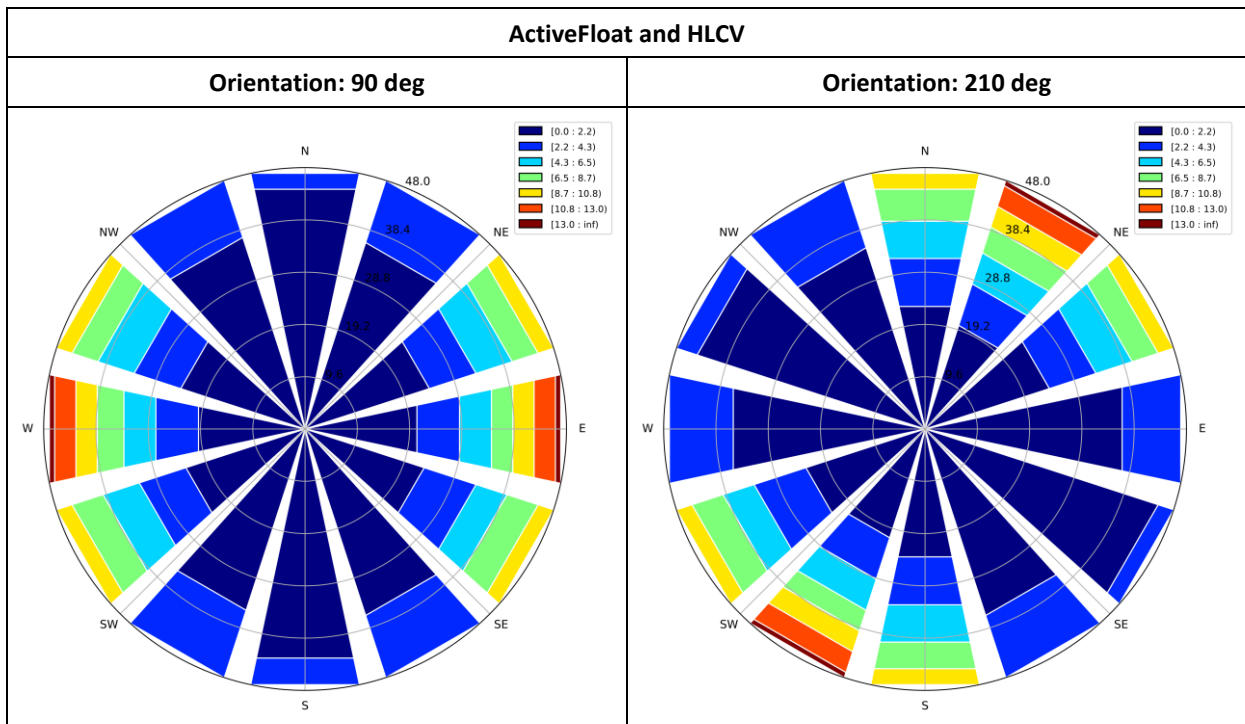


Figure 5-20: Wave rose for maximum relative vertical velocity for floating-to-floating major component exchange of ActiveFloat and generic HLCV for different orientations (left: 90 deg, right: 210 deg) [Source: RAMBOLL].

Limits of the maximum relative vertical velocity are defined as described in Section 5.1.5.1 to derive the operational limits in Figure 5-21 providing low, medium and high motion limit scenarios for the OPEX study. The generic SSCV generally provides better weather limits than the generic HLCV (assuming the conservative assumption of maximum values over all orientations and wave directions).

ActiveFloat													
Generic SSCV							Generic HLCV						
Low motion limit: Relative vertical velocity of 1.0 m/s													
VelZ [m/s]	1.0						VelZ [m/s]	1.0					
Tp/WaveHs	0.5	1	1.5	2	2.5	3	Tp/WaveHs	0.5	1	1.5	2	2.5	3
4	1	1	1	1	1	1	4	1	1	1	1	1	1
6	1	1	1	1	1	1	6	1	1	1	1	0	0
8	1	1	1	1	1	0	8	1	1	0	0	0	0
10	1	1	1	1	0	0	10	0	0	0	0	0	0
12	1	1	0	0	0	0	12	0	0	0	0	0	0
14	1	0	0	0	0	0	14	0	0	0	0	0	0
16	1	0	0	0	0	0	16	0	0	0	0	0	0
18	0	0	0	0	0	0	18	0	0	0	0	0	0
Medium motion limit: Relative vertical velocity of 1.5 m/s													
VelZ [m/s]	1.5						VelZ [m/s]	1.5					
Tp/WaveHs	0.5	1	1.5	2	2.5	3	Tp/WaveHs	0.5	1	1.5	2	2.5	3
4	1	1	1	1	1	1	4	1	1	1	1	1	1
6	1	1	1	1	1	1	6	1	1	1	1	1	1
8	1	1	1	1	1	1	8	1	1	1	0	0	0
10	1	1	1	1	1	1	10	1	0	0	0	0	0
12	1	1	1	0	0	0	12	0	0	0	0	0	0
14	1	1	0	0	0	0	14	0	0	0	0	0	0
16	1	0	0	0	0	0	16	0	0	0	0	0	0
18	1	0	0	0	0	0	18	0	0	0	0	0	0
High motion limit: Relative vertical velocity of 2.5 m/s													
VelZ [m/s]	2.5						VelZ [m/s]	2.5					
Tp/WaveHs	0.5	1	1.5	2	2.5	3	Tp/WaveHs	0.5	1	1.5	2	2.5	3
4	1	1	1	1	1	1	4	1	1	1	1	1	1
6	1	1	1	1	1	1	6	1	1	1	1	1	1
8	1	1	1	1	1	1	8	1	1	1	1	1	0
10	1	1	1	1	1	1	10	1	1	0	0	0	0
12	1	1	1	1	1	0	12	1	0	0	0	0	0
14	1	1	1	0	0	0	14	1	0	0	0	0	0
16	1	1	0	0	0	0	16	1	0	0	0	0	0
18	1	1	0	0	0	0	18	1	0	0	0	0	0

Figure 5-21: Operational limits for ActiveFloat for different motion acceptance criteria; Green cell with “1”: Maximum relative motion of sea state (H_s - T_p combination) below acceptance criterium, Red cell with “0”: Maximum relative motion of sea state (H_s - T_p combination) equal to or above acceptance criterium; Left: Generic SSCV, Right: Generic HLCV [Source: Ramboll].

5.1.5.3 Windcrete and Generic SSCV and HLCV

Results of the relative motions between Windcrete and generic SSCV and HLCV are shown in Figure 5-. Similarly as for ActiveFloat, the generic HLCV shows higher relative motions than the SSCV. The dependency of the results on the wave direction also applies. The maximum relative vertical velocities compare well between the two floating substructure concepts with only minor differences. The influence of the different crane vessel is much more pronounced.

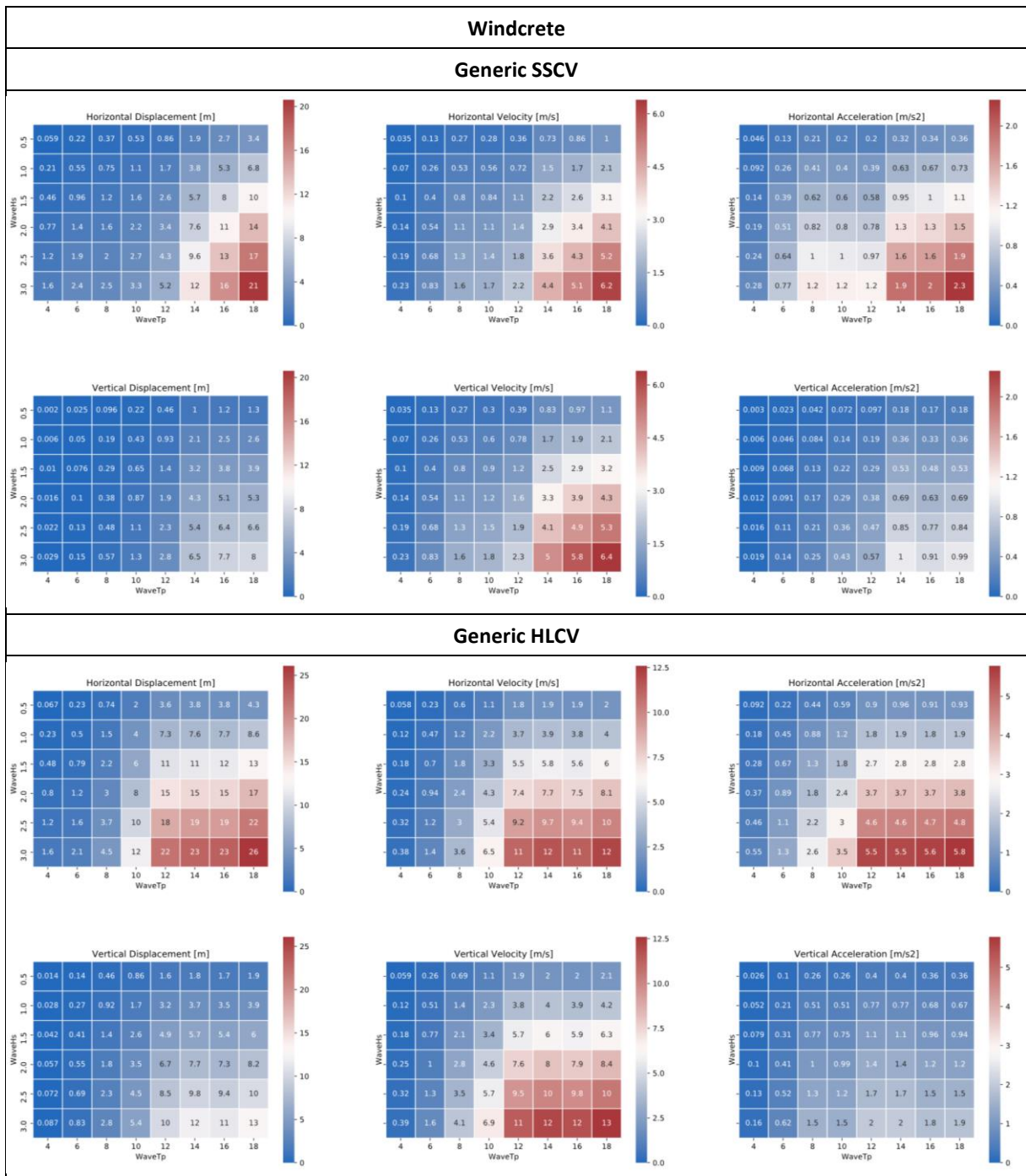


Figure 5-22: Maximum relative motions (first row: horizontal component, second row: vertical component, from left to right: displacement, velocity, acceleration) for floating-to-floating major component exchange of Windcrete; Top: Generic SSCV, Bottom: Generic HLCV [Source: Ramboll].

Limits of the maximum relative vertical velocity are defined as described in Section 5.1.5.1 to derive the operational limits in Figure 5-21 providing low, medium and high motion limit scenarios for the OPEX study. Also, the generic SSCV generally provides better weather limits than the generic HLCV (assuming the conservative assumption of maximum values over all orientations and wave directions).

Windcrete															
Generic SSCV							Generic HLCV								
Low motion limit: Relative vertical velocity of 1.0 m/s															
VelZ [m/s]	1.0							VelZ [m/s]	1.0						
Tp/WaveHs	0.5	1	1.5	2	2.5	3	Tp/WaveHs	0.5	1	1.5	2	2.5	3		
4	1	1	1	1	1	1	4	1	1	1	1	1	1		
6	1	1	1	1	1	1	6	1	1	1	0	0	0		
8	1	1	1	0	0	0	8	1	0	0	0	0	0		
10	1	1	1	0	0	0	10	0	0	0	0	0	0		
12	1	1	0	0	0	0	12	0	0	0	0	0	0		
14	1	0	0	0	0	0	14	0	0	0	0	0	0		
16	1	0	0	0	0	0	16	0	0	0	0	0	0		
18	0	0	0	0	0	0	18	0	0	0	0	0	0		
Medium motion limit: Relative vertical velocity of 1.5 m/s															
VelZ [m/s]	1.5							VelZ [m/s]	1.5						
Tp/WaveHs	0.5	1	1.5	2	2.5	3	Tp/WaveHs	0.5	1	1.5	2	2.5	3		
4	1	1	1	1	1	1	4	1	1	1	1	1	1		
6	1	1	1	1	1	1	6	1	1	1	1	0	0		
8	1	1	1	1	1	0	8	1	1	0	0	0	0		
10	1	1	1	1	1	0	10	1	0	0	0	0	0		
12	1	1	1	0	0	0	12	0	0	0	0	0	0		
14	1	0	0	0	0	0	14	0	0	0	0	0	0		
16	1	0	0	0	0	0	16	0	0	0	0	0	0		
18	1	0	0	0	0	0	18	0	0	0	0	0	0		
High motion limit: Relative vertical velocity of 2.5 m/s															
VelZ [m/s]	2.5							VelZ [m/s]	2.5						
Tp/WaveHs	0.5	1	1.5	2	2.5	3	Tp/WaveHs	0.5	1	1.5	2	2.5	3		
4	1	1	1	1	1	1	4	1	1	1	1	1	1		
6	1	1	1	1	1	1	6	1	1	1	1	1	1		
8	1	1	1	1	1	1	8	1	1	1	0	0	0		
10	1	1	1	1	1	1	10	1	1	0	0	0	0		
12	1	1	1	1	1	1	12	1	0	0	0	0	0		
14	1	1	1	0	0	0	14	1	0	0	0	0	0		
16	1	1	0	0	0	0	16	1	0	0	0	0	0		
18	1	1	0	0	0	0	18	1	0	0	0	0	0		

Figure 5-23: Operational limits for Windcrete for different motion acceptance criteria; Green cell with “1”: Maximum relative motion of sea state (H_s - T_p combination) below acceptance criterium, Red cell with “0”: Maximum relative motion of sea state (H_s - T_p combination) equal to or above acceptance criterium; Left: Generic SSCV, Right: Generic HLCV [Source: Ramboll].

5.2 Tow-In Operation

The seakeeping analyses are described in the following sections in order to identify the weather conditions that allow the towing to harbour or sheltered waters of the FOWT for heavy maintenance operations. The tow-in maintenance scenario requires a complete disconnection of the floaters from cable and mooring. The resulting operational limits are used as input for the O&M cost model representing an alternative scenario for major component exchange as described in Section 5.1 for the floating-to-floating heavy lifting operation. It is assumed that the main limiting criteria for the towing operation is the structural strength of the WTG whose limits are gathered in 5.2.1.

The seakeeping analyses for the tow-in have been carried out in the following steps:

1. **Sensitivity analyses:** Given the amount of parameters involved in the analysis (wind speed, wave height, wave period, wind heading, wave heading, wind-wave misalignment, tow speed) it was deemed necessary to perform a sensitivity analysis to each of the manoeuvre parameters.
2. **Preliminary analyses for weather conditions.** This phase consists in a wide range of analyses with all parameters accounted for. These simulations swept a lot of cases, this is performed in **frequency domain** in order to identify a general frame for the weather conditions.
3. **Detailed analyses for weather conditions.** This last phase consists in a detailed analysis of a final set of cases, in which all parameters are accounted for in a **time domain** analysis.
4. **Tow line tension demand:** Some results of the line tension registered in the simulations are reported in order to have a sensitivity for what size and number of tugs are required for the manoeuvre.

The analyses are performed for both floaters of COREWIND project, Windcrete and ActiveFloat using designs for site C and expressing the results in terms of the metocean data for that site found in the design basis [11].

5.2.1 Acceptance Criteria for Tow-In Operation

The motions and accelerations limitations are shown in the Table 5-7. The acceptance criteria are important because they impact available weather limits for towing operations. The limits are based on conservative assumptions and relate to wind turbine component requirements. It is important to remark that the yaw system is considered active. This allows to orientate the rotor towards the incoming wind and reducing the wind forces on the RNA substantially.

Table 5-7: Motion and acceleration criteria during towing.

Motion Criteria During Towing	
Maximum nacelle acceleration	0.6 m/s ² (0.06 g)
Maximum pitch / roll angle	[-2 deg, +2 deg]

5.2.2 Methodology and Model Description

Models have been defined for each of the floaters by modelling the external geometry of the elements (hull geometry) to be analysed, and defining their mass and hydrodynamic properties.

ANSYS AQWA is the hydrodynamic software selected for performing the analyses. ANSYS AQWA is a commercial software that allows to solve the hydrodynamic problem through diffraction and 3D radiation.

5.2.2.1 Windcrete

The Windcrete model has been built based on the information found in design document in [13]. The main change is to adapt the floater draft from the operational draft to the towing draft. It has been agreed with the designer of Windcrete – UPC - that no ballast modification is to be done and therefore, the mooring hang-off

causes the draft difference between the operational and towing draft because the mooring lines are disconnected for towing.

Floater Geometry

Windcrete is a spar platform. The geometry consists of a semisphere, a cylinder and two truncated cones. The main body has a diameter of 19.40 m. Tower bottom diameter is 14.0 meters and top 6.5 meters. The thickness varies from 0.50 m to 0.28 m. The hub height is set to 141 m (in operating conditions). Figure 5-24 shows the main dimensions of the structure. Note that the configuration shown is operating, i.e. the draft is to be changed for the transport analyses.

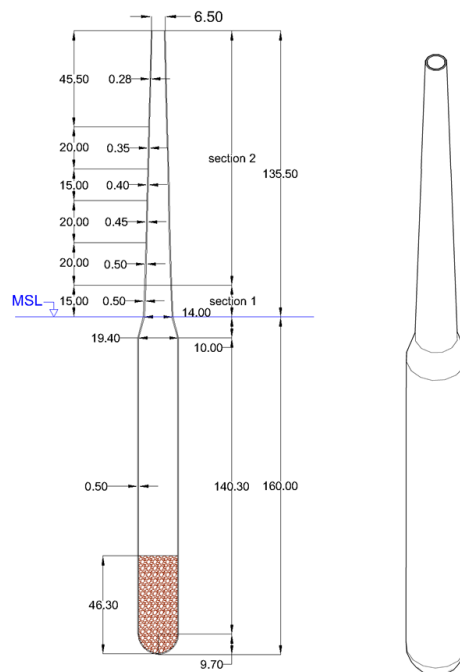


Figure 5-24: Schematic showing geometry and dimensions of Windcrete with Units in meters [Source: UPC].

Mass Properties

The following mass properties in Table 5-8 are used as input in the model.

Table 5-8: Inertias and centre of gravity for Windcrete.

Item	Weight [t]	COG _x [m]	COG _y [m]	COG _z [m]	I _{xx} [tm ²]	I _{yy} [tm ²]	I _{zz} [tm ²]
RNA	1,016.5	7.023	0.000	299.000	5.71E+07	5.72E+07	6.85E+04
Tower	3,291.0	0.000	0.000	223.000	8.91E+07	8.91E+07	8.78E+04
Structure and solid ballast	41,240.0	0.000	0.000	43.000	8.13E+07	8.13E+07	2.23E+06
Water Ballast	0.0	0.000	0.000	6.000	0.00E+00	0.00E+00	0.00E+00
Total	45,547.5	0.000	0.000	62.000	2.27E+08	2.28E+08	2.39E+06
					70.67	70.68	7.24
					r _{xx} [m]	r _{yy} [m]	r _{zz} [m]

Note that the above location of the centre of gravity to the platform bottom and inertias refer to global centre of gravity. The Z values in the table can be changed to the reference axis specified in the document D1.2 Design Basis by subtracting 160 m to these values. Accounting for the above mass and geometry, the draft is recalculated. The towing draft used is 154.30 m, the operational draft is 160.00 m. The RNA has an eccentricity that produces a heeling angle of 0.503 deg towards the rotor direction. This static pitch will be accounted for in all the Windcrete analyses.

Modelling of Wind Forces With Drag Coefficients

Wind forces are modelled through the wind force coefficients which represents the constant part of the force equation:

$$F_i = \frac{1}{2} \cdot \rho \cdot A \cdot C_d \cdot v_{wind}^2$$

with:

- ρ : air density (1.22 kg/m³)
- A: projected area faced to wind direction
- C_d : aerodynamic drag coefficient
- v_{wind} : wind speed at appropriate elevation

The wind profile has been produced following the power law as indicated in IEC 61400-3-1 with an alpha factor of 0.14 (NTM).

$$v_{wind} = \left(\frac{z}{z_{ref}} \right)^{0.14} v_{wind_zref}$$

with:

- z_{ref} : wind speed height reference (hub height)
- z: elevation of the center of projected area.

The drag coefficients are summarized in Table 5-11 there are input to the centre of gravity of the platform as follows:

$$Coef_{F_i} = \frac{1}{2} \cdot \rho \cdot A \cdot C_d$$

$$Coef_{M_i} = Coef_{F_i} \cdot (z_{cop} - z_{cog})$$

Wind Drag Force Coefficients of RNA

Aerodynamic drag coefficient for the parked RNA have been obtained from the wind speed and forces provided by COREWIND partners, see Table 5-9. The OpenFAST model of the IEA 15 MW offshore reference wind turbine was used.

Table 5-9: Wind forces on parked turbine.

	Wind Speed [m/s]	Force [kN]
COREWIND partner 1	20.0	20.2
COREWIND partner 2	28.4	39.0

It was confirmed that above forces only account for the blade aerodynamics. In order to account for the exposed area and drag forces on the nacelle the following geometry in Figure 5-25 was considered.

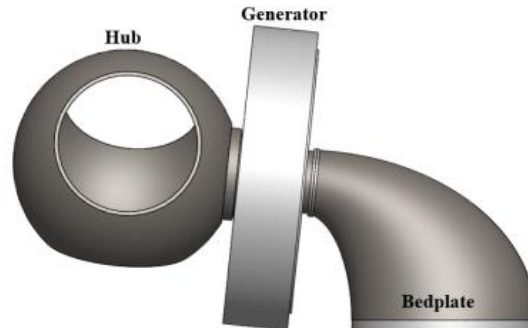


Figure 5-25: Nacelle assembly of IEA-15-240-RWT [Source: [17]].

The generator is assumed with a 10 meter diameter and a C_d of 0.80. The following equivalent, combined C_d is obtained in Table 5-10 when both components are considered:

Table 5-10: Drag coefficients of RNA.

Property	Unit	Blades	Generator
F	[kN]	20.16	15.33
V	[m/s]	20.00	20.00
ρ	[kg/m ³]	1.22	1.22
Diameter	[m]	240	10
A	[m ²]	45,239	79
C_d	[-]	0.0018	0.8000
$C_{d,eq}$ (Blades + Gen)	[-]	0.0034	

Where $C_{d,eq}$ (Blades + Gen) is proportional to the area and C_d of Blades and Generator. Note that the yaw system of the turbine is active during towing (see Section 5.2.1), that is why only a 0 degree wind heading has been investigated.

Wind Drag Force Coefficients of Tower

The tower and other floater structural surfaces are considered with a drag coefficient of 0.70 as recommended for circular sections in DNVGL-RP-C205. Table 5-11 shows the global wind forces and moments on offshore structure above water line for all headings input in the AQWA model at the COG.

Table 5-11: Global wind forces and moments on Windcrete structures above water for all headings.

Heading [deg]	F _x [kN/(m/s) ²]	F _y [kN/(m/s) ²]	F _z [kN/(m/s) ²]	M _x [kN*m/(m/s) ²]	M _y [kN*m/(m/s) ²]	M _z [kN*m/(m/s) ²]
0	0.56	0.00	0.00	0.00	90.64	0.00
15	0.54	0.14	0.00	-23.46	87.55	0.00
30	0.48	0.28	0.00	-45.32	78.49	0.00
45	0.40	0.40	0.00	-64.09	64.09	0.00
60	0.28	0.48	0.00	-78.49	45.32	0.00
75	0.14	0.54	0.00	-87.55	23.46	0.00
90	0.00	0.56	0.00	-90.64	0.00	0.00
105	-0.14	0.54	0.00	-87.55	-23.46	0.00
120	-0.28	0.48	0.00	-78.49	-45.32	0.00
135	-0.40	0.40	0.00	-64.09	-64.09	0.00
150	-0.48	0.28	0.00	-45.32	-78.49	0.00
180	-0.56	0.00	0.00	0.00	-90.64	0.00

Current Force Coefficients

The current forces are modelled using Morison equation with the characteristics in Table 5-12:

Table 5-12: Current force coefficients of Windcrete.

C _d [-]	A [m ²]	Current Force Coefficient [kN/(m/s) ²]
334.36	6.172	1,058.66

The so-called Morison tube is used with an arbitrary diameter (0.04 m), with a height equal to the draft. The drag coefficient is tuned for obtaining the global response. The drag coefficient is obtained as follows, considering a wet projected area of 2,948.1 m² and a drag coefficient of 0.7 as used in the OpenFAST models validated by COREWIND partners.

$$\frac{1}{2} \cdot \rho \cdot A_{tube} \cdot C_{d tube} = \frac{1}{2} \cdot \rho \cdot A_{wc} \cdot C_{d wc}$$

$$C_{d tube} = \frac{A_{wc}}{A_{tube}} \cdot C_{d wc} = \frac{2948.1}{6.172} \cdot 0.7 = 334.36$$

The aim of Morison tubes is to add the drag forces due to the speed of the fluid around the underwater structure. This Morison tubes will produce a force given by the following formula:

$$F = \frac{1}{2} \cdot \rho \cdot A_{tube} \cdot C_{d tube} \cdot v^2$$

Model Coordinate System

The coordinate system is set with Z axis at the platform centre pointing upwards. The X/Y axis are as indicated in the Figure 5-26, where also the wind, wave and advance direction are indicated.

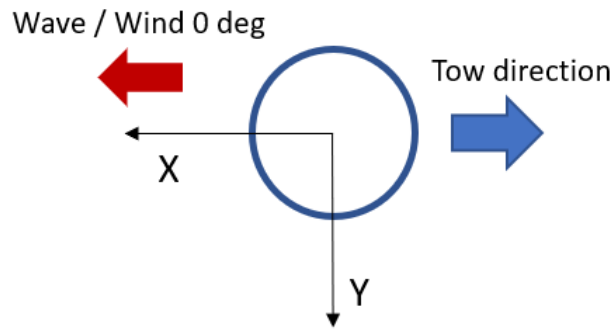


Figure 5-26: Platform coordinate system [Source: ESTEYCO].

Boundary Conditions

Three tug lines are input in the model, see Table 5-13 and Figure 5-27, for restraining the model without affecting any natural period and keeping its water plane position for convergence purposes. One main line aligned with tow direction and two lines at 120 degrees for stabilizing the model. The stiffness input is low, aiming for restraining as little as possible the motions and therefore, minimizing the influence to the results of the analyses.

Table 5-13: Current force coefficients of Windcrete.

Property	Parameter	Line Bow	Line Starboard	Line Portside
Cable properties	Stiffness [kN/m]	31.74	31.74	31.74
	Unstretched length [m]	121.9	121.9	121.9
	Length [m]	149.76	149.76	149.76
Fairlead	X [m]	-9.7	4.85	4.85
	Y [m]	0	8.4	-8.4
	Z [m]	-90	-90	-90
Fixed point	X [m]	-129.4	64.7	64.7
	Y [m]	0	112.064	-112.064
	Z [m]	0	0	0

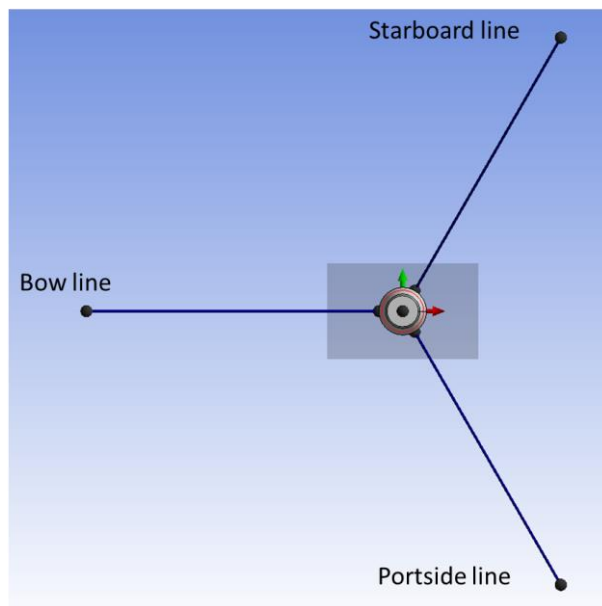


Figure 5-27: Boundary conditions of Windcrete [Source: ESTEYCO].

Additional Hydrodynamic Parameters

One drag disc is added to the bottom of the structure with the following parameters in Table 5-14. A buoyancy point has been added in the centre of buoyancy to compensate small errors in the geometry produced by the mesh.

Table 5-14: Current force coefficients of Windcrete.

Element	C_d [-]	A [m ²]
Drag disc	15,054.4	0.0314

5.2.2.2 ActiveFloat

The ActiveFloat model has been built based on the information found in design document in [13]. The floater draft is set to the transport draft (12.56 m).

Floater Geometry

The platform is a semi-submersible concrete floater with three external vertical columns placed at 120 degrees, see Figure 5-28. The external columns are connected to a central shaft that holds the connection with the tower that ends in the turbine. The three vertical columns are connected to the central shaft through three pontoons. The vertical columns provide the buoyancy and stability to the system while the pontoons are structural members as the central shaft from where the turbine loads are transferred and also add heave damping. The platform external columns have the same height as the central cone where the access platform is located. The platform is made of reinforced concrete, except for the tower that is made of structural steel.

The platform is towed in un-ballasted condition in order to reduce draught requirements of navigation channels or shipyards where the fabrication takes place. For the site C the minimum towing draught that could be achieved is 12.56 meters. Operational draught is set at 27.8 meters.

Circular heave plates are provided at the bottom of each external column, in order to increase damping.

The column diameter (17.40 m) is kept equal towards the pontoons beam. The pontoons have a rectangular cross-section member with a central bulkhead that split the span of the pontoon decks. Hub height is set at 140 m in operating conditions for site C.

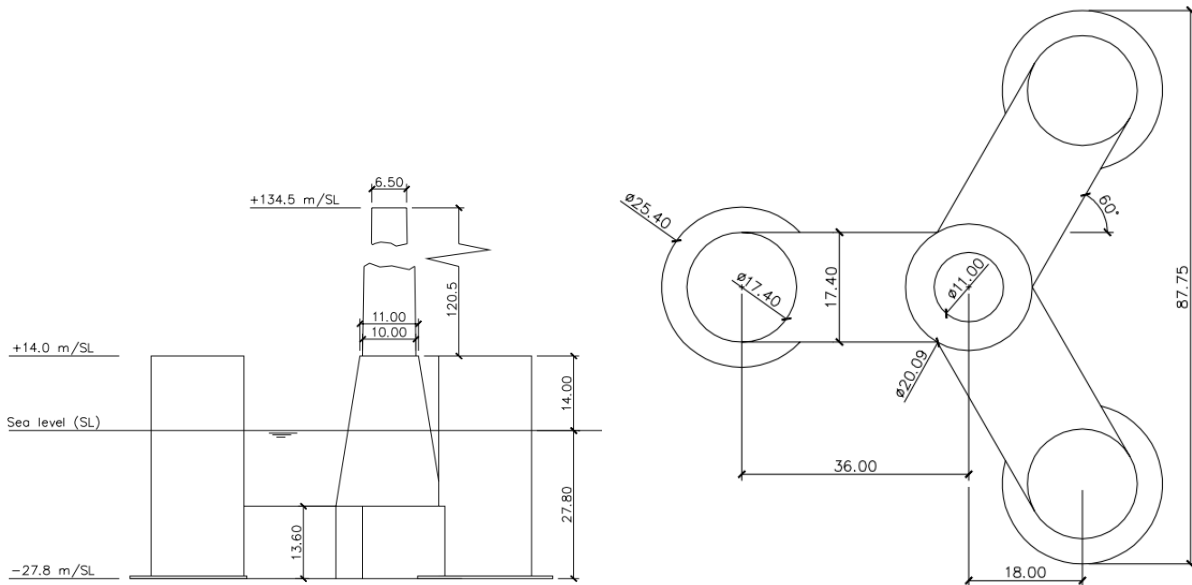


Figure 5-28: Schematic showing geometry and dimensions of ActiveFloat in operation with Units in meters [Source: COBRA].

Mass Properties

The following mass properties in Table 5-15 were input in the model.

Table 5-15: Inertias and centre of gravity for ActiveFloat.

Item	Weight [t]	COG _x [m]	COG _y [m]	COG _z [m]	I _{xx} [tm ²]	I _{yy} [tm ²]	I _{zz} [tm ²]
RNA	1,017	7.020	0.000	167.000	2.14E+07	2.14E+07	2.06E+04
Tower	1,184	0.000	0.000	90.000	6.48E+06	6.48E+06	1.91E+04
Platform	26,327	-0.270	0.000	13.000	1.94E+07	1.94E+07	2.31E+07
Water Ballast	0	0.000	0.000	0.000	0.00E+00	0.00E+00	0.00E+00
Total	28,527.2	0.000	0.000	22.000	4.73E+07	4.73E+07	2.31E+07
					40.71	40.71	28.46
					r _{xx} [m]	r _{yy} [m]	r _{zz} [m]

Note that it is assumed that the static heeling caused by the RNA eccentricity is compensated by the active ballast. Therefore, in the input of the analyses, the platform is assumed with zero pitch as initial equilibrium conditions. In addition, the above location of the centre of gravity and inertias refer to the platform bottom at the central column centreline. The resulting towing draft is 12.56 m, without water ballast.

Wind Drag Force Coefficients

Wind forces are calculated following the same procedure as described in Section 5.2.2.1. The RNA and tower drag coefficients are kept as for Windcrete (0.0034 and 0.70 respectively). The rest of the exposed areas of the structure are modelled with 0.70 (columns, pontoons, etc.). Global wind coefficients input in the AQWA model at the COG are summarised in Table 5-16.

Table 5-16: Global wind forces and moments on ActiveFloat structures above water for all headings.

Heading [deg]	F _x [kN/(m/s) ²]	F _y [kN/(m/s) ²]	F _z [kN/(m/s) ²]	M _x [kN*m/(m/s) ²]	M _y [kN*m/(m/s) ²]	M _z [kN*m/(m/s) ²]
0	0.85	0.00	0.00	0.00	40.61	0.00
15	0.82	0.22	0.00	-10.52	39.26	0.00
30	0.74	0.43	0.00	-20.32	35.19	0.00
45	0.60	0.60	0.00	-28.72	28.72	0.00
60	0.43	0.74	0.00	-35.12	20.27	0.00
75	0.22	0.82	0.00	-39.23	10.51	0.00
90	0.00	0.85	0.00	-40.61	0.00	0.00
105	-0.22	0.83	0.00	-39.22	-10.51	0.00
120	-0.43	0.74	0.00	-35.17	-20.30	0.00
135	-0.60	0.60	0.00	-28.72	-28.72	0.00
150	-0.74	0.43	0.00	-20.30	-35.17	0.00
180	-0.85	0.00	0.00	0.00	-40.61	0.00

Current Force Coefficients

The current forces are modelled by three Morison tubes (one per cylinder) and additional current force coefficients with the characteristics in Table 5-17.

Table 5-17: Current force coefficients of ActiveFloat.

Element	C _d [-]	A [m ²]	Current Force Coefficient [kN/(m/s) ²]
Morison tube column 1	304.5	0.5236	81.7
Morison tube column 2	304.5	0.5236	81.7
Morison tube column 3	304.5	0.5236	81.7

Morrison Tubes emulate the hydrodynamic drag forces of floaters from the drag coefficient and projected area against the current direction, additional current forces are included to model the other parts of the structures that are affected by the current forces. The projected area is obtained from an arbitrary diameter of 0.04 m and tube height equal to draft. The drag coefficient is obtained from the following equation:

$$\frac{1}{2} \cdot \rho \cdot A_{tube} \cdot C_{d\ tube} = \frac{1}{2} \cdot \rho \cdot A_{flt} \cdot C_{d\ flt} ; C_{d\ tube} = \frac{A_{flt}}{A_{tube}} \cdot C_{d\ flt} = \frac{227.8}{0.5236} \cdot 0.7 = 304.5$$

The drag coefficient for the floater is assumed as 0.7 (cylinder drag coefficient).

Once the Morison tubes are defined, the additional current forces and moments are obtained calculating the current force coefficient without Morison tubes and subtracting the Morison tube coefficient. Table 5-18 shows the current force and moment coefficients.

Table 5-18: Additional current force coefficients of ActiveFloat.

Heading [deg]	F_x [kN/(m/s) ²]	F_y [kN/(m/s) ²]	F_z [kN/(m/s) ²]	M_x [kN*m/(m/s) ²]	M_y [kN*m/(m/s) ²]	M_z [kN*m/(m/s) ²]
-180	-130.89	0.00	0.00	0.00	1,640.59	0.00
-150	-79.36	-45.82	0.00	-574.60	995.23	0.00
-135	-85.48	-85.48	0.00	-1,071.57	1,071.57	0.00
-120	-65.45	-113.35	0.00	-1,420.79	820.29	0.00
-105	-31.29	-116.77	0.00	-1,463.79	392.22	0.00
-90	0.00	-91.63	0.00	-1,149.19	0.00	0.00
-75	31.29	-116.77	0.00	-1,463.79	-392.22	0.00
-60	65.45	-113.35	0.00	-1,420.79	-820.29	0.00
-45	85.48	-85.48	0.00	-1,071.57	-1,071.57	0.00
-30	79.36	-45.82	0.00	-574.60	-995.23	0.00
-15	116.77	-31.29	0.00	-392.22	-1,463.79	0.00
0	130.89	0.00	0.00	0.00	-1,640.59	0.00
15	116.77	31.29	0.00	392.22	-1,463.79	0.00
30	79.36	45.82	0.00	574.60	-995.23	0.00
45	85.48	85.48	0.00	1,071.57	-1,071.57	0.00
60	65.45	113.35	0.00	1,420.79	-820.29	0.00
75	31.29	116.77	0.00	1,463.79	-392.22	0.00
90	0.00	91.63	0.00	1,149.19	0.00	0.00
105	-31.29	116.77	0.00	1,463.79	392.22	0.00
120	-65.45	113.35	0.00	1,420.79	820.29	0.00
135	-85.48	85.48	0.00	1,071.57	1,071.57	0.00
150	-79.36	45.82	0.00	574.60	995.23	0.00
180	-130.89	0.00	0.00	0.00	1,640.59	0.00

Model Coordinate System

The coordinate system is identical as for the Windcrete model in Section 5.2.2.1.

Boundary Conditions

Three soft mooring lines are input in the model for restraining the model without affecting any natural period and keeping its water plane position for convergence purposes. One main line aligned with tow direction and two lines at 120 degrees for stabilizing the model coinciding with each column are used, see Table 5-19 and Figure 5-29. The stiffness input is low, aiming for restraining as little as possible the motions and therefore, minimizing the influence to the results of the analyses.

Table 5-19: Current force coefficients of ActiveFloat.

Property	Parameter	Line Bow	Line Starboard	Line Portside
Cable properties	Stiffness [kN/m]	31.74	31.74	31.74
	Unstretched length [m]	76.44	76.44	76.44
	Length [m]	84.71	84.71	84.71
Fairlead	X [m]	-44.7	22.35	22.35
	Y [m]	0	38.71	-38.71
	Z [m]	0.51	0.51	0.51
Fixed point	X [m]	-129.4	64.7	64.7
	Y [m]	0	112.064	-112.064
	Z [m]	0	0	0

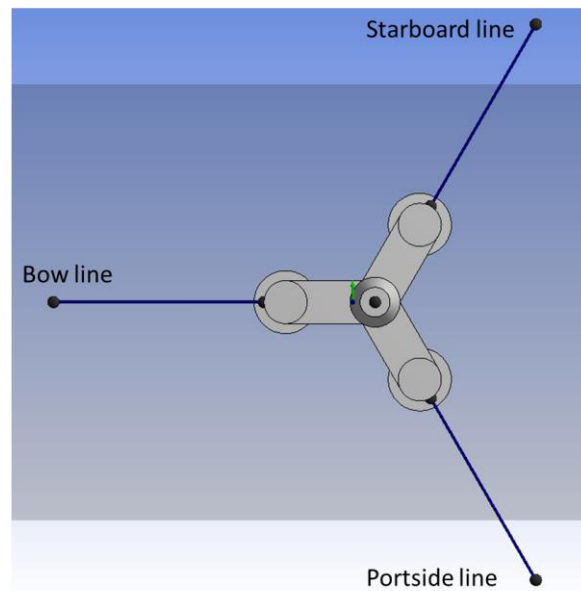


Figure 5-29: Boundary conditions of ActiveFloat [Source: ESTEYCO].

Additional Hydrodynamic Parameters

Three drag discs (one per column) are added to the bottom of the structure with the parameters in Table 5-20.

Table 5-20: Current force coefficients of Windcrete.

Element	C_d [-]	A [m ²]
Drag disc column 1	1,032,256	0.0314
Drag disc column 2	1,032,256	0.0314
Drag disc column 3	1,032,256	0.0314

A buoyancy point has been added in the centre of buoyancy to compensate small errors in the geometry produced by the mesh.

5.2.3 [Sensitivity Analysis](#)

The aim of these analyses is to know the effect of each parameter involved in the towing operation in the structure motions and accelerations. Four analyses are carried out:

- **Wind speed and heading sensitivity**
 - For heading sensitivity, simulations with average wind speeds of 8 m/s and wind directions of 0, 45 and 90 deg are performed.
 - Wind speed sensitivity analysis is carried out in time domain in order to find the limiting wind speed in the absence of waves/current.
- **Tow speed sensitivity:** This time-domain analysis simulates different transport speeds. The speed is input as a constant current profile.
- **Wave sensitivity:** This frequency-domain analysis aims to obtain the RAO of the structure for pitch and roll. It shows a first approach of the effect of the wave in the structures motions.
- **Wind and wave misalignment:** The aim of this analysis is to find the combination of wind and wave directions that produce the worst load situation. To carry out this sensitivity, simulations with varying wind and wave headings from 0 to 180 degrees have been run. These analyses are run in time domain, so that an indication of the accelerations caused by the waves can be inferred.

The sensitivity analyses intend to provide information on what parameter are governing the behaviour of the platforms during towing and which would be a reasonable matrix reflecting the cases to investigate the platform limits. The following sections show the results of these analyses based on the monitoring results that are nacelle COG motions and accelerations (pitch, roll, acceleration in X and acceleration in Y).

5.2.3.1 [Windcrete](#)

The sensitivity analyses of Windcrete are described in the following sections.

Wind Sensitivity

The wind sensitivity cases will show the effect of a range of wind speeds on the structures motions and acceleration. The wind fields are introduced in ANSYS AQWA as time series of wind speeds. They are calculated by COREWIND partners using NREL's tool TurbSim following the procedure according to IEC 61400-1 for normal turbulence model (NTM) wind fields. The wind speeds are defined at hub height with a 10-min average wind speed. In the conclusions these will be scaled at 10 meters and 1-hour average for better comparison to the scatter diagrams, see 5.2.7.

The following Table 5-21 summarizes the monitored parameters obtained from 10,400 s simulations. These are the platform pitch and roll, and the accelerations at the nacelle COG. The wind speed used for the initial wind heading sensitivity is an arbitrary value, which is chosen near the mean wind speed at site C and within the operational range of the wind turbine. The results confirms that, given the symmetry of the Windcrete spar-type floating substructure and the nacelle yaw system being active, there is no influence of the wind direction and results are symmetric.

Table 5-21: Wind heading sensitivity of Windcrete.

Wind Speed [m/s]		8.0	8.0	8.0
Wind Direction [deg]		0.0	45.0	90.0
Roll [deg]	Max	0.00	0.63	0.90
	Average	0.00	0.32	0.45
Pitch [deg]	Max	0.91	0.63	0.00
	Average	-0.45	-0.32	0.00
Acc. X [m/s ²]	Max	0.0444	0.0308	0.0005
	Average	0.00	0.00	0.00
Acc. Y [m/s ²]	Max	0.0004	0.0304	0.0441
	Average	0.00	0.00	0.00

The following Table 5-22 shows results for increasing wind speed until reaching the acceptance criteria that are established for the towing. It can be seen that larger wind speeds induce higher pitch angles of the platform as well as accelerations. It is important to note that the accelerations are not affected as much as the heeling by the wind turbulence. A quick conclusion of this analysis is that Windcrete could be towed with wind speeds up to 28 m/s (10-min at hub height, i.e. 16 m/s at 10 meters) in absence of waves/current.

Table 5-22: Wind speed sensitivity of Windcrete.

Wind Speed [m/s]		8.0	12.0	16.0	24.0	26.0	28.0
Wind Direction [deg]		0.0	0.0	0.0	0.0	0.0	0.0
Roll [deg]	Max	0	0.01	0.01	0.01	0.01	0.01
	Average	0	0	0	0	0	0
Pitch [deg]	Max	0.91	1.16	1.33	1.66	1.78	2.08
	Average	-0.45	-0.4	-0.32	-0.09	-0.02	0.06
Acc. X [m/s ²]	Max	0.04	0.08	0.1	0.158	0.176	0.209
	Average	0	0	0	0	0	0
Acc. Y [m/s ²]	Max	0.0004	0.0005	0.0005	0.001	0.001	0.001
	Average	0	0	0	0	0	0

Tow Speed Sensitivity

The tow speed sensitivity cases in Table 5-23 show the effect of a range of towing speeds on the platform pitch. As mentioned above the analyses are carried out using a constant current profile as input condition.

Table 5-23: Considered cases for forward speed sensitivity of Windcrete.

Current Speed / Tow Speed Sensitivity (only current)	
U _c [m/s]	Heading [deg]
0.5 ≤ U _c ≤ 2.5	0

The following Table 5-24 summarises the results of the sensitivity analyses to the tow speed obtained from 10,400 s simulations. The results, as expected, show a constant heeling in the platform. The rotation is counterclockwise, i.e. the rotor moves backwards. It must be noted that tow speed will be limited to around 3 knots or less, because of the potential large towing force required. The results for higher speeds are for reference only.

Table 5-24: Results for forward speed sensitivity of Windcrete.

Tow Speed		0.5 m/s	1.0 m/s	1.5 m/s	2.0 m/s	2.5 m/s
		1 knot	2 knot	3 knot	4 knot	5 knot
Pitch [deg]	Average	0.05	0.16	0.31	0.48	0.69

Wave Height Sensitivity

As mentioned, the RAO of the pitch mode is obtained. It is shown in Figure 5-30. The RAOs are characterised by a mainly linear response that increases in magnitude with the wave period. This means that the pitch/roll motion increase fairly linearly with the wave period. In order to achieve the maximum heeling angle allowed, of 2 degrees, for an average wave period of 12 s, the wave height should be approximately 6.5 m. However, it is important to bear in mind that the accelerations will govern the weather windows. The effect of the waves on the accelerations is determined in further analyses.

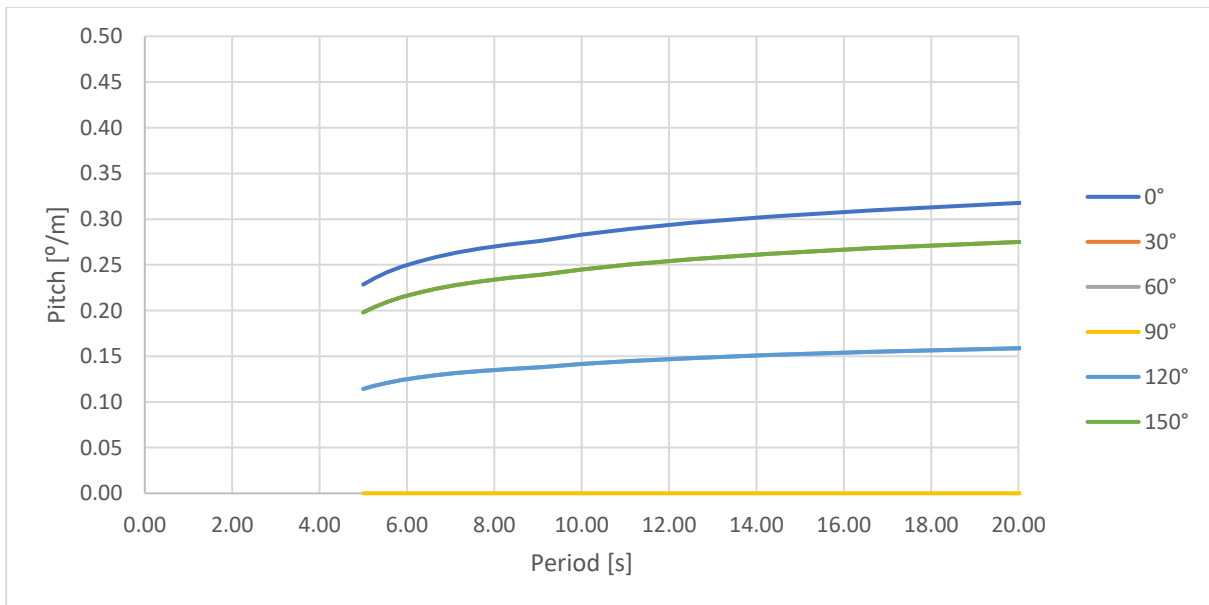


Figure 5-30: Pitch RAO of Windcrete [Source: ESTEYCO].

Wind and Wave Misalignment

The wind and wave misalignment sensitivity shows the effect of the misalignment of wave and wind direction on the platform motions and accelerations. This analysis consists of cases with 0 deg wind direction increasing up to 180 deg.

The irregular waves are simulated using the JONSWAP spectrum. The peak enhancement factor has been calculated for each sea state using the equation from DNVGL-RP-C205:

$$\gamma = 5 \text{ for } \frac{T_p}{\sqrt{H_s}} \leq 3.6$$

$$\gamma = \exp\left(5.75 - 1.15 \frac{T_p}{\sqrt{H_s}}\right) \text{ for } 3.6 < \frac{T_p}{\sqrt{H_s}} < 5$$

$$\gamma = 1 \text{ for } 5 \leq \frac{T_p}{\sqrt{H_s}}$$

Wind fields are included with the same basis as explained before in the paragraph “Wind Sensitivity” of Section 5.2.3. The turbine eccentricity is included in the results reported here.

The H_s and T_p values are obtained from the design basis [11] using the wave scatter diagram at site C (Morro Bay) as the most probable H_s - T_p combination.

Table 5-25: Cases for wind/wave misalignment of Windcrete.

Wind		Wave		
U_w [m/s]	Head. [deg]	H_s [m]	T_p [s]	Head. [deg]
8	0	2.5	13	$0 \leq \text{Dir (deg)} \leq 180$
8	$0 \leq \text{Dir (deg)} \leq 180$	2.5	13	0

The results obtained from 10,400 s simulations are summarised in the Table 5-26. The results show that the worst situation takes place when wind and wave are aligned in 0 deg direction, although this situation is very similar to the others directions due to the symmetry of the platform (and yaw system active). Therefore, in the Windcrete analyses the wind and wave angles will be considered to be aligned, in order to obtain the most onerous situation.

Table 5-26: Results for wind/wave misalignment of Windcrete.

Wave/Wind Misalignment												
T_p [s]		13.00	13.00	13.00	13.00	13.00	13.00	13.00	13.00	13.00	13.00	13.00
H_s [m]		2.50	2.50	2.50	2.50	2.50	2.50	2.50	2.50	2.50	2.50	2.50
Wave angle [deg]		0.00	30.00	60.00	90.00	120.00	180.00	0.00	0.00	0.00	0.00	0.00
U_w [m/s]		8.00	8.00	8.00	8.00	8.00	8.00	8.00	8.00	8.00	8.00	8.00
Wind angle [deg]		0.00	0.00	0.00	0.00	0.00	0.00	30.00	60.00	90.00	120.00	180.00
Pitch [deg]	MAXABS	1.22	1.13	0.98	1.00	1.06	1.13	1.14	0.91	0.60	0.71	1.21
	AVERAGE	-0.45	-0.45	-0.45	-0.45	-0.46	-0.46	-0.39	-0.22	0.00	0.23	0.54
Roll [deg]	MAXABS	0.00	0.44	0.57	0.59	0.51	0.00	0.54	0.88	1.00	0.89	0.00
	AVERAGE	0.00	0.00	0.00	0.00	0.00	0.00	0.23	0.39	0.45	0.39	0.00
Acc. Y [m/s²]	MAXABS	0.001	0.349	0.604	0.697	0.603	0.001	0.031	0.049	0.055	0.051	0.001
	AVERAGE	0.000	0.000	0.000	0.000	0.000	0.000	0.000	0.000	0.000	0.000	0.000
Acc. X [m/s²]	MAXABS	0.714	0.620	0.364	0.056	0.359	0.688	0.712	0.706	0.698	0.689	0.685
	AVERAGE	0.000	0.000	0.000	0.000	0.000	0.000	0.000	0.000	0.000	0.000	0.000

It is worth comparing one case with the previous wind-only sensitivity. The same wind speed has been used as input (8 m/s, 10-min, at hub height). The results in Table 5-27 indicate that the pitch is mainly caused by the wind action (70%, right column), while 90% of the acceleration peak is caused by waves (left column). Actually, the input wave causes an acceleration over the acceptance criteria of 0.06 g. It will be seen in Section 5.2.3.2, where the same analysis is done for ActiveFloat, that Windcrete is more sensible to waves in terms of peak acceleration.

Table 5-27: Wave impact on accelerations of Windcrete.

Wave/Wind Misalignment			
T_p [s]		13.00	-
H_s [m]		2.50	-
Wave angle [deg]		0.0	0.0
U_w [m/s]		8.0	8.0
Wind angle [deg]		0.0	0.0
Pitch [deg]	MAXABS	1.22	0.91
	AVERAGE	-0.45	-0.45
Roll [deg]	MAXABS	0.00	0.9100
	AVERAGE	0.00	-0.4500
Acc. Y [m/s²]	MAXABS	0.001	0.0004
	AVERAGE	0.000	0.00
Acc. X [m/s²]	MAXABS	0.714	0.0444
	AVERAGE	0.000	0.00

5.2.3.2 ActiveFloat

The sensitivity analyses of ActiveFloat are described in the following sections.

Wind Sensitivity

The wind sensitivity analysis is performed with the same basis as described in Section 5.2.3.1 using the case of Table 5-28.

Table 5-28: Cases for wind speed sensitivity of ActiveFloat.

Wind Speed Sensitivity (only current)	
U_w [m/s]	Head. [deg]
8	$0 \leq \text{Dir. (deg)} \leq 90$
$10 \leq U_w \leq 16$	Worst wind direction

The following Table 5-29 summarizes the monitored parameters obtained from 10,400 s simulations, that are the platform pitch and roll, and the accelerations at the nacelle COG. The results confirms that given the symmetry of the ActiveFloat and the yaw system being active, there is no influence in the wind direction and results are symmetric.

Table 5-29: Results for wind heading sensitivity of ActiveFloat.

Wind Speed [m/s]		8.0	8.0	8.0
Wind direction [deg]		0.0	45.0	90.0
Roll [deg]	Max	0.00	0.33	0.45
	Average	0.00	-0.04	-0.06
Pitch [deg]	Max	0.46	0.32	0.02
	Average	0.06	0.04	0.00
Acc. X [m/s^2]	Max	0.0513	0.0357	0.0028
	Average	0.0000	0.0000	0.0000
Acc. Y [m/s^2]	Max	0.0005	0.0371	0.0509
	Average	0.0000	0.0000	0.0000

The following Table 5-30 shows results for increasing wind speed until reaching the acceptance criteria that are established for the towing. It can be seen that larger wind speeds induce higher pitch angles to the platform as well as accelerations. It is important to note that the accelerations are not affected as much as the heeling by the wind turbulences. A quick conclusion of this analysis is that ActiveFloat could be transported with wind speeds up to 24 m/s (10-min at hub height, i.e. 14 m/s at 10 meters) in absence of waves/current.

Table 5-30: Wind speed sensitivity of ActiveFloat.

Wind Speed [m/s]		10.0	12.0	14.0	16.0	24.0	10.0
Wind direction [deg]		0.0	0.0	0.0	0.0	0.0	0.0
Roll [deg]	Max	0.00	0.00	0.00	0.00	0.00	0.00
	Average	0.00	0.00	0.00	0.00	0.00	0.00
Pitch [deg]	Max	0.64	0.81	1.02	1.23	2.02	0.64
	Average	0.09	0.13	0.18	0.24	0.53	0.09
Acc. X [m/s ²]	Max	0.0705	0.0869	0.1090	0.1313	0.2070	0.0705
	Average	0.0000	0.0000	0.0000	0.0000	0.0000	0.0000
Acc. Y [m/s ²]	Max	0.0005	0.0005	0.0005	0.0004	0.0000	0.0005
	Average	0.0000	0.0000	0.0000	0.0000	0.0000	0.0000

Tow Speed Sensitivity

The tow speed sensitivity is carried as described in Section 5.2.3.1 and with cases defined in Table 5-31. As mentioned above the analyses are carried out using a constant current profile as input.

Table 5-31: Considered cases for forward speed sensitivity of ActiveFloat.

Current Speed / Tow Speed Sensitivity (only current)	
U _c [m/s]	Heading [deg]
0.5 ≤ U _c ≤ 2.5	0

Table 5-32 summarizes the results of the sensitivity analyses to the tow speed obtained from 10,400 s simulations. The results, as expected, showed a constant heeling in the platform. The rotations is in this case clockwise, i.e. the rotor falls forward. The direction of this rotation is different to the Windcrete rotation due to the tug lines fairleads position, in the case of Windcrete, the fairlead Z is -90 m and the centre of pressure of the current faced area is ~-80 m; ActiveFloat fairlead Z is 0.51 m and the centre of pressure of the current faced area is ~-6.25 m. It must be noted that tow speed will be limited to around 3 knots or less, because of the potential large towing force required. The results for higher speeds are for reference only.

Table 5-32: Results for forward speed sensitivity of ActiveFloat.

Tow speed		0.5 m/s	1.0 m/s	1.5 m/s	2.0 m/s	2.5 m/s
		1 knot	2 knot	3 knot	4 knot	5 knot
Pitch [deg]	Average	-0.01	-0.05	-0.1	-0.18	-0.28

Wave Height Sensitivity

The RAO of the pitch mode is obtained. It is shown in Figure 5-31. The RAOs are characterised by a non-linear response. It is more or less flat for periods lower than 14 s, and linearly growing from 14 s and higher. For an average period of 12 s, a wave of 17 m is needed in order to reach the limiting heeling angle of 2 degrees. However, it is important to bear in mind that the accelerations will govern the weather windows. The effect of the waves on the accelerations is determined in further analyses.

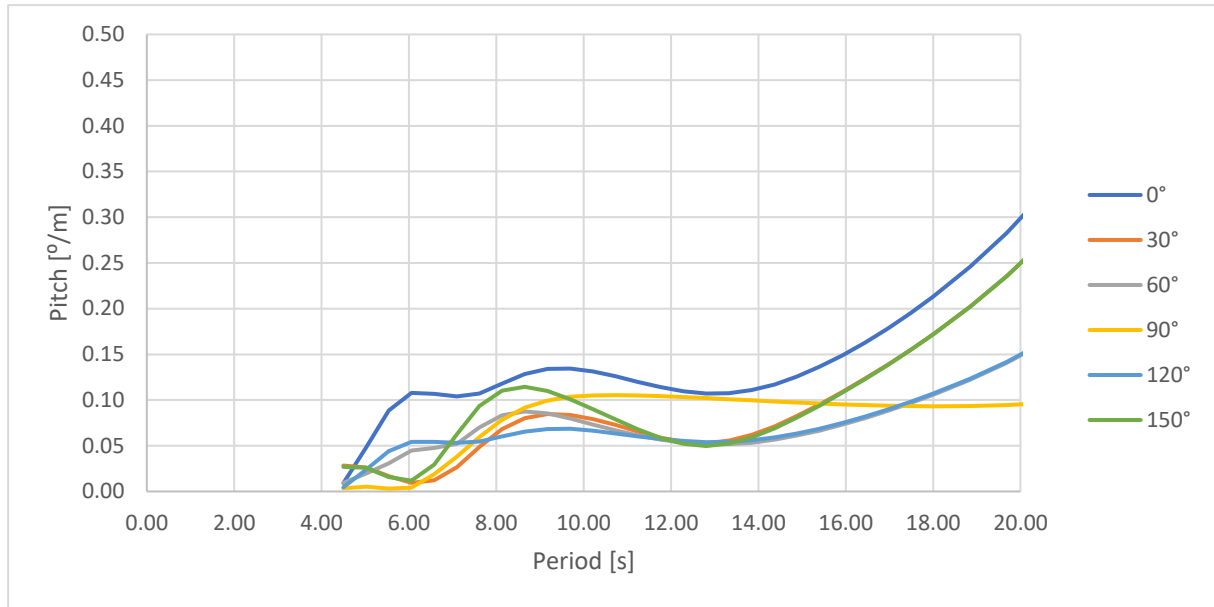


Figure 5-31: Pitch RAO of ActiveFloat [Source: ESTEYCO].

Wind and Wave Misalignment

The same basis is used for the ActiveFloat wind-wave misalignment as described in Section 5.2.3.1 and summarised in Table 5-33.

Table 5-33: Cases for wind/wave misalignment of ActiveFloat.

Wind		Wave		
U_w [m/s]	Head. [deg]	H_s [m]	T_p [s]	Head. [deg]
8	0	2.5	13	$0 \leq \text{Dir (deg)} \leq 180$
8	$0 \leq \text{Dir (deg)} \leq 180$	2.5	13	0

The results obtained from 10,400 s simulations are summarized in Table 5-34. The results show that the worst situation in terms of pitch occurs for 0 –120 degree (wave – wind) misalignment, while for accelerations occurs at 30 – 0 deg misalignment. Results are fairly similar for all directions, however different misalignments will be analysed in the following steps of the seakeeping analyses.

Table 5-34: Results for wind/wave misalignment of ActiveFloat.

Wave/Wind Misalignment												
T_p [s]		13.00	13.00	13.00	13.00	13.00	13.00	13.00	13.00	13.00	13.00	13.00
H_s [m]		2.50	2.50	2.50	2.50	2.50	2.50	2.50	2.50	2.50	2.50	2.50
Wave angle [deg]		0.00	30.00	60.00	90.00	120.00	180.00	0.00	0.00	0.00	0.00	0.00
U_w [m/s]		8.00	8.00	8.00	8.00	8.00	8.00	8.00	8.00	8.00	8.00	8.00
Wind angle [deg]		0.00	0.00	0.00	0.00	0.00	0.00	30.00	60.00	90.00	120.00	180.00
Pitch [deg]	MAXABS	0.57	0.44	0.28	0.46	0.43	0.52	0.56	0.60	0.66	0.72	0.77
	AVERAGE	0.05	0.06	0.07	0.07	0.05	0.02	0.05	0.02	-0.01	-0.04	-0.07
Roll [deg]	MAXABS	0.03	0.33	0.39	0.39	0.54	0.03	0.09	0.16	0.18	0.16	0.03
	AVERAGE	0.00	-0.02	-0.03	-0.01	0.00	0.00	-0.03	-0.05	-0.06	-0.05	0.00
Acc. Y [m/s²]	MAXABS	0.011	0.273	0.406	0.396	0.330	0.008	0.014	0.017	0.018	0.017	0.011
	AVERAGE	0.000	0.000	0.000	0.000	0.000	0.000	0.000	0.000	0.000	0.000	0.000
Acc. X [m/s²]	MAXABS	0.389	0.333	0.236	0.171	0.193	0.462	0.389	0.387	0.384	0.381	0.382
	AVERAGE	0.000	0.000	0.000	0.000	0.000	0.000	0.000	0.000	0.000	0.000	0.000

It worth comparing one case with the previous wind only sensitivity. The same wind speed is input (8 m/s, 10-min, at hub height). The results in Table 5-35 indicate that the pitch is mainly caused by the wind action (80%), while 90% of the accelerations peak are caused by waves. It can be seen that the acceleration caused by a 2.5 m wave at 13 s in ActiveFloat is 60% of the value of Windcrete. This means that ActiveFloat shows a smaller sensitivity to waves in terms of accelerations.

Table 5-35: Wave impact on accelerations of ActiveFloat.

Wave/Wind Misalignment			
T_p [s]		13.00	-
H_s [m]		2.50	-
Wave angle [deg]		0.0	0.0
U_w [m/s]		8.0	8.0
Wind angle [deg]		0.0	0.0
Pitch [deg]	MAXABS	0.57	0.46
	AVERAGE	0.05	0.06
Roll [deg]	MAXABS	0.03	0.00
	AVERAGE	0.00	0.00
Acc. Y [m/s²]	MAXABS	0.011	0.001
	AVERAGE	0.000	0.000
Acc. X [m/s²]	MAXABS	0.389	0.051
	AVERAGE	0.000	0.000

5.2.4 Preliminary Analysis in Frequency Domain

From the results of the previous sections, the proposed set of frequency domain simulations comprises two load case sets as shown in Table 5-36. The first set of load cases defines a more detailed wind/wave misalignment study, although for Windcrete it has been noted that not much difference is found. The second set of load cases investigates a wide range combinations.

Wind speeds are still referred to the hub height. For the conclusions, the wind speeds will be transferred to 10 m height and 1 hour reference time in order to filter the scatter diagrams. The time-domain wind fields described in Section 5.2.3.1 are transformed into a (frequency-domain) spectrum through the Fourier transform.

Table 5-36: Summary of load cases in frequency domain for preliminary weather conditions estimation.

Set no.	U_w [m/s]	H_s [m]	T_p [s]	Wind Direction [deg]	Wave Direction [deg]
1st Set	14	2.5	13	0, 30, 60, 90, 120, 150, 180	0, 90, 180
2nd Set	12, 14, 16	1.5, 2, 2.5, 3, 3.5, 4, 4.5, 5	6, 8, 10, 13, 16	As above misalignment analysis	As above misalignment analysis
	6, 8, 10	3.5, 4, 4.5, 5	6, 8, 10, 13, 16	As above misalignment analysis	As above misalignment analysis

A wide range of H_s , T_p , U_w combinations have been analysed to mostly cover all the situations in which the operation could take place. The objective is to identify the upper threshold for this operation which depending on the platform is usually within the proposed simulations. These simulations are calculated taking into account all parameters (the eccentricity of turbine is included in Windcrete case and fully compensated by the active ballast system for ActiveFloat), except for the tow speed whose effect will be added in a postprocessing step.

The outputs obtained from AQWA are the significant values. Significant values can be transformed into the most probable maximum expected for the magnitude being measured and the 90% percentile, defined as:

$$MPM = \sigma_a + \sigma_s \cdot \sqrt{0.5 \cdot \ln(N)}$$

$$P90 = \sigma_a + \sigma_s \cdot \sqrt{-0.5 \cdot \ln\left(1 - 0.9\frac{1}{N}\right)}$$

With σ_a as average value, σ_s as significant value and N as numbers of cycles. Considering on average 1,080 cycles for the 3 hour sea states the equations are:

$$MPM = \sigma_a + \sigma_s \cdot 1.87$$

$$P90 = \sigma_a + \sigma_s \cdot 2.15$$

The statistic used to calculate the maximum value in the frequency domain analysis is percentile 90 of maximums value.

5.2.4.1 Windcrete

The results for Windcrete are summarised in the following sections.

Misalignment Detailed Analysis

The results in Table 5-37 show that the accelerations are very similar for all simulations (when the resultant is calculated, all simulations indicate a maximum acceleration of 0.804 m/s²). Peaks of pitch mode are, however, slightly higher when the wind direction is 0 deg and wave direction is 180 deg (load case 15 in bold in Table 5-37).

Table 5-37: Misalignment detailed analysis for Windcrete.

Load Case	U _w [m/s]	H _s [m]	T _p [s]	Wind Dir. [deg]	Wave Dir. [deg]	Max (P90)			
						Roll [deg]	Pitch [deg]	Nac. Acc. Y [m/s ²]	Nac. Acc. X [m/s ²]
1	14.00	2.50	13.00	0.00	0.00	0.01	0.70	0.001	0.804
2	14.00	2.50	13.00	30.00	0.00	0.31	0.94	0.060	0.801
3	14.00	2.50	13.00	60.00	0.00	0.54	0.67	0.105	0.797
4	14.00	2.50	13.00	90.00	0.00	0.62	0.55	0.120	0.794
5	14.00	2.50	13.00	120.00	0.00	0.54	0.53	0.105	0.797
6	14.00	2.50	13.00	150.00	0.00	0.31	0.70	0.060	0.801
7	14.00	2.50	13.00	180.00	0.00	0.01	0.73	0.001	0.804
8	14.00	2.50	13.00	0.00	90.00	0.55	0.90	0.794	0.120
9	14.00	2.50	13.00	30.00	90.00	0.53	0.78	0.796	0.105
10	14.00	2.50	13.00	60.00	90.00	0.70	0.45	0.801	0.060
11	14.00	2.50	13.00	90.00	90.00	0.77	0.01	0.803	0.001
12	14.00	2.50	13.00	120.00	90.00	0.70	0.31	0.801	0.060
13	14.00	2.50	13.00	150.00	90.00	0.53	0.54	0.796	0.105
14	14.00	2.50	13.00	180.00	90.00	0.55	0.58	0.794	0.120
15	14.00	2.50	13.00	0.00	180.00	0.01	1.05	0.001	0.804
16	14.00	2.50	13.00	30.00	180.00	0.31	0.94	0.060	0.801
17	14.00	2.50	13.00	60.00	180.00	0.54	0.67	0.105	0.796
18	14.00	2.50	13.00	90.00	180.00	0.62	0.55	0.120	0.794
19	14.00	2.50	13.00	120.00	180.00	0.54	0.53	0.105	0.796
20	14.00	2.50	13.00	150.00	180.00	0.31	0.70	0.060	0.801
21	12.00	2.50	13.00	180.00	180.00	0.01	0.73	0.001	0.804

Full Case Matrix

Due to the long size of the load case table, the following results only show a summary. Table 5-38 shows the cases that fulfil the acceptance criteria, and also the cases that are close to the limits and, therefore, need to be analysed in detail using time domain simulations. The results are shown for the worst case situation of the wind/wave misalignment. The main limiting parameter is the acceleration which is very similar for all the wind/wave misalignments. Table 5-39 shows unsuccessful cases not fulfilling the acceptance criteria.

Table 5-38: 2nd Set frequency domain analysis successful cases fulfilling the acceptance criteria for Windcrete.

Successful Load Cases		
U _w [m/s]	H _s [m]	T _p [s]
12 ≤ U _w ≤ 16	1.5	6 ≤ T _p ≤ 16
	2	6

Table 5-39: 2nd Set frequency domain analysis unsuccessful cases not fulfilling the acceptance criteria for Windcrete.

Unsuccessful Load Cases		
U _w [m/s]	H _s [m]	T _p [s]
12 ≤ U _w ≤ 16	2	8 ≤ T _p ≤ 13
	2.5 ≤ H _s ≤ 5	6 ≤ T _p ≤ 16
6 ≤ U _w ≤ 10	3.5 ≤ H _s ≤ 5	

The following Table 5-40 includes a summary of the results.

Table 5-40: 2nd set frequency domain analysis near limit LCs for Windcrete.

Load Case	U _w [m/s]	H _s [m]	T _p [s]	Wind Dir. [deg]	Wave Dir. [deg]	Max (P90)			
						Roll [deg]	Pitch [deg]	Nac. Acc. Y [m/s ²]	Nac. Acc. X [m/s ²]
24	12.00	1.50	10.00	0.00	180.00	0.00	1.00	0.001	0.518
27	12.00	2.00	6.00	0.00	180.00	0.01	1.20	0.001	0.540
28	12.00	2.00	8.00	0.00	180.00	0.01	1.12	0.001	0.655
29	12.00	2.00	10.00	0.00	180.00	0.01	1.08	0.001	0.685
30	12.00	2.00	13.00	0.00	180.00	0.00	1.08	0.000	0.643
31	12.00	2.00	16.00	0.00	180.00	0.00	1.13	0.000	0.573
32	12.00	2.50	6.00	0.00	180.00	0.01	1.57	0.002	0.700
48	14	1.5	8	0	180	0.01	1.40	0.001	0.500
49	14	1.5	10	0	180	0.01	1.42	0.001	0.523
52	14	2	6	0	180	0.01	1.58	0.001	0.545
53	14	2	8	0	180	0.01	1.52	0.001	0.659
54	14	2	10	0	180	0.01	1.49	0.001	0.689
55	14	2	13	0	180	0.01	1.51	0.001	0.647
56	14	2	16	0	180	0.00	1.50	0.001	0.577
73	16	1.5	8	0	180	0.01	1.80	0.001	0.506
74	16	1.5	10	0	180	0.01	1.81	0.001	0.528
77	16	2	6	0	180	0.01	1.94	0.001	0.550
78	16	2	8	0	180	0.01	1.92	0.001	0.664
79	16	2	10	0	180	0.01	1.89	0.001	0.694
80	16	2	13	0	180	0.01	1.88	0.001	0.651
81	16	2	16	0	180	0.01	1.91	0.001	0.583
82	16	2.5	6	0	180	0.01	2.26	0.002	0.706
83	16	2.5	8	0	180	0.01	2.08	0.001	0.824
84	16	2.5	10	0	180	0.01	1.97	0.001	0.861
85	16	2.5	13	0	180	0.01	1.97	0.001	0.807
86	16	2.5	16	0	180	0.01	2.00	0.001	0.720

Table 5-41 shows the selected cases of the previous table that are calculated using more detailed time domain simulations in Section 5.2.5.

Table 5-41: Time domain detailed analysis load case list parameters for Windcrete.

Load Case	U _w [m/s]	H _s [m]	T _p [s]	Wind Dir. [deg]	Wave Dir. [deg]
48	14.00	1.50	8.00	0.00	180
49	14.00	1.50	10.00	0.00	180
52	14.00	2.00	6.00	0.00	180
53	14.00	2.00	8.00	0.00	180
54	14.00	2.00	10.00	0.00	180
55	14.00	2.00	13.00	0.00	180
56	14.00	2.00	16.00	0.00	180
73	16.00	1.50	8.00	0.00	180
74	16.00	1.50	10.00	0.00	180
77	16.00	2.00	6.00	0.00	180
78	16.00	2.00	8.00	0.00	180
79	16.00	2.00	10.00	0.00	180
80	16.00	2.00	13.00	0.00	180
81	16.00	2.00	16.00	0.00	180
82	16.00	2.50	6.00	0.00	180
86	16.00	2.50	16.00	0.00	180

5.2.4.2 ActiveFloat

The results for ActiveFloat are summarised in the following sections.

Misalignment Detailed Analysis

Accelerations are clearly higher for wave headings of 180 degree. The maximum pitch occurs for 180 degree wind heading for load case 21 (marked in bold in Table 5-42).

Table 5-42: Misalignment detailed analysis for ActiveFloat.

Load Case	U _w [m/s]	H _s [m]	T _p [s]	Wind Dir. [deg]	Wave Dir. [deg]	Max (P90)			
						Roll [deg]	Pitch [deg]	Nac. Acc. Y [m/s ²]	Nac. Acc. X [m/s ²]
1	14	2.50	13.00	0.00	0.00	0.02	0.59	0.003	0.396
2	14	2.50	13.00	30.00	0.00	0.12	0.76	0.028	0.395
3	14	2.50	13.00	60.00	0.00	0.21	0.64	0.047	0.393
4	14	2.50	13.00	90.00	0.00	0.30	0.52	0.054	0.392
5	14	2.50	13.00	120.00	0.00	0.21	0.64	0.047	0.393
6	14	2.50	13.00	150.00	0.00	0.12	0.76	0.028	0.395
7	14	2.50	13.00	180.00	0.00	0.02	0.59	0.005	0.396
8	14	2.50	13.00	0.00	90.00	0.30	0.68	0.398	0.144
9	14	2.50	13.00	30.00	90.00	0.27	0.63	0.398	0.142
10	14	2.50	13.00	60.00	90.00	0.29	0.47	0.400	0.137
11	14	2.50	13.00	90.00	90.00	0.10	0.31	0.401	0.135
12	14	2.50	13.00	120.00	90.00	0.28	0.47	0.400	0.137
13	14	2.50	13.00	150.00	90.00	0.25	0.63	0.399	0.142
14	14	2.50	13.00	180.00	90.00	0.29	0.68	0.398	0.144
15	14	2.50	13.00	0.00	180.00	0.03	0.82	0.006	0.447
16	14	2.50	13.00	30.00	180.00	0.10	0.77	0.025	0.446
17	14	2.50	13.00	60.00	180.00	0.17	0.63	0.043	0.445
18	14	2.50	13.00	90.00	180.00	0.00	0.51	0.049	0.444
19	14	2.50	13.00	120.00	180.00	0.17	0.63	0.043	0.445
20	14	2.50	13.00	150.00	180.00	0.10	0.77	0.025	0.446
21	12	2.50	13.00	180.00	180.00	0.03	0.82	0.006	0.447

Full Case Matrix

In the same way as in Section 5.2.4.1 the following tables show a summary of the results.

Table 5-43: 2nd Set frequency domain analysis successful cases fulfilling the acceptance criteria for ActiveFloat.

Successful Load Cases		
U _w [m/s]	H _s [m]	T _p [s]
6 ≤ U _w ≤ 16	1.5 ≤ H _s ≤ 3	6 ≤ T _p ≤ 16
	3.5	6 ≤ T _p ≤ 10
	4	6 ≤ T _p ≤ 8
	4.5 ≤ H _s ≤ 5	6

Table 5-44: 2nd Set frequency domain analysis unsuccessful cases not fulfilling the acceptance criteria for ActiveFloat.

Unsuccessful Load Cases		
U _w [m/s]	H _s [m]	T _p [s]
6 ≤ U _w ≤ 16	3.5	13 ≤ T _p ≤ 16
	4	10 ≤ T _p ≤ 16
	4.5 ≤ H _s ≤ 5	8 ≤ T _p ≤ 16

The following Table 5-45 includes a summary of the results.

Table 5-45: 2nd set frequency domain analysis near limit LCs for ActiveFloat.

Load Case	U _w [m/s]	H _s [m]	T _p [s]	Wind Dir. [deg]	Wave Dir. [deg]	Max (P90)			
						Roll [deg]	Pitch [deg]	Nac. Acc. Y [m/s ²]	Nac. Acc. X [m/s ²]
40	12	3	13	180	180	0.04	0.84	0.007	0.537
41	12	3	16	180	180	0.03	0.84	0.006	0.560
44	12	3.5	10	180	180	0.05	1.12	0.009	0.539
45	12	3.5	13	180	180	0.05	0.99	0.008	0.630
46	14	3.5	16	180	180	0.09	0.96	0.007	0.655
65	14	3	13	180	180	0.22	0.93	0.007	0.538
66	14	3	16	180	180	0.25	0.93	0.006	0.561
69	14	3.5	10	180	180	0.20	1.19	0.009	0.540
70	14	3.5	13	180	180	0.26	1.07	0.008	0.630
71	16	3.5	16	180	180	0.29	1.04	0.007	0.655
90	16	3	13	180	180	0.22	1.04	0.007	0.539
91	16	3	16	180	180	0.25	1.05	0.006	0.562
94	16	3.5	10	180	180	0.20	1.29	0.009	0.541
95	16	3.5	13	180	180	0.26	1.16	0.008	0.631
96	6	3.5	16	180	180	0.29	1.14	0.007	0.656
99	6	3.5	10	180	180	0.20	0.98	0.009	0.539
100	6	3.5	13	180	180	0.26	0.85	0.009	0.630
101	6	3.5	16	180	180	0.29	0.81	0.007	0.655
103	6	4	8	180	180	0.15	1.06	0.009	0.517
104	6	4	10	180	180	0.24	1.19	0.011	0.624
108	6	4.5	8	180	180	0.18	1.26	0.010	0.601
113	6	5	8	180	180	0.21	1.46	0.011	0.685
119	8	3.5	10	180	180	0.20	1.01	0.009	0.539
120	8	3.5	13	180	180	0.26	0.89	0.009	0.630
121	8	3.5	16	180	180	0.29	0.85	0.007	0.654
123	8	4	8	180	180	0.05	1.09	0.009	0.516
124	8	4	10	180	180	0.07	1.23	0.011	0.624
128	8	4.5	8	180	180	0.06	1.29	0.010	0.601
133	8	5	8	180	180	0.07	1.49	0.011	0.685
139	10	3.5	10	180	180	0.05	1.06	0.009	0.539
140	10	3.5	13	180	180	0.05	0.93	0.008	0.630
141	10	3.5	16	180	180	0.03	0.90	0.007	0.654
143	10	4	8	180	180	0.05	1.14	0.009	0.516
144	10	4	10	180	180	0.07	1.27	0.011	0.624
148	10	4.5	8	180	180	0.06	1.33	0.010	0.601
153	10	5	8	180	180	0.07	1.53	0.011	0.685
158	12	4	8	180	180	0.05	1.20	0.009	0.517
159	12	4	10	180	180	0.07	1.32	0.011	0.624
163	12	4.5	8	180	180	0.06	1.39	0.010	0.601
168	12	5	8	180	180	0.07	1.58	0.011	0.684
173	14	4	8	180	180	0.05	1.28	0.009	0.517
174	14	4	10	180	180	0.07	1.39	0.011	0.624
178	14	4.5	8	180	180	0.06	1.46	0.010	0.602
183	14	5	8	180	180	0.07	1.65	0.011	0.690
188	16	4	8	180	180	0.05	1.38	0.009	0.520
189	16	4	10	180	180	0.07	1.47	0.011	0.625
193	16	4.5	8	180	180	0.06	1.55	0.010	0.602
198	16	5	8	180	180	0.07	1.74	0.011	0.684

Table 5-46 shows the selected cases of the previous table that are calculated using more detailed time domain simulations in Section 5.2.5.

Table 5-46: Time domain detailed analysis load case list parameters for ActiveFloat.

Load Case	U _w [m/s]	H _s [m]	T _p [s]	Wind Dir. [deg]	Wave Dir. [deg]
121	8	3.5	16	180	180
140	10	3.5	13	180	180
141	10	3.5	16	180	180
159	12	4	10	180	180
163	12	4.5	8	180	180
168	12	5	8	180	180
174	14	4	10	180	180
178	14	4.5	8	180	180
183	14	5	8	180	180
189	16	4	10	180	180
193	16	4.5	8	180	180
198	16	5	8	180	180
69	14	3.5	10	180	180
91	16	3	16	180	180
188	16	4	8	180	180
90	16	3	13	180	180
94	16	3.5	10	180	180
173	14	4	8	180	180

5.2.5 Detailed Analysis in Time Domain

Time domain analyses are conducted to derive detailed weather limit estimations based on the identified load cases in Table 5-41 for Windcrete and Table 5-46 for ActiveFloat.

5.2.5.1 Windcrete

The results for the time domain analyses of Windcrete are shown in Table 5-47.

Table 5-47: Time domain detailed analysis results for Windcrete.

Load Case	U _w [m/s]	H _s [m]	T _p [s]	Wind Dir. [deg]	Wave Dir. [deg]	Max (P90)			
						Roll [deg]	Pitch [deg]	Nac. Acc. Y [m/s ²]	Nac. Acc. X [m/s ²]
48	14.00	1.50	8.00	0	180	0.006	1.118	0.458	0.001
49	14.00	1.50	10.00	0	180	0.006	1.105	0.483	0.001
52	14.00	2.00	6.00	0	180	0.012	1.203	0.550	0.002
53	14.00	2.00	8.00	0	180	0.007	1.183	0.615	0.001
54	14.00	2.00	10.00	0	180	0.007	1.129	0.619	0.001
55	14.00	2.00	13.00	0	180	0.008	1.176	0.599	0.001
56	14.00	2.00	16.00	0	180	0.008	1.170	0.508	0.001
73	16.00	1.50	8.00	0	180	0.006	1.261	0.467	0.001
74	16.00	1.50	10.00	0	180	0.006	1.259	0.494	0.001
77	16.00	2.00	6.00	0	180	0.012	1.360	0.560	0.002
78	16.00	2.00	8.00	0	180	0.007	1.338	0.617	0.001
79	16.00	2.00	10.00	0	180	0.008	1.282	0.630	0.001
80	16.00	2.00	13.00	0	180	0.008	1.330	0.606	0.001
81	16.00	2.00	16.00	0	180	0.009	1.308	0.513	0.001
82	16.00	2.50	6.00	0	180	0.013	1.377	0.628	0.002
86	16.00	2.50	16.00	0	180	0.008	1.372	0.630	0.001

The time domain analyses improve the results in general, i.e. the maximum motions and accelerations are reduced, therefore the environmental limits fulfilling the acceptance criteria can be expanded. Table 5-48 shows the new conditions for successful load cases fulfilling the acceptance criteria. The influence of the tow speed is finally discussed in the conclusions in Section 5.2.7.1.

Table 5-48: Final successful parameters fulfilling the acceptance criteria for Windcrete.

Successful Load Cases		
U_w [m/s]	H_s [m]	T_p [s]
$12 \leq U_w \leq 16$	1.5	$6 \leq T_p \leq 16$
	2	6
		16
$12 \leq U_w \leq 14$	2	13

5.2.5.2 ActiveFloat

Contrary to Windcrete, the time domain analysis worsens the results for ActiveFloat obtained preliminary in the frequency domain analyses, i.e. the maximum motions and accelerations are increased as shown in Table 5-49. Time-domain analysis takes into account second order effects, non-linearised drag forces etc. contrary to the frequency-domain analysis of Section 5.2.4.

Table 5-49: Time domain detailed analysis results for ActiveFloat.

Load Case	U_w [m/s]	H_s [m]	T_p [s]	Wind Dir. [deg]	Wave Dir. [deg]	Max (P90)			
						Roll [deg]	Pitch [deg]	Nac. Acc. Y [m/s^2]	Nac. Acc. X [m/s^2]
121	8	3.5	16	180	180	0.06	0.92	0.013	0.717
121	8	3.5	16	180	180	0.06	0.92	0.013	0.717
140	10	3.5	13	180	180	0.06	1.03	0.020	0.709
141	10	3.5	16	180	180	0.06	0.91	0.013	0.718
159	12	4	10	180	180	0.11	1.86	0.044	0.729
163	12	4.5	8	180	180	0.06	1.81	0.016	0.752
168	12	5	8	180	180	0.07	1.95	0.020	0.904
174	14	4	10	180	180	0.11	1.79	0.041	0.728
178	14	4.5	8	180	180	0.06	1.85	0.016	0.754
183	14	5	8	180	180	0.07	1.99	0.020	0.904
189	16	4	10	180	180	0.11	1.74	0.040	0.720
193	16	4.5	8	180	180	0.06	1.88	0.015	0.762
198	16	5	8	180	180	0.07	2.03	0.020	0.894
69	14	3.5	10	180	180	0.08	1.46	0.026	0.608
91	16	3	16	180	180	0.04	0.94	0.009	0.606
188	16	4	8	180	180	0.05	1.71	0.012	0.633
90	16	3	13	180	180	0.04	1.04	0.012	0.598
94	16	3.5	10	180	180	0.09	1.52	0.026	0.613
173	14	4	8	180	180	0.05	1.63	0.012	0.622

The number of successful load cases shown in Table 5-43 is overestimated, the new successful parameters fulfilling the acceptance criteria are shown in Table 5-50. The main difference between both tables is that the load cases with $H_s \geq 4$ m do not comply the transport criteria limitations, and for $H_s = 3$ m and 3.5 m there is a reduced number of wave periods that comply the acceptance criteria. Influence of tow speed is finally discussed in the conclusions in Section 5.2.7.2.

Table 5-50: Final successful parameters fulfilling the acceptance criteria for ActiveFloat.

Successful Load Cases		
U_w [m/s]	H_s [m]	T_p [s]
$6 \leq U_w \leq 16$	$1.5 \leq H_s \leq 2.5$	$6 \leq T_p \leq 16$
	3	$6 \leq T_p \leq 13$
$6 \leq U_w \leq 13$	3	16

5.2.6 Tow Line Tension Demand

In this section a sensitivity analysis is included with respect to what type of tug is generally required for the towing operation.

5.2.6.1 Windcrete

Table 5-51 shows the maximum tow line tensions (bow line in Figure 5-27) based on a set of load cases of the detailed analysis in time domain in Section 5.2.5.1. A forward speed of 1.5 m/s and the wind and wave direction of 0 deg are used. Assuming an efficiency factor for the tug boat of 78% according to DNVGL-ST-N001 (Section 11.12.2.8, assuming LOA > 45 m, BP > 100 t), and a maximum number of two tug boats for the operation, Windcrete would require two tug boats of 180 tons BP each one for sailing at 1.5 m/s.

Table 5-51: Tow line tension for Windcrete.

Load Case	U_w [m/s]	H_s [m]	T_p [s]	Wind Dir. [deg]	Wave Dir. [deg]	Avg. Tension Mooring Line (@Fs = 1.5 m/s) [kN]
79	16	2	10	0	0	2,737
82	16	2.5	6	0	0	2,777
86	16	2.5	16	0	0	2,727

5.2.6.2 ActiveFloat

Table 5-52 shows the tow line tension (bow line in Figure 5-29) based on a set of load cases of the detailed analysis in time domain in Section 5.2.5.2. A forward speed of 1.5 m/s and the wind and wave direction of 0 deg are used. Assuming an efficiency factor for the tug boat of 78% according to DNVGL-ST-N001 (Section 11.12.2.8, assuming LOA > 45 m, BP > 100 t), ActiveFloat would require one tug boat of 180 tons BP, for sailing at 1.5 m/s.

Table 5-52: Tow line tension for ActiveFloat.

Load Case	U_w [m/s]	H_s [m]	T_p [s]	Wind Dir. [deg]	Wave Dir. [deg]	Avg. Tension Mooring Line (@Fs = 1.5 m/s) [kN]
121	8	3.5	16	0	0	949
140	10	3.5	13	0	0	1,042
141	10	3.5	16	0	0	980
69	14	3.5	10	0	0	1,314
91	16	3	16	0	0	1,101
90	16	3	13	0	0	1,148
94	16	3.5	10	0	0	1,286

5.2.7 Operational Limits for Tow-In

Based on above considerations the operational limits for the tow-in operation for both Windcrete and ActiveFloat can be derived as input for the O&M cost model simulations.

5.2.7.1 Windcrete

The conditions shown in Table 5-53 fulfil the acceptance criteria based on the evaluated motion and acceleration values of Windcrete.

Table 5-53: Operational limits for the tow-in operation for Windcrete.

Successful Load Cases		
U_w [m/s]	H_s [m]	T_p [s]
$U_w \leq 9.5$	$1.5 \leq H_s \leq 2$	$6 \leq T_p \leq 16$
	$H_s \leq 2.5$	$T_p \leq 6$
		$T_p = 16$

Note that above wind speeds are transferred to 1-hour average at 10 m height from the previous convention used throughout the report, that was 10-min average at hub height. This is done in order to compare the environmental conditions fulfilling the acceptance criteria against the scatter diagrams provided in the COREWIND design basis [11], which refers to 1-hour average wind speed at 10 m height.

A constant pitch angle is resulting from the tow speed. This factor does not affect the results reported before, because the limiting parameter is the acceleration. The results are rounded up since the scatter diagrams derived are not as detailed as the analyses performed. Concluding, there is the tendency to expand the weather conditions in which the towing operation can be performed. In the scatter diagrams in Table 5-54 and Table 5-55, the green cells are parameters where the motions and accelerations comply with the transport criteria at site C, while red cells do not comply.

Table 5-54: Operational limits for the tow-in operation as H_s/T_p filtered scatter diagram for Windcrete. Green cells indicate conditions complying with the acceptance criteria (red cells do not comply).

T_p/H_s	0.5	1.5	2.5	3.5	4.5	5.5	6.5	7.5
1								
3								
5		x	x					
7		x	x	x				
9	x	x	x	x	x			
11	x	x	x	x	x	x		
13	x	x	x	x	x	x	x	
15	x	x	x	x	x	x	x	
17	x	x	x	x	x	x	x	x
19	x	x	x	x	x	x	x	
21		x	x	x	x	x		
23		x	x	x				

Table 5-55: Operational limits for the tow-in operation as wind speed/ H_s filtered scatter diagram for Windcrete. Green cells indicate conditions complying with the acceptance criteria (red cells do not comply).

H_s [m]	U_w (1-hour at 10 m)										
	0.0 – 2.0	2.0 – 4.0	4.0 – 6.0	6.0 – 8.0	8.0 – 10.0	10.0 – 12.0	12.0 – 14.0	14.0 – 16.0	16.0 – 18.0	18.0 – 20.0	> 24.0
0.5	x	x	x	x	x						
1.5	x	x	x	x	x	x	x	x			
2.5	x	x	x	x	x	x	x	x	x	x	
3.5	x	x	x	x	x	x	x	x	x	x	x
4.5	x	x	x	x	x	x	x	x	x	x	x
5.5	x	x	x	x	x	x	x	x	x	x	x
6.5	x	x	x	x	x	x	x	x	x	x	x
> 7.0		x	x	x	x	x	x	x	x	x	

5.2.7.2 ActiveFloat

The operational limits of ActiveFloat for the tow-in study are included in Table 5-56. The results already account for the mean pitch from tow speed. Similarly to Windcrete if speed is kept under 3 knots the previous results are valid.

Table 5-56: Operational limits for the tow-in operation for ActiveFloat.

Successful Load Cases		
U_w [m/s]	H_s [m]	T_p [s]
$U_w \leq 7.5$	$H_s \leq 3$	$6 \leq T_p \leq 16$
$7.5 < U_w \leq 9.5$	$H_s \leq 2.5$	$6 \leq T_p \leq 16$
	3	$6 \leq T_p \leq 13$

Table 5-57 shows a H_s/T_p scatter diagram for site C, filtered by valid sea states for performing the tow manoeuvre. The green cells are parameters where the motions and accelerations comply with the transport criteria, while red cells do not comply.

Table 5-57: Operational limits for the tow-in operation as H_s/T_p filtered scatter diagram for ActiveFloat. Green cells indicate conditions complying with the acceptance criteria (red cells do not comply).

T_p/H_s	0.5	1.5	2.5	3.5	4.5	5.5	6.5	7.5
1								
3								
5		x	x					
7		x	x	x				
9	x	x	x	x	x			
11	x	x	x	x	x	x		
13	x	x	x	x	x	x	x	
15	x	x	x	x	x	x	x	
17	x	x	x	x	x	x	x	x
19	x	x	x	x	x	x	x	
21		x	x	x	x	x		
23		x	x	x				

Table 5-58: Operational limits for the tow-in operation as wind speed/ H_s filtered scatter diagram for ActiveFloat. Green cells indicate conditions complying with the acceptance criteria (red cells do not comply).

H_s [m]	U_w (1-hour at 10 m)										
	0.0 – 2.0	2.0 – 4.0	4.0 – 6.0	6.0 – 8.0	8.0 – 10.0	10.0 – 12.0	12.0 – 14.0	14.0 – 16.0	16.0 – 18.0	18.0 – 20.0	> 24.0
0.5	x	x	x	x	x						
1.5	x	x	x	x	x	x	x	x			
2.5	x	x	x	x	x	x	x	x	x	x	
3.5	x	x	x	x	x	x	x	x	x	x	x
4.5	x	x	x	x	x	x	x	x	x	x	x
5.5	x	x	x	x	x	x	x	x	x	x	x
6.5	x	x	x	x	x	x	x	x	x	x	x
> 7.0		x	x	x	x	x	x	x	x	x	

5.3 Workability and Transportability

This section builds on Chapter 8 - “Maintainability” of Deliverable D4.1 [12] published in August 2020, where the concept of workability is described in detail and references to relevant research is made.

Here, a short introduction to the topic is given and the difference between workability and transportability is explained. The focus of this section is the description of the assessment methodology and the application of the motion criteria on the floater motions of the ActiveFloat and the Windcrete and on the CTV and SOV during transfer. The section ends with a discussion on the simulation results and conclusions drawn on the developed workability and transportability limits.

The complex motion behaviour of vessels and floating wind turbines show a motion response in all translational and rotational directions of all six degrees of freedom. The surge, sway, heave and rotational oscillations of a vessel lie, from the point of view of human comfort as described by Mansfield [18], in the low frequency range below 1 Hz, which can provoke motion sickness to those exposed to the moving environment. According to the studies from McCauley [19], Griffin [20], and Mansfield [18] especially translational accelerations such as those in the vertical direction are the main driver for motion sickness.

Due to increased pressure on cost reduction during the operating phase, this topic is becoming increasingly important. Cost intensive maintenance campaigns for wind farms with long travel times depend on the success of the operation to keep up the target availability of the wind farm. Seasickness can have a massive impact on the worker’s performance and poses an HSE risk. It is therefore advisable to carry out a workability & transportability assessment early in the design process in order to identify possible risks for the O&M phase.

Workability is understood here as the ability of technicians to perform their work without being impaired by negative factors influencing their human comfort. As the maintenance work is usually performed on the asset itself, the workability assessment focusses on the floater motions and their influence on the technician’s ability to work.

Transportability is understood as the ability to transport the technicians without impairing their human comfort through negatively influencing factors. It focusses on the vessel motions the workers are exposed to during transport and assesses the potential for seasickness from the motion response of the ship.

5.3.1 Standards and Motion Limit Criteria

This section introduces the standards and guidelines which offer the most promising evaluation methodologies and motion criteria for the assessment of low frequency motions of floating offshore wind structures. This also includes literature from the railway industry, where human comfort has been assessed to a much larger extent due to its day-to-day application and the resulting public interest. For a thorough evaluation of these and further standards on their applicability to floating wind and the potential adverse effect of the motions on human comfort, it is referred to Schwarzkopf et al. in [21]. This gap analysis proved a deficiency in guiding literature to this topic for the offshore industry.

The threshold limits suggest limitations on the motion exposure of personnel, such as a maximum average acceleration over time. An evaluation of existing threshold values has been made by Schwarzkopf et al. in [21]. The paper concludes that most standards suggest limit criteria only for frequencies above 1 Hz and that the guidance of standards on acceleration thresholds for low frequency responses is very limited. Those are not applicable to motions in floating wind as this is outside the expectable frequency range of the structures assessed in COREWIND.

Apart from the standard literature, the "Assessment of ship performance in a seaway" published by the Nordic research collaboration Nordforsk (1987), [22], provides relevant motion limit criteria for ship motions. The work is practically oriented and aims to develop criteria and methods for the verification of the seakeeping performance of vessels. Nordforsk addresses the decrease in performance due to deck wetness or motion sickness and provides threshold values of the vibration magnitude for different kinds of works on vessels. These limit criteria, presented in Table 5-, are suggested for the evaluation of floating offshore wind turbine motions by [21].

Table 5-59: Limit criteria for r.m.s. accelerations and roll motions on vessels for different types of activities, [Source: Nordforsk (1987), [22]]

Root Mean Square Criterion			Description
Vertical Acc.	Lateral Acc.	Roll	
0.2 g	0.10 g	6.0°	Light manual work
0.15 g	0.07 g	4.0°	Heavy manual work
0.10 g	0.05 g	3.0°	Intellectual work
0.05 g	0.04 g	2.5°	Transit passengers
0.02 g	0.03 g	2.0°	Cruise liner

5.3.2 Workability Method

From the floater RAOs provided from the OrcaFlex simulations described in Section 5.1.4 the accelerations at the reference points (e.g. tower top, platform height, ...) are calculated and prepared for subsequent analysis. Accelerations are calculated for all horizontal and vertical directions as well as the pitch and roll motion of the floater.

By taking square root of the sum of the squares of both horizontal accelerations it is possible to combine both surge- and sway-directions. The resulting values describe the lateral displacement in space. With the same procedure the roll and pitch rotational motions can be combined into a resulting rotation and benchmarked against the rotational motion criteria. The contribution of pitch and roll to surge, sway, and heave have been taken into account. Yaw motions are not considered as they showed very small magnitudes under the studied conditions. Heave motions are not combined with other signals for the postprocessing.

The following postprocessing aims at benchmarking the floater accelerations against general motion criteria for human comfort and to calculate a **Workability Index (WI)** for each sea state condition. The assessment follows the methods presented in [23], [24], calculating the weighted r.m.s. values according to the formulas presented therein, except for one aspect: The time signal of the acceleration signals are divided into bins of a fixed duration (here 10 minutes) and the r.m.s. acceleration value is calculated for each bin. This way each time signal is described by a list of multiple r.m.s. accelerations instead of only one r.m.s. value.

This method is known from railway applications where it allows the evaluation of the r.m.s. accelerations along the route of the train, denoted Continuous Comfort, and to assign the values to their corresponding track section (BS EN 12299, 2009, [25]). In offshore application, it is of interest to observe the changes in the accelerations during the simulation time. The bin size can be understood as the acceptance criterion for exposure time of a technician being located in the moving environment. Scheu et al. 2018 [26] indicates that the Workability Index changes with the bin size chosen; the parameter must therefore be treated with care. Based on the studies by Caicedo et al. 2012, [27], a bin size of 10 min has been chosen. A sensitivity analysis of different bin sizes has also

been carried out by Scheu et al. 2018 [26] in order to illustrate the effects. The frequency weighting of the acceleration signal is done according to ISO 2631-1, 1997, [24].

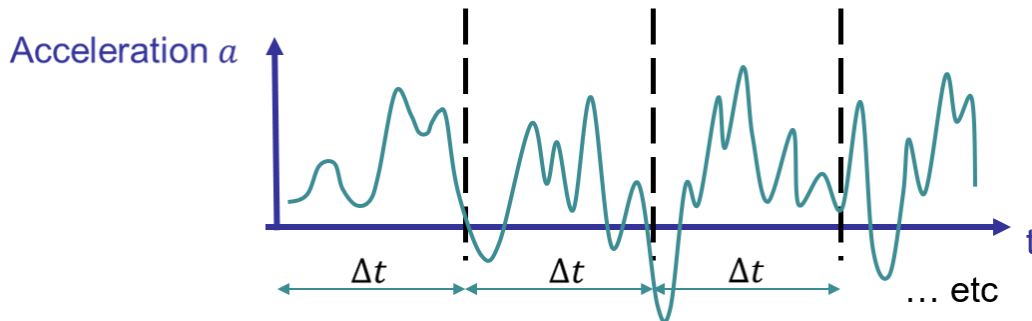


Figure 5-32: Division of the acceleration time signal into bins of a fixed duration [Source: Ramboll].

For the further assessment the conservative assumption presented by Scheu et al. 2018 and based on the studies from Boggs, 1995, [23], has been used. Boggs [23] presents the theory that the largest individual peak cycles affect a person most and that lesser cycles are “forgotten” about. For this, not all accelerations occurring during a certain sea state condition are treated equally, but more emphasis is given to local acceleration maxima. (Scheu et al, 2018 [26])

In this assessment the r.m.s. values is calculated from the maxima contained in each bin. The resulting values r.m.s. accelerations are lower than peak-to-peak values but account for actually occurring peak accelerations more than the traditional r.m.s. method described in ISO 2631-1, 1997, [24]. For this calculation the absolute values of the studied acceleration signal are assessed in order to account for negative peaks. Figure 5- illustrates the procedure.

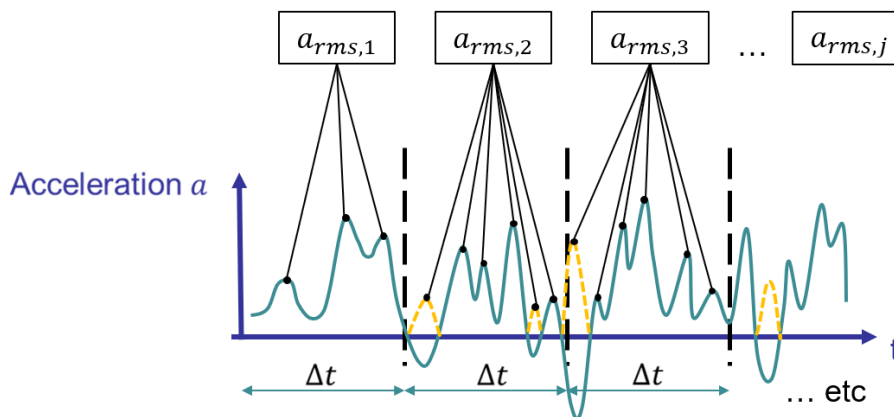


Figure 5-33: Calculation of r.m.s. of local acceleration maxima [Source: Ramboll].

The results of every specific H_s - T_p combination can be visualised in a histogram displaying the r.m.s. acceleration in the y-axis and the different bins on the x-axis. For every direction (lateral, vertical, and rotational) the r.m.s. values are compared to their specific r.m.s. acceleration limits.

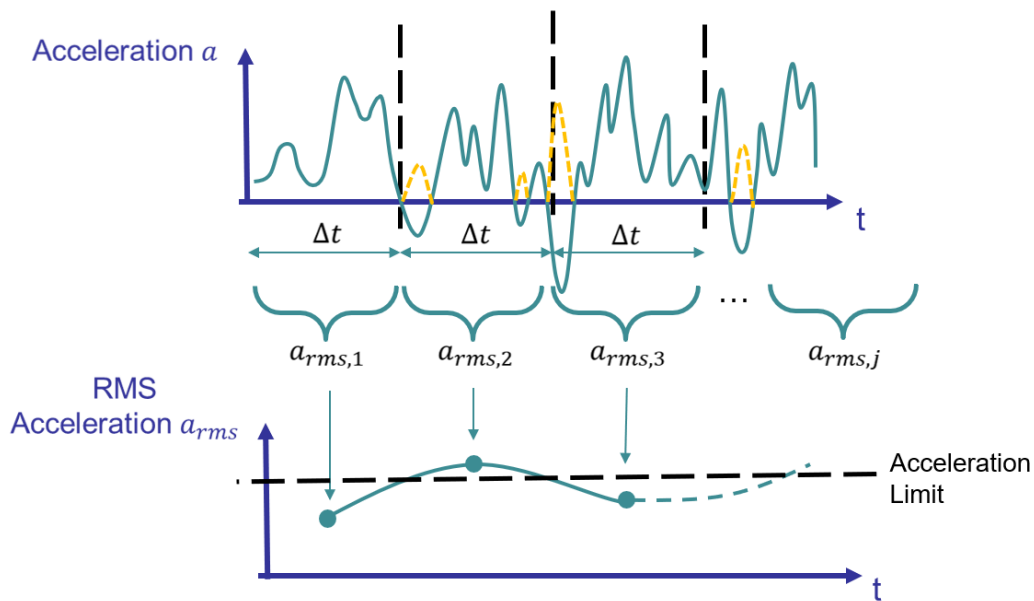


Figure 5-34: Calculation of r.m.s. acceleration of each bin and comparison against r.m.s. acceleration limit [Source: Ramboll].

The percentage of occurrences outside the given limit values is denoted as a non-workable condition; **the fraction of time in which the respective limiting motion exposure threshold is not exceeded is further denoted as the Workability Index (WI):**

$$WI = \frac{\text{Workable Time}}{\text{Total Duration}}$$

For one sea state condition individual WIs from the different directions (lateral, vertical, and rotational) are calculated and multiplied to provide the WI of the specific H_s - T_p combination. The resulting WI is calculated for each H_s - T_p combination of interest for a given site.

As limitation threshold the motion limit criteria from Nordforsk, [22], have been chosen because of their wide applicability and for providing limits for all degrees of freedom except for yaw, see Table 5-. More information on other motion limit criteria have been summarised in [21] and [12].

On the one side, failure finding tasks and repair work on the wind turbine include complex cognitive tasks so that the motion limit of intellectual work is regarded as appropriate for the assessment. On the other side, some technicians might not be used to motions of the sea, which according to Nordforsk, [22], applies to the category of the “transit passenger” limit criteria. For this reason the assessment is made for both motion criteria categories. This approach will further underline the influence the choice of the limit has on the final workability and transportability matrix.

5.3.3 [Workability Limits for Offshore Maintenance Works](#)

Generic Workability Index Matrices have been created showing the workable and non-workable sea states for the Windcrete and ActiveFloat substructure at site C - Morro Bay. The coloured cells highlight the sea states which according to D1.2 [11] occur at site C. The numbers in the cells show the Workability Index. When the index is below 1 the sea state allows only a reduced workability.

ActiveFloat and Transit Passenger Motion Criterion										
Tp/Hs	0.5	1.5	2.5	3.5	4.5	5.5	6.5	7.5	8.5	
1	1	1	1	1	1	1	1	1	1	1
3	1	1	1	1	1	1	1	1	1	1
5	1	1	1	1	1	0.9	0.71	0.62	0.48	
7	1	1	1	0.9	0.71	0.43	0.33	0.14	0.1	
9	1	1	1	1	0.86	0.43	0.24	0.14	0	
11	1	1	1	1	1	0.86	0.57	0.29	0.14	
13	1	1	1	1	1	1	0.95	0.76	0.52	
15	1	1	1	1	1	1	1	1	0.95	
17	1	1	1	1	1	1	1	1	1	1
19	1	1	1	1	1	1	1	1	1	1
21	1	1	1	1	1	1	1	1	1	1
23	1	1	1	1	1	1	1	1	1	1

ActiveFloat and Intellectual Work Motion Criterion										
Tp/Hs	0.5	1.5	2.5	3.5	4.5	5.5	6.5	7.5	8.5	
1	1	1	1	1	1	1	1	1	1	1
3	1	1	1	1	1	1	1	1	1	1
5	1	1	1	1	1	0.99	0.94	0.78	0.63	
7	1	1	1	0.95	0.82	0.68	0.5	0.35	0.22	
9	1	1	1	1	0.93	0.67	0.45	0.28	0.19	
11	1	1	1	1	1	0.95	0.77	0.52	0.37	
13	1	1	1	1	1	1	1	0.94	0.76	
15	1	1	1	1	1	1	1	1	0.99	
17	1	1	1	1	1	1	1	1	1	1
19	1	1	1	1	1	1	1	1	1	1
21	1	1	1	1	1	1	1	1	1	1
23	1	1	1	1	1	1	1	1	1	1

Figure 5-35: Workability Matrix for ActiveFloat applying the transit passenger (top) and intellectual work (bottom) motion criteria [Source: Ramboll].

Windcrete and Transit Passenger Motion Criterion										
Tp/Hs	0.5	1.5	2.5	3.5	4.5	5.5	6.5	7.5	8.5	
1	1	1	1	1	1	1	1	1	1	1
3	1	1	1	1	1	1	1	1	1	1
5	1	1	1	1	0.94	0.75	0.51	0.44	0.41	
7	1	1	1	0.73	0.46	0.41	0.29	0.17	0.16	
9	1	1	1	1	0.62	0.41	0.25	0.16	0.14	
11	1	1	1	1	1	0.81	0.43	0.35	0.16	
13	1	1	1	1	1	1	1	0.6	0.43	
15	1	1	1	1	1	1	1	1	0.95	
17	1	1	1	1	1	1	1	1	1	
19	1	1	1	1	1	1	1	1	1	
21	1	1	1	1	1	1	1	1	1	
23	1	1	1	1	1	1	1	1	1	

Windcrete and Intellectual Work Motion Criterion										
Tp/Hs	0.5	1.5	2.5	3.5	4.5	5.5	6.5	7.5	8.5	
1	1	1	1	1	1	1	1	1	1	1
3	1	1	1	1	1	1	1	1	1	1
5	1	1	1	1	1	1	0.9	0.71	0.52	
7	1	1	1	1	0.71	0.52	0.43	0.33	0.33	
9	1	1	1	1	0.9	0.52	0.43	0.33	0.24	
11	1	1	1	1	1	1	0.71	0.43	0.33	
13	1	1	1	1	1	1	1	0.9	0.71	
15	1	1	1	1	1	1	1	1	1	
17	1	1	1	1	1	1	1	1	1	
19	1	1	1	1	1	1	1	1	1	
21	1	1	1	1	1	1	1	1	1	
23	1	1	1	1	1	1	1	1	1	

Figure 5-36: Workability Matrix for Windcrete applying the transit passenger (top) and intellectual work (bottom) motion criteria [Source: Ramboll].

Looking at the resulting matrices it is a non-intuitive outcome that the workability does not decrease with higher sea states. On the contrary, even for very high significant waves workable conditions exist. It becomes apparent that the workability is affected by the peak wave period of the sea state. Especially in the wave period range between 7 s and 9 s the workability is always the lowest. For further information on the probability distribution of the wave scatter diagram of site C refer to D1.2 [2] of COREWIND.

The generic workability matrices show that for both floaters the conservative motion criteria “Transit passenger” allows for less workable conditions than the motion criteria “Intellectual Work”. The acceleration limit values have a high impact on the results and floating-specific standards are lacking a consistent methodology for the assessment of motion sickness for floating offshore structures in the low frequency range. Limit values for different working activities from expert literature should be revised and compared with field data of maintenance personal of existing floating offshore wind farms.

The purpose of the workability assessment was to use these matrices as input to the O&M cost model simulations in Chapter 6. However, when comparing the matrices with the weather limits of the SOV and CTV it becomes apparent that the non-workable conditions are in no case the limiting factor and are always higher than the weather limits of the vessels. Therefore no effect could be seen, when trying to study the influence of workability on the OPEX and availability of the wind farm. It can therefore be concluded that for the studied large scale

15 MW wind turbines the non-workable conditions lie outside the wave conditions relevant for the operation and maintenance activities. As smaller wind turbines have a different motion response, the outcomes of this study cannot be generalised and the workability needs to be assessed for each case individually.

5.3.4 Transportability Method

The methodology used for the transportability study is analogous to the methodology used for the workability study in Section 5.3.2, expect from three differences between both approaches. For the transportability study:

- the RAOs are provided from AQWA simulations, also considering the vessels transfer speeds,
- the accelerations on deck are compared directly to the total acceleration r.m.s., instead of considering bins, and
- the cases where the waves are above breaking limits are not considered suitable for transportability.

5.3.5 Transportability Limits for Crew Transfer

Figure 5- and Figure 5- display the transportability results for both vessels. It was found that the limits for transportability are high for both vessels. In fact, the main limitation is imposed by the vessel recommended limitations ($H_s \leq 4\text{m}$ for CTV and $H_s \leq 6\text{m}$ for SOV), chosen based on previous experience and vessel provider recommendations. For shorter periods, the main limitation is the condition of no breaking waves (short period waves break with less significant height).

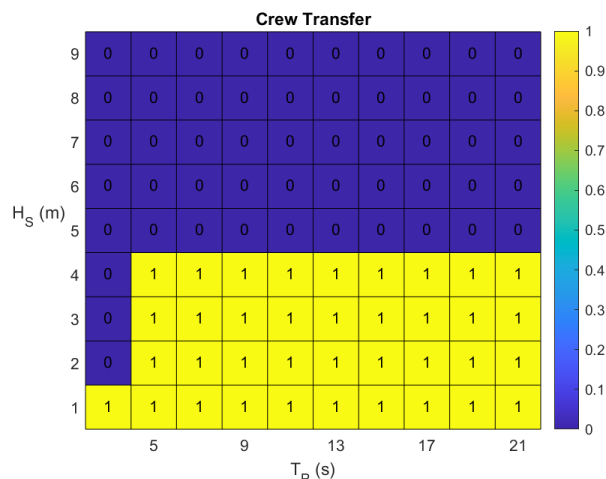


Figure 5-37. Transportability results for the CTV, [Source: FIHAC].

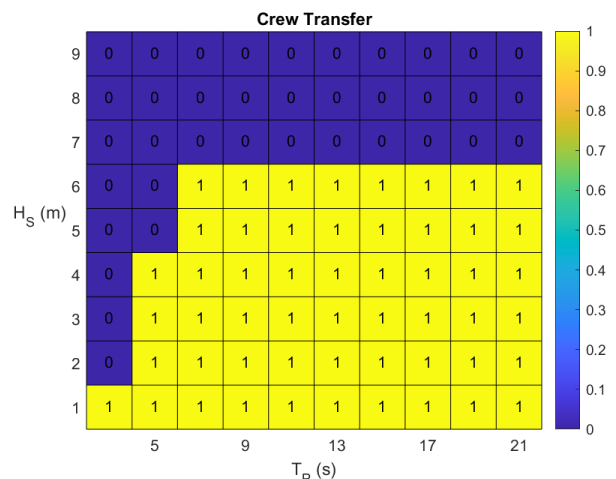


Figure 5-38. Transportability results for the SOV, [Source: FIHAC].

5.4 Accessibility for CTV and SOV

5.4.1 [Accessibility Method](#)

The accessibility methodology is based on the specific landing procedure of the vessel studied. The landing procedure on a floating platform from a CTV is the following:

- The CTV lands on the bumpers mounted on the platform. The platform displaces until the system reaches equilibrium.
- The bow-mounted fender helps in absorbing the impact energy and providing friction at the contact surface.
- O&M technician step-over from the vessel to a platform mounted ladder.
- Access is possible when no-slip conditions occur at the fender and the relative rotations are below limits.



Figure 5-39. CTV in crew transfer manoeuvre [Source: [28]].



Figure 5-40. SOV in crew transfer manoeuvre [Source: Esvagt Faraday].

The landing procedure on a floating platform from a SOV is the following:

- The SOV uses a motion compensated gangway through which crew can walk to the tower (or transition piece), without any contact between the vessel and the turbine structure.
- The gangway helps in providing a path to technicians and limiting motions during transfer.
- O&M technician step-over to the transition piece.
- Access is possible when relative motions between gangway and platform are below compensation limits.

The methodology starts with computing the RAOs of the coupled system consisting of the floating platform and the vessel, see Figure 5-. For the SOV, the RAOs are computed as usual with no mechanical constraints. For the CTV, the fender acts as a ball joint, not allowing relative translations at the contact point. Consequently, for the CTV, the RAOs are computed including a constraint matrix in the system, which allows to find the forces at the contact point.

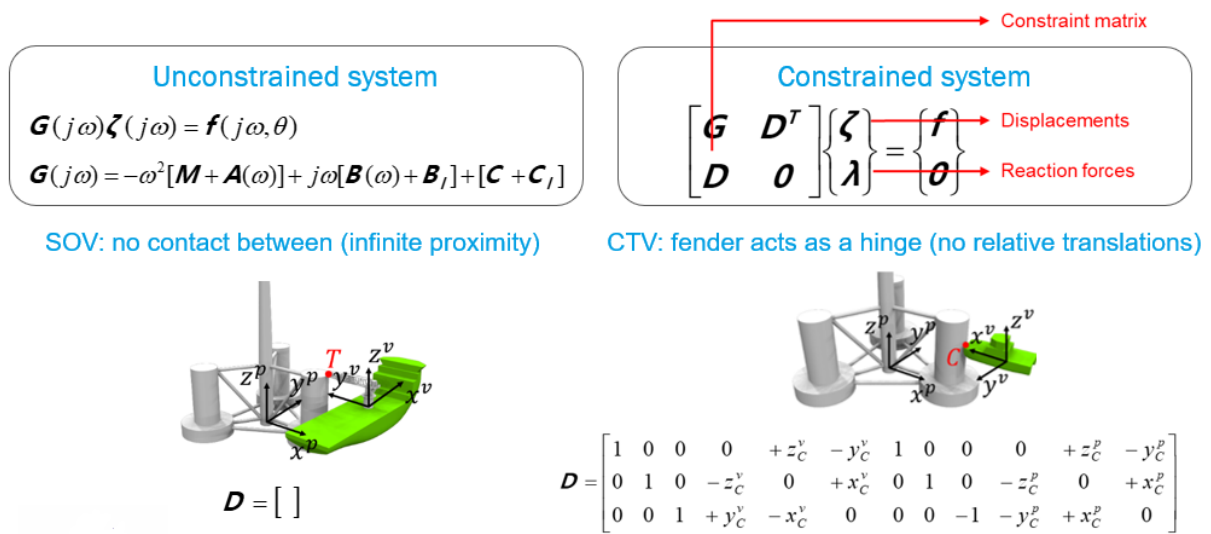


Figure 5-41. Equations used in the computations of the motions and forces response amplitude operators [Source: FIHAC].

Once the RAOs are obtained, they are used to evaluate the crew transfer for a specific sea state. Every sea state is defined with a frequency spectrum and a directional spreading function. The RAOs and the sea state definition are combined following these steps, see also Figure 5-:

- 1) Generate random phases for the wave components in the sea state in order to obtain a free surface time series. Check that the time series meets the statistical properties to be a realistic wave (significant wave height, peak period and maximum wave height).
- 2) With the RAOs and the wave components and their phases, the system movements and forces are reproduced.
- 3) The system movements and forces are analysed to check when the crew transfer restrictions are met, in particular:
 - a. For the CTV, check that the relative rotations are below the thresholds and that the no-slip condition is met. For the no-slip condition, first the normal force on the fender is computed (sum of the trust of the vessel and the joint forces obtained from the RAOs) and, for a given static friction coefficient, it is checked that the tangent forces (obtained from the RAOs) are below the maximum static friction force.
 - b. For the SOV, check that the relative motions at the gangway contact point are below the motion compensation limits.
- 4) Finally, the access windows are found: time intervals of enough length (transfer window length) when crew transfer was found to be possible. To compute the percentage of time for which access is possible, the durations of all these access windows are added up together and divided by the duration of the total sea state. The sea state is considered suitable for crew transfer if this percentage is above a threshold (minimum percentage of access time).

The sea states where the wave height was above the wave breaking limit were not considered suitable for crew transfer, since a sudden snap load on the vessel would risk the personnel.

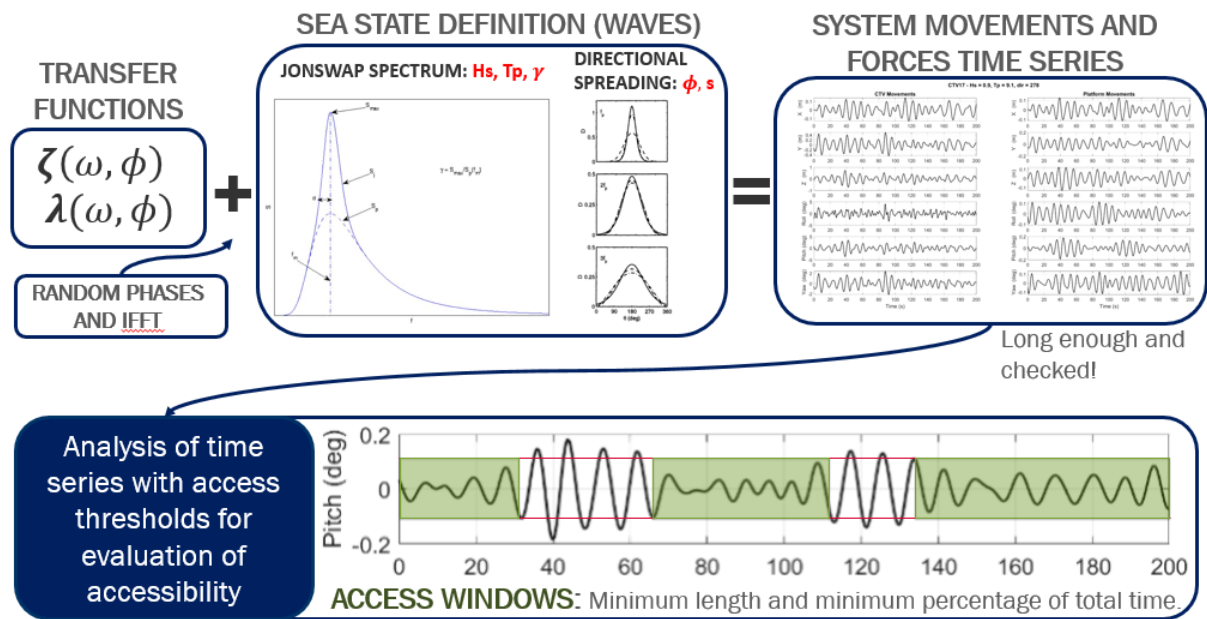


Figure 5-42. Strategy used to evaluate if crew transfer was possible for a sea state [Source: FIHAC].

5.4.2 Accessibility Limits for CTV and SOV

The methodology was applied in two different sites: Grand Canaria Island in Spain (site B) and Morro Bay in the USA (site C). West Barra Island in Scotland (site A) was not analysed in this work because data was incomplete for the study. Two different platforms Windcrete and ActiveFloat are studied, with two different vessels, CTV and SOV. Figure 5- displays the basic information of the used platforms and vessels. Also, the sensitivity of the results to parameters as the viscous damping or the minimum percentage of access time was studied.

ActiveFloat – Site B		ActiveFloat – Site C	
Displacement	36431.22 m ³	Displacement	43755.57 m ³
Operation draft	26.50 m	Operation draft	27.80 m
Central cone base / top diameter	19.6 / 11.0 m	Central cone base / top diameter	20.09 / 11.0 m
Offset columns / heave plates diameter	17.0 / 25.0 m	Offset columns / heave plates diameter	17.4 / 25.4 m
Columns center to tower center	34.0 m	Columns center to tower center	36.0 m
Pontoons width	17.0 m	Pontoons width	17.4 m
Surge / heave / pitch / yaw natural period	163.9 / 18.2 / 32.7 / 81.9 s	Surge / heave / pitch / yaw natural period	163.83 / 18.21 / 32.77 / 81.9 s

WindCrete – Site B		WindCrete – Site C	
Displacement	40540 m ³	Displacement	45570 m ³
Operation draft	155 m	Operation draft	160 m
Central cone base / top diameter	18.60 / 13.20 m	Central cone base / top diameter	19.40 / 14.00 m
Surge / heave / pitch / yaw natural period	81.9 / 32.77 / 40.97 / 10.92 s	Surge / heave / pitch / yaw natural period	81.9 / 32.77 / 40.97 / 13.65 s

CTV		SOV	
Displacement	102 T	Displacement	5568 t
Length / Beam / Draft	24 / 10 / 1.37 M	Length / Beam / Draft	80.0 / 16.45 / 5.64 m
Water plane area	94.45 M ²	Water plane area	1286 m ²
Fender friction coefficient	1.2 -		
Bollard push force	135 kN		
Heave / roll / pitch natural period	3.0 / 3.5 / 4.5 s	Heave / roll / pitch natural period	6.0 / 6.0 / 8.5 s

Figure 5-43. Platforms and vessels characteristics [Source: FIHAC].

The accessibility limits are given in scatter matrices containing combinations of significant wave heights (H_s) and peak periods (T_p). Each H_s - T_p combination was also studied for 16 different wave headings, the matrices of the following figures (Figure 5- to Figure 5-53) display the proportion of headings for which crew transfer was possible.

The operational limits considered for the CTV are maximum relative rotations of 2.5° in roll, 10.0° in pitch and 2.5° in yaw, a transfer window length of 15 s, and a minimum percentage of transfer time of 50%. For the SOV, the motion compensation limits were of 3 m for all relative movements and 10.0° for all relative rotations.

5.4.2.1 Results for Site B: Grand Canaria Island

Figure 5- and Figure 5- display the accessibility results for Windcrete at Gran Canaria, for CTV and SOV, respectively. Figure 5-46 and Figure 5-47 show the results for ActiveFloat. All the presented results are averaged from the different ones obtained for each direction. The accessibility limits as the transportability ones (Section 5.3.5) are imposed by both vessel recommendations ($H_s \leq 4$ m for CTV and $H_s \leq 6$ m for SOV) and the condition of no breaking waves for shorter periods. In general with a CTV, the accessibility to the Windcrete platform (Figure 5-) is higher than to the ActiveFloat platform (Figure 5-46), specially for $H_s = 4$ m. Conversely with a SOV, the accessibility to the Windcrete platform (Figure 5-) is lower than to the ActiveFloat platform (Figure 5-47) for large H_s .

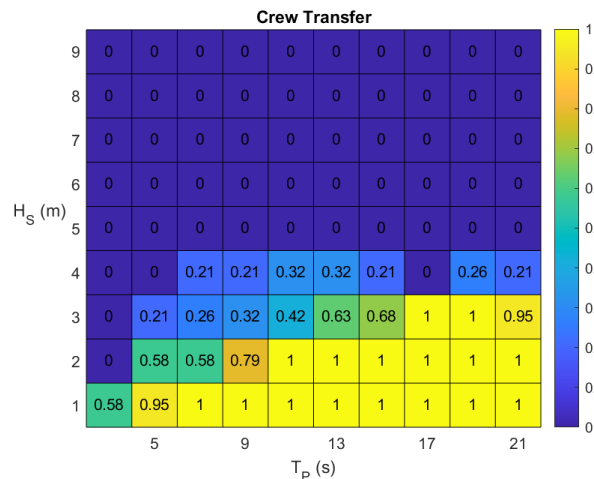


Figure 5-44. Windcrete-CTV accessibility limits for Gran Canaria [Source: FIHAC].

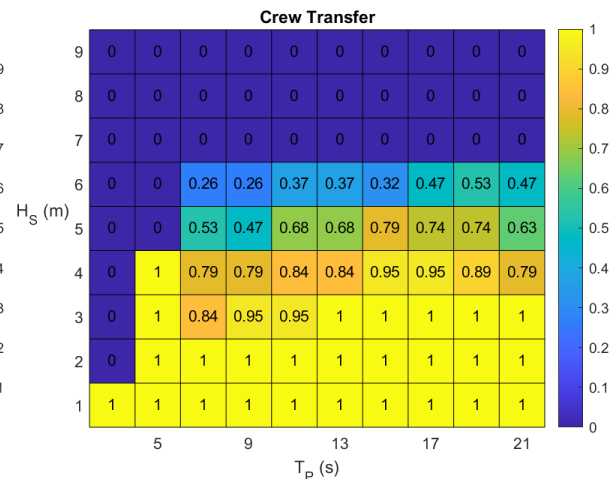


Figure 5-45. Windcrete-SOV accessibility limits for Gran Canaria [Source: FIHAC].

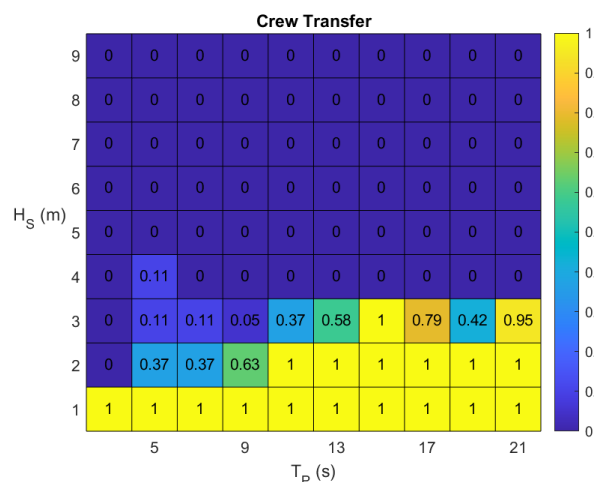


Figure 5-46. ActiveFloat-CTV accessibility limits for Gran Canaria [Source: FIHAC].

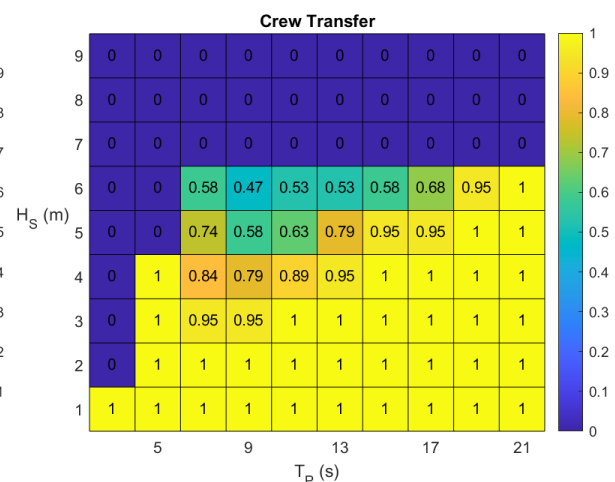


Figure 5-47. ActiveFloat-SOV accessibility limits for Gran Canaria [Source: FIHAC].

5.4.2.2 Results for Site C: Morro Bay

Figure 5-48 and Figure 5-49 compare the results for Windcrete from the previous section with the results at Morro Bay. The discrepancies observed are caused by the water depth difference, which implies different wave breaking limits, different wave forces and different mooring stiffness. For the CTV, it is observed that accessibility is better for shorter periods at Morro Bay, while for the SOV, the accessibility is increased in the longer periods. Over all the discrepancies in the results between both locations are not significantly large.

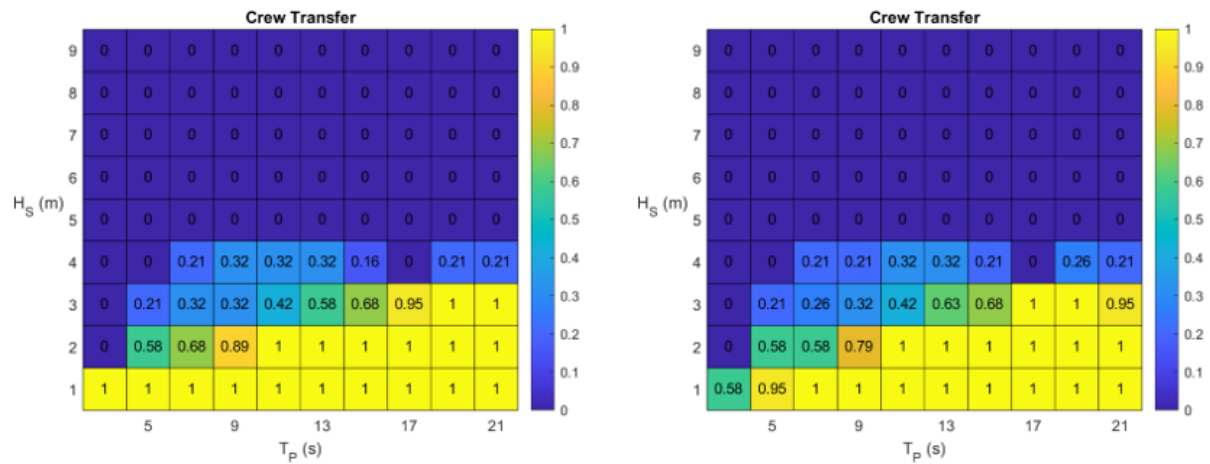


Figure 5-48. Comparison of the Windcrete-CTV accessibility limits of Morro Bay (left) and Gran Canaria (right) [Source: FIHAC].

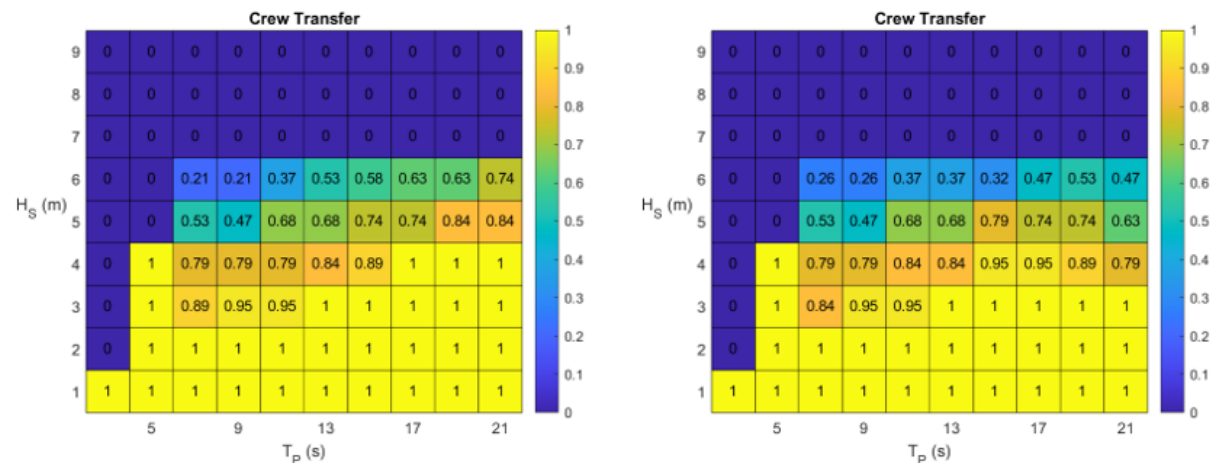


Figure 5-49. Comparison of the Windcrete-SOV accessibility limits of Morro Bay (left) and Gran Canaria (right) [Source: FIHAC].

Figure 5-50 and Figure 5-51 compare the results for ActiveFloat from the previous section with the results at Morro Bay. With this platform for the CTV, it is observed that accessibility is worse for shorter periods at Morro Bay, while for the SOV, the accessibility is decreased in the longer periods. In the latter SOV results, the discrepancies between both locations are larger.

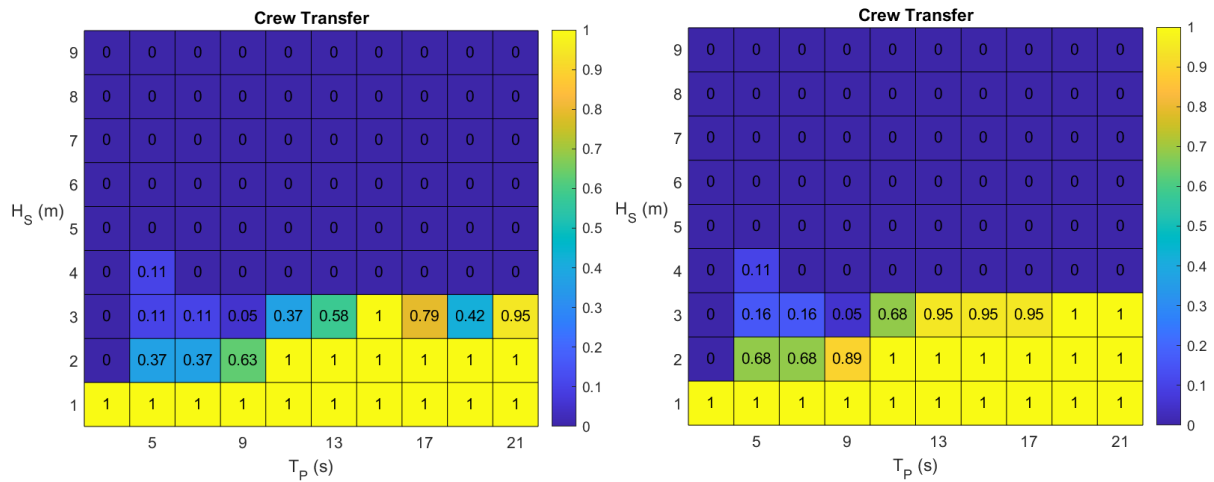


Figure 5-50. Comparison of the ActiveFloat-CTV accessibility limits of Morro Bay (left) and Gran Canaria (right) [Source: FIHAC].

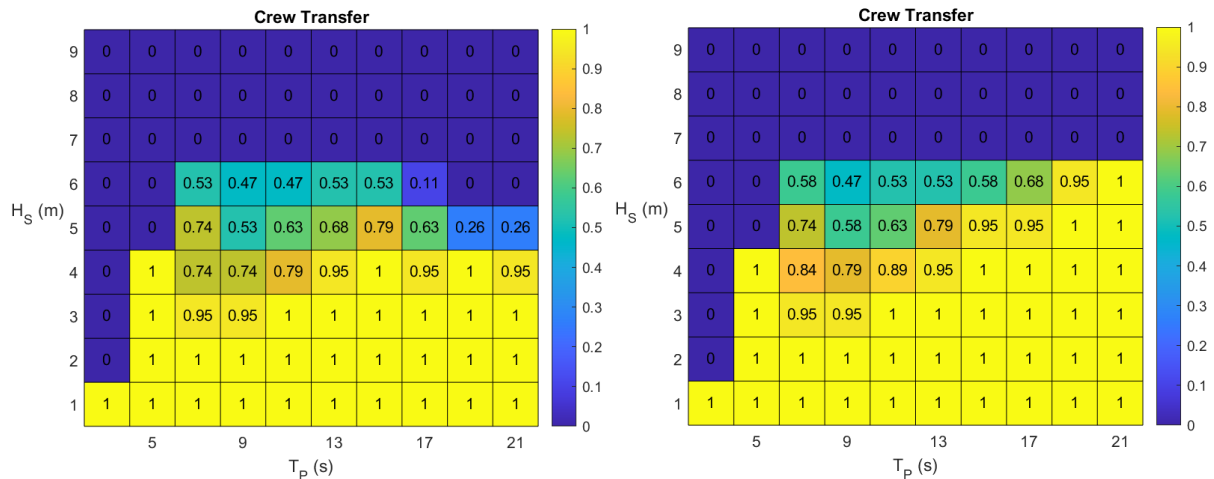


Figure 5-51. Comparison of the ActiveFloat-SOV accessibility limits of Morro Bay (left) and Gran Canaria (right) [Source: FIHAC].

5.4.2.3 Sensitivity Analysis to Viscous Damping

Figure 5-52 compares the accessibility results for Windcrete and CTV at Gran Canaria with low (3.5%) and high (7.0%) damping coefficients (fraction of critical damping). As expected, with higher viscous damping, the movement amplitudes are lower and the accessibility increases. This is specially observed for large periods, where accessibility is ensured for H_s of 3 m.

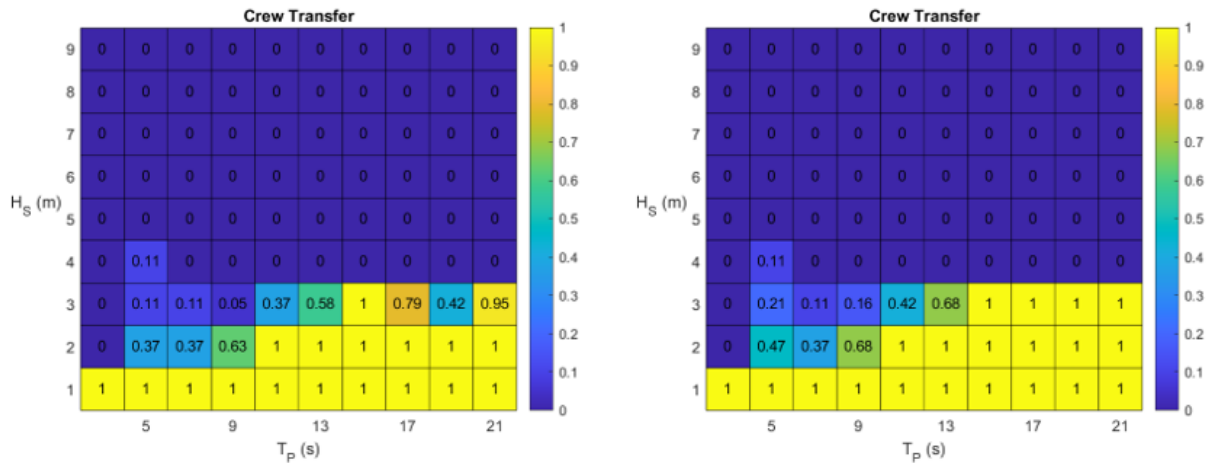


Figure 5-52. Comparison of the Gran Canaria Windcrete-CTV accessibility limits with viscous damping coefficient of 3.5% (left) and 7% (right) (fractions of critical damping) [Source: FIHAC].

5.4.2.4 Sensitivity Analysis to Lower Transfer Time

Figure 5-53 compares the accessibility results for Windcrete-CTV at Gran Canaria with low (25%) and high restriction (50%) on the minimum percentage of access time. With the lower restrictions, the accessibility limits increase, as expected. In this sensitivity analysis the accessibility limits increase significantly, rising from 2 m to 4 m for the longer wave periods.

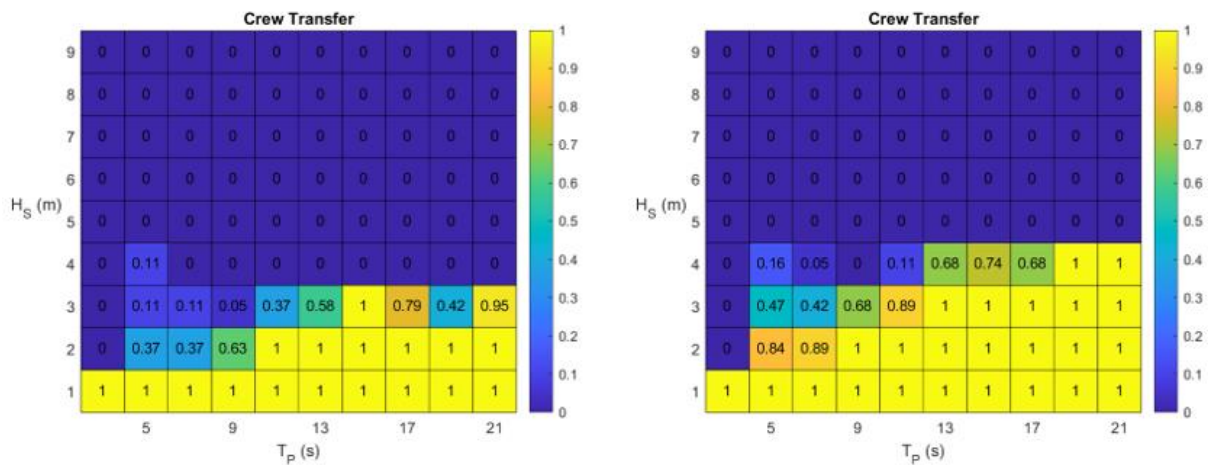


Figure 5-53. Comparison of the Gran Canaria Windcrete-CTV accessibility limits with a minimum proportion of transfer time of 50% (left) and 25% (right) [Source: FIHAC].

6 Results and Interpretation

As discussed in Chapter 4, the Morro Bay site is taken as reference site for the parameter analysis of Section 6.1. The convergence behaviour in section 6.1.1, as well as the sensitivity analysis from Section 6.1.2, are performed on the baseline scenario considering that the access is performed via bow-transfer with a CTV, and that the major component exchanges are executed inshore (tow-in strategy). In contrast, the impact analyses of Section 6.2 and 6.3 are performed for all three sites.

The targeted availability metrics (i.e. TBA and PBA, see chapter 4) in the simulation scenarios are set to 98.0%. The baseline scenario at Morro Bay was tuned as such that this availability target is achieved. The variables influencing the availability are the number of CTVs and personnel. Furthermore, the OPEX estimate has to lie within a realistic range. The ORE Catapult evaluation in [29] is taken as a comparative value, considering the average operating costs per megawatt and year of about 90,000 €.

6.1 Parameter Analysis

A sensitivity analysis is conducted to evaluate the influence of the following settings: vessel dayrates, mobilization costs, failure rates, and personnel costs. The variation in the overall OPEX is measured for changes of the input parameters values of + 10% of their baseline reference value.

6.1.1 Monte Carlo Convergence Behaviour

The Shoreline simulation engine performs time-based modelling and probabilistic forecasting of failure events. The failure events are calculated based on an exponential failure distribution of each of the turbines' component. Due to the probabilistic approach, deviations in the calculated failures lead to different outcomes for the KPIs of availability and OPEX. To stochastically reduce the deviation in the simulation results, multiple runs are performed for each simulation, following a Monte-Carlo approach. After analysing the convergence behaviour of the simulation tool, 70 runs have been found to be sufficient to guarantee a small deviation, with a maximum variation of 0.5% on the OPEX, and of 0.4% on the availabilities. The decreasing trend of OPEX and availability variations can be observed in Figure 6-1 and Figure 6-2 for the increasing number of runs per simulation.

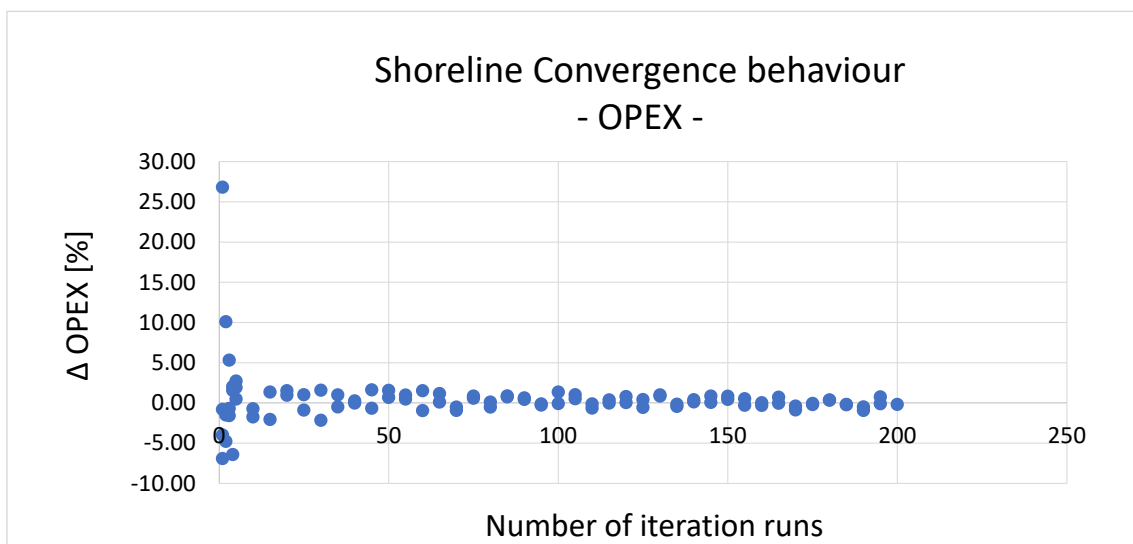


Figure 6-1: Convergence behaviour of the simulation engine for the baseline scenario, displaying the change in OPEX [%] over the number of iterations [Source: Ramboll].

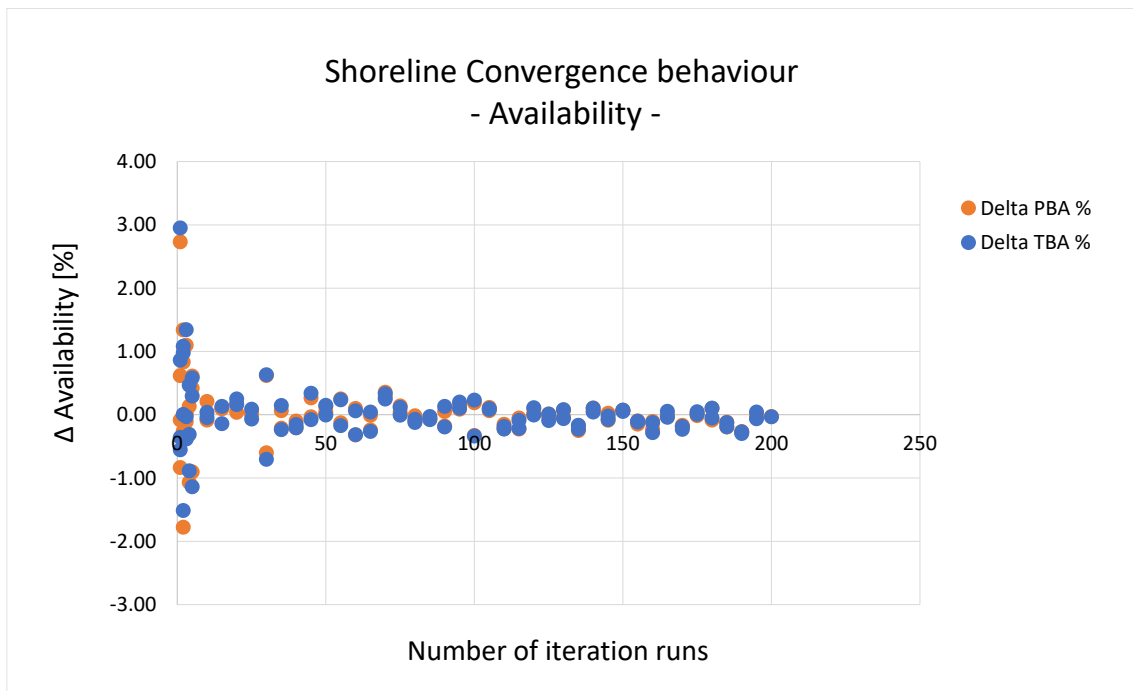


Figure 6-2: Convergence behaviour of the simulation engine for the baseline scenario, displaying the change in production-based and time-based availability [%] over the number of iterations [Source: Ramboll].

6.1.2 Sensitivity Analyses

A certain degree of uncertainty cannot be ruled out for the majority of the inputs. For this reason, a first sensitivity study is carried out (see section 6.1.2.1) for the most relevant parameters. The input parameters of the simulation can affect the results in different ways and with a varying impact on OPEX and availability metrics. A sensitivity analysis helps to identify those parameters whose deviation, even when small, affect at most the output results. Additionally, the preliminary studies of Chapter 5 indicated a higher and a lower bound of the operational limits of the floating crane vessel, the CTV and the SOV. In a separate sensitivity analysis (see section 6.1.2.2), the limit influences the final result of the simulation is investigated.

6.1.2.1 Sensitivity of Relevant Input Parameters

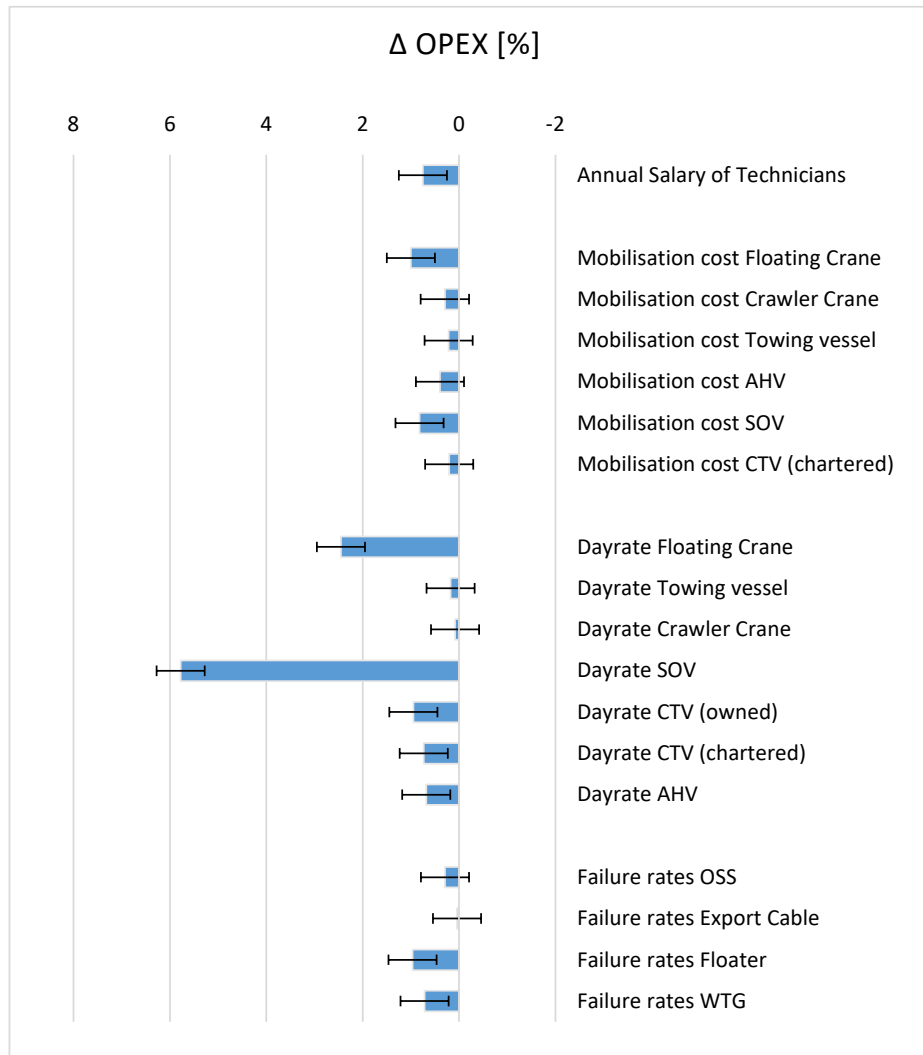


Figure 6-3: Sensitivity study displaying the change in OPEX [%] for an increase of 10 % of different input parameters. Error bars indicating the ± 0.5 % uncertainty of the OPEX results of the simulation tool [Source: Ramboll].

The sensitivity study presented in Figure 6-3 is performed on all parameters on the baseline scenario, except for the impact of the floating crane vessel, which is studied in the F2F scenario described in Section 6.2. The procedure consisted of increasing each one of these parameters' value by 10 %, while keeping the others unchanged. It can be observed that, especially for the deployment of SOV, the dayrate has a remarkable impact on the OPEX. In the baseline scenario, the SOV is only used for the subsea repairs and inspections, when a ROV is required. The high impact of its dayrate can be explained by the fact that these campaigns require long chartering times of the vessel. It can be further noticed that the mobilisation costs and the dayrate of the floating crane vessel have a significant impact on the OPEX. This is relatable to the high cost of the floating crane (see Table 4-10), for which a 10% only increase can already cause a noticeable variation of the overall OPEX.

In conclusion, the vessel prices fluctuate strongly and are dependent on the current demand on the market. The variability of the vessel costs can have a strong impact on the total operational costs of a floating wind farm.

6.1.2.2 Sensitivity of Weather Windows

The sensitivities on the floating crane vessel, CTV and SOV operability limits are described in the following paragraphs.

Floating Crane Vessel

Figure 6-4 shows the influence of the weather window boundaries for the monohull (HLCV) and semi-submersible floating crane vessel (SSCV) on the TBA and PBA of the wind farm. It indicates the percentage deviation of the availability of the wind farm compared to the reference case. Figure 6-5 shows this percentage deviation for the lifetime OPEX. The SSCV scenario for medium weather limits is used as a benchmark for the other results. It looks clear from the graph that either the lowering or the raising of the weather limits of the SSCV only slightly affects the wind farm availability metrics. By contrast, the weather limits of the HLCV are more restrictive than the one of the SSCV. Thus, their variation leads to availability losses almost 40% higher than those of the SSCV. The differences between the low, medium and high weather criteria are more dominant for the HLCV than for the SSCV.

A significant deviation of the wind farm availability between both floater types is observed, in Figure 6-4, for the high boundary conditions of the HLCV. When comparing the high motion limits in Figure 5-21 and Figure 5-23 of section 5.1, it becomes clear that the Windcrete weather window is restricted by 2 sea state combinations at a wave height of 2.0 m and 2.5 m and a T_p of 8 s. These conditions are, however, operable for the ActiveFloat. A comparison with the weather time series at Morro Bay shows that these two sea states account for 58% of the available weather window of ActiveFloat. Restricting them for the heavy lift operation at the Windcrete floater results in a reduction of the weather windows and thus of the wind farm availability. The further reduction of the weather windows by the medium and low motion limits of the HLCV does not result in such a strong gradation anymore. It is therefore necessary to have in particular the frequent sea states included in the possible weather windows of the floating crane vessel in order to favour a high availability of the wind farm.

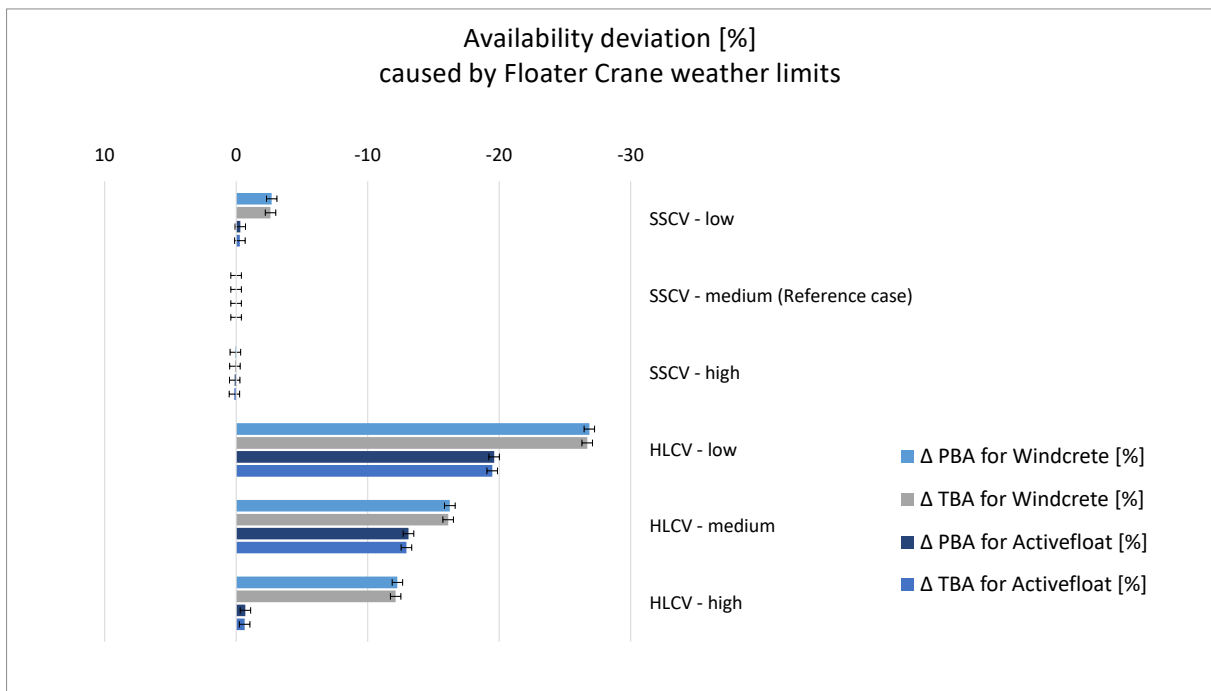


Figure 6-4: Influence of the weather window boundaries for the monohull (HLCV) and semi-submersible floating crane vessel (SSCV) on the time-based availability (TBA) and production-based availability (PBA) for the Windcrete and ActiveFloat substructure. Error bars indicating the $\pm 0.4\%$ uncertainty of the availability results of the simulation tool [Source: Ramboll].

As for the availability metrics, changes in OPEX can be observed in Figure 6-5 when altering the weather limits of the floating crane vessels to a higher and a lower limit. For the lower, and thus more severe, the OPEX increases. This can be explained by the fact, that smaller weather windows for the component replacements cause longer waiting times, increasing the downtimes and the vessel costs, as the maintenance actions are interrupted to be finished at a later stage. Higher limits, and thus bigger weather windows, are related to an amelioration of the OPEX compared to the medium or low limits. It can be observed that the monohull crane vessel does have the stricter limits causing higher OPEX throughout the lifetime.

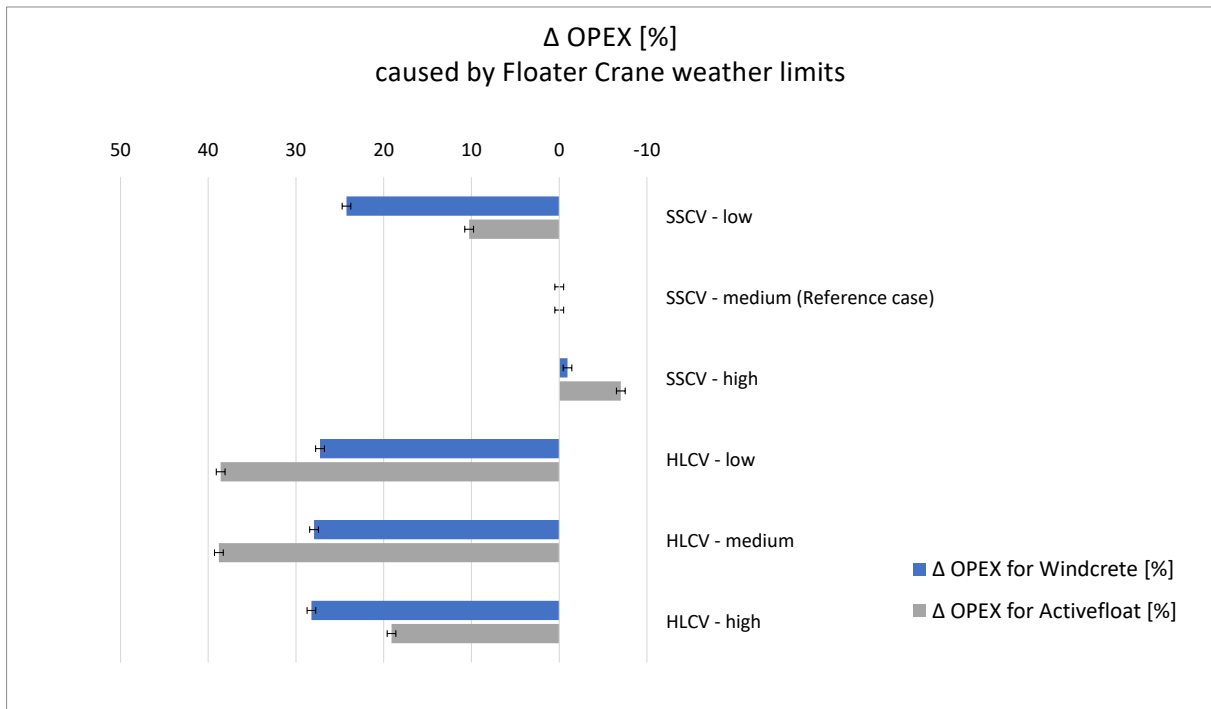


Figure 6-5: Influence of the weather window boundaries for the monohull (HLCV) and semi-submersible floating crane vessel (SSCV) on the lifetime OPEX for the Windcrete and ActiveFloat substructure. Error bars indicating the ±0.5 % uncertainty of the OPEX results of the simulation tool [Source: Ramboll].

In conclusion to the observations from this sensitivity study, **the SSCV with the medium weather limits is chosen for the scenario analyses at the three sites**, presented in the following sections. The medium weather limit follows the recommendation from industry on the crane compensation limits to be applied on the operational scatter tables of the floating crane vessels (see Section 5.1.5). It is seen as the most realistic weather limitation.

Crew Transfer Vessel and Service Operation Vessel

To study the sensitivity on the weather limits of the SOV and CTV, the limits identified in Section 5.4.2 are used to set lower and higher boundaries for the acceptable sea states in the scatter tables. The “low” boundary condition allows the access of the CTV and the SOV only if the accessibility in the scatter table is equal 1. This is set as the reference case against which the “high” boundary condition is compared to. The “high” condition includes all the H_s-T_p combinations for which the accessibility is not zero (> 0).

Figure 6-6 and Figure 6-7 show only a very small deviation of the OPEX and the availability metrics for both floaters in either cases.

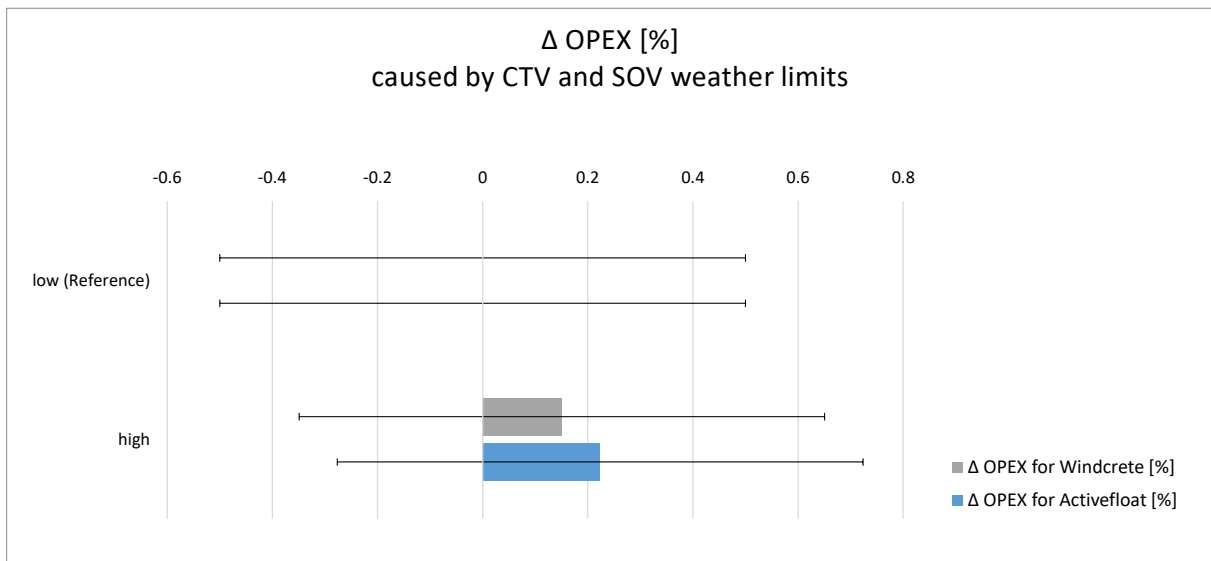


Figure 6-6: Influence of the weather window boundaries for the CTV and SOV on the lifetime OPEX for the Windcrete and ActiveFloat substructure. Error bars indicating the ± 0.5 % uncertainty of the OPEX results of the simulation tool [Source: Ramboll].

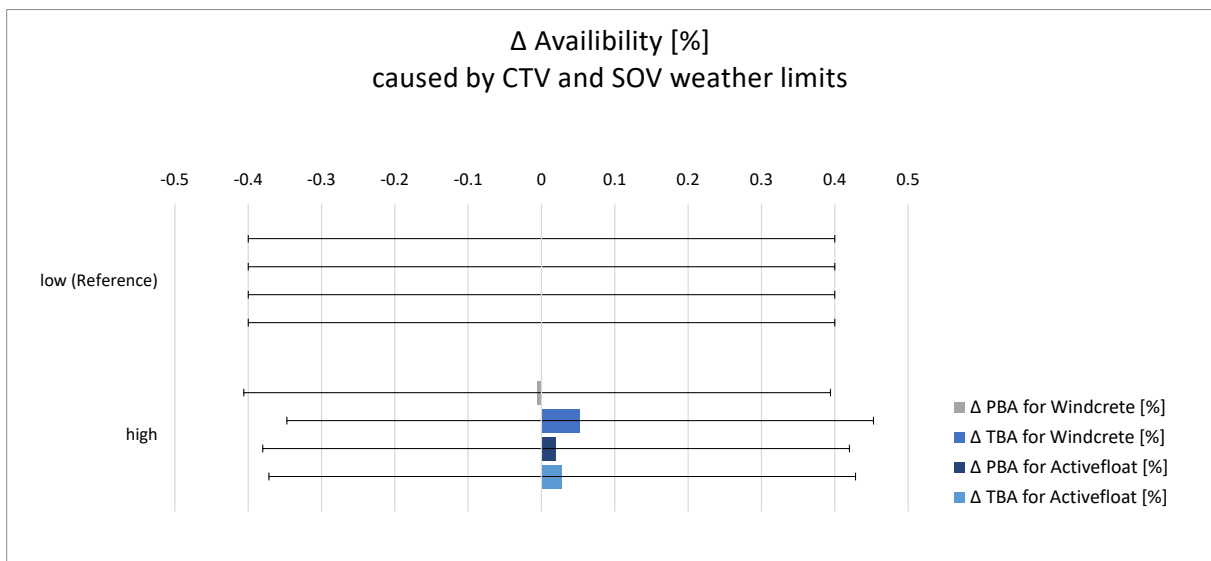


Figure 6-7: Influence of the weather window boundaries for the CTV and SOV on the time-based availability (TBA) and production-based availability (PBA) for the Windcrete and ActiveFloat substructure. Error bars indicating the ± 0.4 % uncertainty of the availability results of the simulation tool [Source: Ramboll].

However, the influence of the weather limitation is noticeable in the accessibility of each vessel type. Figure 6-8 shows a clear reduction in the number of days during which the wind turbines can be accessed via CTVs and SOVs when applying the lower (and more conservative) weather limits. This means that there are less weather windows available for the maintenance actions. For the other vessels, the weather limits remained unchanged and so did their accessibility. It can be noticed, in Figure 6-7, that the change in the accessibility for the SOV and CTV has a very low impact on the availability, meaning that there are enough vessels available to compensate the lack of weather windows.

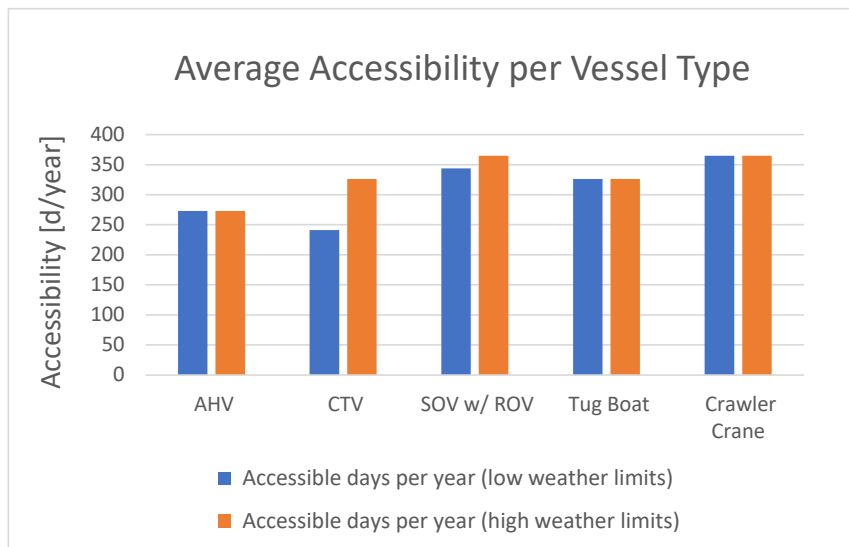


Figure 6-8: Impact of weather limit on wind turbine accessibility [Source: Ramboll].

In conclusion to the observations from this sensitivity study, the **low SOV and CTV weather limits are chosen for the scenario analyses at the three sites**, presented in the following sections. The more conservative weather limits are preferred to the optimistic limits due to the low impact the latter would have on the wind farm KPIs.

6.2 Influence of Major Component Exchange Strategy on Lifetime OPEX

The first scenario analysis focusses on the question: “Which strategy for the major component exchange is more favourable for a large commercial-size floating offshore wind farm: tow-to shore (tow-in) with a major component exchange in calm waters (at quayside), or a heavy lift operation offshore using a floating crane vessel?”.

To give an indicative answer to this question the baseline scenario for a tow-to-shore strategy is compared to the offshore heavy lift scenario (F2F). The following table gives an overview of the inputs used for the simulated processes.

Table 6-1: Durations of the major component exchange operations for the tow-in scenario (tug boat) and the F2F scenario (floating crane vessel), according to inhouse expertise.

Vessel Type	Mobilisation [h]	Demobilisation [h]	Tow-in Preparation at Port [h]	Mooring Line and Cable Hook-off [h]	Tow-out Preparation at Port [h]	Mooring Line and Cable Hook-on [h]
Tug Boat	1	1	8	3	8	3
Floating Crane	8	8	-	-	-	-

6.2.1 Simulation Results

The results of the influence of major component exchange strategy are summarised in the following tables for site A, B and C. As mentioned in simulation scenario description (Section 4.2) a maintenance tow-in is not foreseen for the Windcrete floater, due to the draft of the spar structure and potential port restrictions in (see also the description of the maintenance strategy in the design basis [11] based on partial submersion of the Windcrete spar for major repairs). Nevertheless and for the sake of completeness, the theoretical scenario of a tow-in solution was modelled.

Site A – West of Barra

Table 6-2: Tow-in vs. F2F – Availability, OPEX and Lost Production results at West of Barra for ActiveFloat.

Floater Type	Scenario	TBA [%]	PBA [%]	Total OPEX [€]	OPEX [€/MW/yr]	Lost Production [MWh]
ActiveFloat	Tow-in	39.70	39.62	1,920,991,987	64,033	106,767,911
	F2F	34.30	34.08	4,524,359,112	150,812	116,556,903

Site B - Gran Canaria

Table 6-3: Tow-in vs. F2F – Availability, OPEX and Lost Production results at Gran Canaria for ActiveFloat and Windcrete.

Floater Type	Scenario	TBA [%]	PBA [%]	Total OPEX [€]	OPEX [€/MW/yr]	Lost Production [MWh]
ActiveFloat	Tow-in	98.70	98.95	2,316,419,630	77,214	1,910,026
	F2F	98.68	98.91	2,530,931,822	84,364	1,967,521
Windcrete	Tow-in*	98.70	98.96	2,319,154,711	77,305	1,892,913
	F2F	98.67	98.90	2,533,618,601	84,454	1,986,517

*Theoretical scenario due to draft of Windcrete spar and port restrictions.

Site C - Morro Bay

Table 6-4: Tow-in vs. F2F – Availability, OPEX and Lost Production results at Morro Bay for ActiveFloat and Windcrete.

Floater Type	Scenario	TBA [%]	PBA [%]	Total OPEX [€]	OPEX [€/MW/yr]	Lost Production [MWh]
ActiveFloat	Tow-in	98.63	98.97	2,333,482,615	77,782	1,275,433
	F2F	98.39	98.74	2,961,801,300	98,726	1,560,215
Windcrete	Tow-in*	98.62	98.96	2,334,512,981	77,817	1,283,326
	F2F	98.02	98.33	3,494,669,406	116,489	2,067,675

*Theoretical scenario due to draft of Windcrete spar and potential port restrictions.

Looking at these results, one can observe that for the site of Morro Bay and Gran Canaria the availabilities lie above the target of 98%. The achieved OPEX for these cases range between 77.000 €/((MW/year) and 116.000 €/((MW/year), which is a realistic range comparing it to the reference OPEX of ~90.000 €/((MW/year) by ORE Catapult [29], of 90.000 €/((MW/year)., of 90.000 €/((MW/year). Only the site of West of Barra shows an availability loss above 60% and unrealistic OPEX values, for both the tow-in and F2F cases. This is due to the very harsh weather conditions at the site. In combination with the applied weather limits of the vessels, only very small weather windows are available. The simulation results for West of Barra show that no replacements could be performed, which leads to unfinished workorders and downtimes. Summarizing these over the lifetime causes the availability losses. The extremely high OPEX for the F2F case is due to the fact that the expensive crane vessel is chartered but cannot sail out, adding up the dayrates during the waiting time. This does not reflect a realistic scenario for West of Barra. Under the weather conditions of that site cost-effective maintenance activities cannot be performed. Neither one of the two major component exchange strategies appear advantageous in this harsh environment.

At Gran Canaria, the differences in OPEX and availability metrics for the two floater types are low. In the case of Morro Bay, the slightly harsher environment, in combination with the slightly more severe weather limits when

considering the Windcrete structure, achieves a higher OPEX for the F2F scenario than for the ActiveFloat system. In contrast, similar values between Windcrete and ActiveFloat are seen for the tow-in scenario.

When comparing the two strategies for major component exchange, the **tow-in scenario presents in all cases a lower OPEX for almost the same availabilities.**

6.2.2 Outlook and Conclusion

The results lead to the conclusion that the tow-in solution for the major component exchange is the more favourable option for both floater types. However, it shall be noted that the tow-in operation highly depends on the distance to a suitable port, having the required capacities and infrastructure. The draft of the Windcrete spar buoy is very deep, therefore, it might not be suited for a tow-in to a harbour facility. Alternative solutions are either to tow the spar to a location with smoother weather conditions but sufficiently deep waters to perform the lifting operation, or to use a floating crane vessel for onsite heavy lift maintenance. Furthermore, the OPEX of the F2F solution highly depend on the vessel dayrates and mobilisation costs. As the vessel costs vary significantly depending on the market situation, it is difficult to make tangible assumptions on their actual value. Lower costs are possible, and they would make the OPEX for the scenario of using the crane vessel more attractive. In addition, considering the discussion in Section 5.1.5.2, less conservative assumptions for the operational limits of the floating-to-floating heavy lift maintenance operation – by using optimal orientation between FOWT and crane vessel - would have a positive effect on the resulting OPEX.

6.3 Influence of Vessel Type on Lifetime OPEX

The second scenario studies the influence of using the bow-transfer method, or alternatively a motion compensated gangway to access the wind turbines. The access from a moving vessel to a ladder attached to a floating substructure is challenged by the relative motions between both bodies, which needs to be compensated to ensure a safe passing of the personnel.

Two methods exist for personnel transfer. The most common one is the access method via bow-transfer (see Figure 6-9) where the fender-protected bow of the CTV pushes against the boat landing of the substructure [30]. The thrust force creates a friction, at the point of contact, strong enough to compensate the heave motions induced by the waves. The time for the transfer of the personnel is often short because the CTV can, on occasion, lose its position due to too large waves or current, [31].

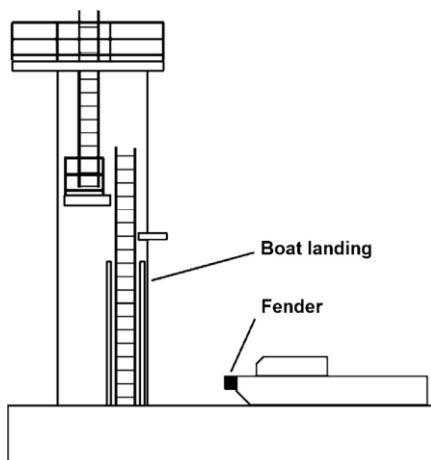


Figure 6-9: Access via bow-transfer method, [32] adapted by [30].

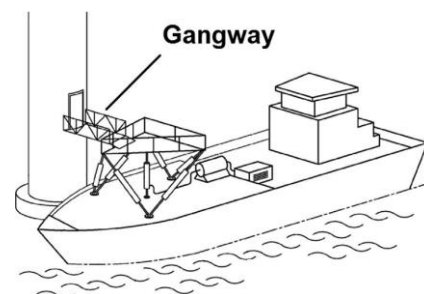


Figure 6-10: Access via motion compensated gangway, [33] adapted by [30].

The access using the motion compensated gangway requires larger vessels, like SOVs, to carry the gangway support structure (see Figure 6-10). The gangway is an extendable bridge to carry personnel and cargo which is

attached to the external platform of the wind turbine. The hydraulic system in the support structure of the gangway compensates the motions of the vessel. This allows a safe transfer of the maintenance crew over a stationary bridge. The access is possible at higher sea states, in which the bow-transfer would not be feasible anymore, [31], [30].

6.3.1 Simulation Results

The results for the influence of access strategy are summarised in the following tables for site A, B and C.

Site A – West of Barra

Table 6-5: CTV vs. SOV – Availability, OPEX and Lost Production results at West of Barra for ActiveFloat.

Floater Type	Scenario	TBA [%]	PBA [%]	Total OPEX [€]	OPEX [€/MW/yr]	Lost Production [MWh]
ActiveFloat	CTV	39.70	39.62	1,920,991,987	64,033	106,767,911
	SOV	32.00	31.69	1,486,073,108	49,536	120,796,218

Site B - Gran Canaria

Table 6-6: CTV vs. SOV – Availability, OPEX and Lost Production results at Gran Canaria for ActiveFloat and Windcrete.

Floater Type	Scenario	TBA [%]	PBA [%]	Total OPEX [€]	OPEX [€/MW/yr]	Lost Production [MWh]
ActiveFloat	CTV	98.70	98.95	2,316,419,630	77,214	1,910,026
	SOV	98.74	98.98	2,353,124,153	78,437	1,847,794
Windcrete	CTV	98.70	98.96	2,319,154,711	77,305	1,892,913
	SOV	98.73	98.99	2,339,995,187	78,000	1,837,044

Site C - Morro Bay

Table 6-7: CTV vs. SOV – Availability, OPEX and Lost Production results at Morro Bay for ActiveFloat and Windcrete.

Floater Type	Scenario	TBA [%]	PBA [%]	Total OPEX [€]	OPEX [€/MW/yr]	Lost Production [MWh]
ActiveFloat	CTV	98.63	98.97	2,333,482,615	77,783	1,275,433
	SOV	98.66	98.95	2,211,357,787	73,712	1,293,430
Windcrete	CTV	98.62	98.96	2,334,512,981	77,817	1,283,326
	SOV	98.67	98.97	2,205,546,597	73,518	1,269,712

The results show that the availabilities for the Morro Bay and Gran Canaria sites are all above the target value of 98.0 %. The OPEX realised for these cases range from 73,000 €/MW/year to 78,000 €/MW/year, a range lying below the reference OPEX of ORE Catapult, [20], of 90.000 €/MW/year). Only the site of West of Barra shows again a significant availability loss above 60% associated with unrealistic OPEX values for both the SOV and CTV-access case. This is due to the same reasons described earlier for the major component exchange impact study, in section 6.2.1. The harsh weather conditions of West of Barra do not allow for any maintenance actions. As major component exchange strategy, in both Access-scenarios the tow-in solution of the baseline scenario is applied. As no replacements and very little maintenance work are performed, low maintenance costs apply causing an unrealistically small OPEX. Changing the strategy from CTV use to SOV use for the day-to-day maintenance activities, does not improve the availability nor the OPEX results. This leads to the conclusion that

under the weather conditions of the site West of Barra, no cost-effective maintenance activities can be performed. None of the two access solutions show a clear advantage against the other in this harsh environment.

At Gran Canaria the differences in OPEX and availability for the two floater types are negligibly small. In the case of Morro Bay no real difference can be observed between the floater types for both scenarios. This means that the difference in the weather limitations of the two floaters for the SOV and the CTV-access has a small impact on the weather window only, such that it is not visible in the results.

When comparing the two access strategies – i.e. the bow-transfer (CTV) against motion compensated gangway (SOV) – it can be noted that **the SOV scenario gives better results at Morro Bay. At Gran Canaria the results are very similar but slightly better for the CTV case.**

6.3.2 [Outlook and Conclusions](#)

The results lead to the conclusion that for Morro Bay the access using a motion compensated gangway (SOV) is more favourable for either floater type. At Gran Canaria accessing the turbine via bow-transfer and by using CTVs is recommended. Due to the bad weather conditions, no clear recommendation can be made for the site of West of Barra.

6.4 Optimised Scenario for Each Floater Type at Each Site

The impact analyses of the previous section have provided valuable information on the influences of different strategic O&M approaches on the wind farm KPIs and how they are affected by the FOWT type and the site location. This information is now used to conclude on the best (“optimised”) major component exchange and accessibility strategy for each floater type at each site. The intention is to provide a general conclusion on the most promising strategies.

The findings presented in chapter 6.2 and 6.3 have shown that no reasonable results could be extracted for site A (West of Barra). This site is therefore excluded from the selection of an optimal scenario. For site B (Gran Canaria) - for either the Windcrete and ActiveFloat floater type - the combination of towing the floaters for inshore major component exchange, together with deploying a CTV to perform the daily maintenance campaigns, is the most favourable option. At site C (Morro Bay) the tow-in solution also leads to better results and is most favourable in combination with the access via motion compensated gangway, using a SOV for the corrective and scheduled maintenance.

At this point it shall be noted that the draft of the Windcrete floater presents technical challenges that were not considered in detail in this assessment. The results are therefore theoretical. In reality, the turbine would be towed to a location with calmer weather conditions but sufficiently deep waters to perform the lifting operation, or a floating crane vessel would be deployed on site.

The most optimal scenarios of both sites and for both floaters, and their resulting OPEX and availabilities, are listed in Table 6-8.

Table 6-8: Optimised O&M scenarios for Site B (Gran Canaria) and C (Morro Bay).

Optimised Scenario				Availability		OPEX		Lost Production	
Site	Floater Type	Major Exchange Strategy	Access Vessel	TBA [%]	PBA [%]	Per Lifetime [€]	Per MW and Year [€/MW/yr]	Per Lifetime [MWh]	Per MW and Year [MWh/MW/yr]
B	ActiveFloat	Tow-in	CTV	98.70	98.95	2,316,419,630	77,214	1,910,026	63.67
	Windcrete	Tow-in*	CTV	98.70	98.96	2,319,154,711	77,305	1,892,913	63.10
C	ActiveFloat	Tow-in	SOV	98.66	98.95	2,211,357,787	73,712	1,293,430	43.11
	Windcrete	Tow-in*	SOV	98.67	98.97	2,205,546,597	73,518	1,269,712	42.32

**Theoretical scenario due to draft of Windcrete spar and potential port restrictions.*

7 Validation with Real O&M Data and Experience

The findings of Chapter 6 are validated below with experience for O&M in real floating wind farms.

7.1 O&M Experience in Real Floating Wind Farms

The floating wind farm operators taking part in the COREWIND project, shared insights on the operation and maintenance phase of floating wind farms. For confidentiality reasons, the operators and the name of the respective wind farms remain anonymous. Based on their experience, floating offshore wind farms face some specific challenges compared to bottom fixed wind farms, due to some extra equipment and the coupling between the wind turbine and the platform. These challenges lead to an additional effort and cost for the O&M contractor into preventive and corrective maintenance tasks.

The floating platform can include a system to compensate for rotational motions resulting from turbine thrust. The potential failures of this system - requiring pumps, instrumentations and control system, communications, as well as sensors - can be reduced by its preventive maintenance. Its inspections will be performed periodically. Likewise, these components can have unexpected issues resulting in downtimes of the wind turbine and minor corrective actions. To increase the availability, and shorten the repair times, it is recommended to have the most common spare parts and the personnel ready to solve the failure. How well this recommendation may be implemented depends on available weather windows and the wind farm location.

The floating substructure has dedicated scheduled inspections. According to DNVGL-ST-0119 [34] the time interval for periodic inspections shall be at most 5 years, if the Design Fatigue Factor (DFF) is applied as specified in Section 7 of [34]. The periodic inspections of the floating substructure at one of the wind farms are performed every 3 years. Furthermore, annual above-water-inspection are performed on the steel structures. The subsea inspection runs during one week, if and when the weather conditions are appropriate. The execution of these inspections differs between the operators using ROVs and divers for the subsea inspections respectively. It is expected that larger wind farms will enable to mitigate the investment in ROVs against divers. In one of the wind farms, for the time being, divers are performing the inspections. The operators suggest that in the future the subsea inspections should be improved because the ROVs can smooth the process and reduce Health & Safety (HSE) requirements. In other wind farms, where no divers are required anymore, different ROV types perform the underwater inspections. According to the operators, ROVs are able to carry out almost every offshore operation, making it possible to replace all diver operations relevant for the inspection campaigns. The high HSE risk associated with diving campaigns would thus be removed.

Conventional ROVs are tethered to a vessel for the inspection of the mooring chains, the floating substructures and the in-field cables including the J-tubes. In shallow water below a depth of 30 m a USV equipped with a sonar and multi-beam echo is used to inspect the export cable. It is controlled remotely by an onshore operation control centre and does not require a support vessel. In deeper water and higher currents much larger and heavier work-class ROVs are used.

In the future, it is likely that a risk-based 5-year inspection schedule is going to be followed, to check the integrity of the mooring system at different turbines location in different years. If defects are identified they will be tracked and an educated assumption (extrapolation) for the other turbines will be made.

Regarding the O&M operation, the coupling between the wind turbine and the platform is essential due to the nacelle's restrictive motion limits (tilt angle, motions and accelerations). This motion induces vibrations on the wind turbine leading to the need for additional maintenance actions, such as, for instance, at the greasing and the lubrication system. This might result in downtimes affecting the energy production.

The maintenance strategy foresees to go out when the weather is good. Therefore, the summer months are targeted for the surveys; when wind speeds are the lowest the production loss is minimized and the wind-induced waves are smaller, allowing an easier access to the structure. In general, the cost of the production loss is lower than the rent for the survey vessel. Hence, the survey programme needs to be adjusted to the actual metocean conditions. This makes the weather windows the real bottleneck. The crew transfers and accessibility, however, do not pose the biggest challenge as reliable solutions have already been found. In one of the respective wind farms, CTVs are preferred for the crew transfer, while the option of using an helicopter is too expensive and does not offer any significant advantages. Prior to the crew transfer, the wind turbine is stopped to stabilised the platform. Once stability is achieved, the access via CTV is quick and safe.

The major component replacement requires disconnecting the mooring lines and transporting the wind turbine up to the operation port.

In the following list selected lessons learnt from the operation of a real floating wind farm are summarised:

- Control strategy and coupling between wind turbine and platform is the most relevant aspect.
- Subsea inspections should be improved and the inspections must be taken into account in the engineering phases.
- ROVs will be commonly used in the near future.
- Redundancy is justified to avoid long downtimes.
- Corrosion can harm the steel structures and auxiliary equipment.
- Connection and disconnection should be faster once it is required for major repairs.
- The draught of the floating substructure should be minimized during the towing in order to increase the available harbours where the repairs can be performed.

7.2 Validation of Results

To validate the results of the simulation study, the wind farm operators collaborating to the project were asked to estimate the magnitude of realistic OPEX results. The OPEX costs of a commercial floating offshore wind farm were estimated in the range of 70,000 €/ (MW/year) – 90,000 €/ (MW/year). This coincides with the OPEX value given by the most recent evaluation of ORE Catapult of approximately 90,000 €/ (MW/year), [29]. Although an estimate is generally difficult to make as the figures depend largely on details (such as crew, vessels, distances, number of turbines, etc.), the OPEX estimated for all optimised scenario cases of this study fall within this range.

The operators estimated the availability of the turbines at around 95 %. However, the time loss caused by a major repair in a real floating wind farm is predicted to be higher than assumed in the simulations. A simulated operation took, in average, from one to three weeks to be completed. According to the realistic estimation of the operators, such an operation would take at least one month, taking into account the disconnection/connection, towing and repair times. This could partly explain why the wind farm availability of the simulations is more favourable and lies above 98 % for all cases.

8 Conclusions

This study presents an estimation of the OPEX of a theoretical, commercial-scale, reference floating offshore farm, deploying 15 MW turbines, installed on either a semi-submersible or a spar type floating substructure, and installed at three potential sites. The investigation of several scenarios was aimed at identifying the challenges and opportunities that lie in the possible maintenance strategies, and at identifying key trends. The modelled data reflects current market conditions and attempts to represent the maintenance decision-making process as close as possible to reality. However, the extent of the uncertainty related to the inaccuracies in the estimation of highly fluctuating parameters, and the assumptions taken into the simulation models, cannot be excluded. The calculations underlying this study represent only one possible way of estimating maintenance costs. They do not include the operational costs of the control centre or O&M base, insurance or rental costs of infrastructure, but focus solely on costs directly caused by maintenance activities. Energy losses due to downtime were calculated but neither converted into financial losses, nor added to the final OPEX results.

The results of the study showed an estimated OPEX in the range of 73,000 €/ (MW/year) – 78,000 €/ (MW/year), with an availability of over 98% and an energy production loss of 42 MWh/(MW/year) – 64 MWh/(MW/year). These values were validated by the floating wind farm operators who are part of the COREWIND project.

The preliminary studies, in Chapter 5, provide the ranges of the operational limits (possible H_s - T_p combinations) given as input to the scenarios of the cost calculations. When considering the operational limits of the floating crane vessels, the maximum relative motions (in particular the maximum relative vertical velocity representing an exemplary active heave compensator) between FOWT and crane vessel were studied for several wave directions and floater-vessel orientations. In reality, some orientations would not be approached by the crane vessel in relation to the wave direction, to avoid resonance phenomena and excessive vessel motions. For this reason, the presented operational limits for the floating-to-floating major component exchange are assumed to be rather conservative. This was balanced by altering the limit value of the maximum relative vertical velocity of the crane compensation in a sensitivity study.

It can be expected that the number of vessels adapted to large scale floating wind turbines will increase with future vessel generations. This will impact the vessel prices, making the current predictions more unreliable. The prices included in this study reflect a best estimate of the current market situation. The motion compensation systems will be further improved and most likely adjusted to the challenges posed by floating wind turbines in different wave regimes. The same applies to accessibility options.

The analyses and findings of this report helped to derive the following main conclusions:

- The major component exchange strategies, i.e. performing a floating-to-floating lifting operation offshore and towing the structure to port to perform the heavy lift operations in calm water, were compared. The findings showed that the tow-in solution is the most economically effective solution based on the assumptions taken in the simulation model.
- In the matter of this solution, the feasibility and effectiveness of the tow-in operation depends on the distance to a suitable port, having a sufficient berth draft to accommodate the FOWT. Additionally, the ease of the disconnection and re-connection procedures for mooring lines and dynamic power cable(s) as well as the suitability of the floater archetype for towing in shallow waters plays a significant role in the choice of the adequate maintenance strategy.
- The dayrates and mobilisation costs of the floating crane vessel cause high OPEX of the F2F-scenarios. As the vessel costs vary significantly depending on the market situation, it is difficult to make tangible assumptions about dayrates. In the future, a positive development of these rates is possible if more large crane vessels will be available.

- The deployment of the two considered floater types only slightly varied the OPEX and availability estimates in the optimal scenario settings. A clear trend is observed for the semi-submersible crane vessel, which is more cost effective over the lifetime than the monohull crane vessel.
- The operational limits have a significant impact on the wind farm availability. An early comparison of the project's weather time series with the operating limits already gives a good indication of how the available weather windows will look like for the corresponding operation.
- The workability assessment showed that, for large 15 MW floating wind turbine structures, the workability limits are rather high. Therefore, the accessibility limits are the decisive factor for defining and restricting the weather window for the operation. A similar trend is observed for the access vessels: the larger is the vessel, the smaller is the impact of the vessel motions on the transportability of the passengers.
- The selection of the access vessel was mainly driven by the weather conditions at site. It was apparent that, in the calm region of Gran Canaria, either of the access solutions provided have similar impact to OPEX estimate, which was only slightly better with the bow-transfer access of the CTV. At Morro Bay, where the average wave heights are higher, a clear trend towards the SOV solution, by using a motion compensated gangway, was observed.
- The results for the site of West of Barra showed significant availability losses and unrealistic OPEX. This can be explained by the very harsh weather conditions at the site. Only very small weather windows are available for maintenance, leading to unfinished workorders and downtimes summarised over the farm's lifetime. Under the weather conditions of that site no cost-effective maintenance strategy was deduced.

Using these conclusions, an optimal strategy was found for the two sites of Morro Bay and Gran Canaria, for both FOWT concepts.

Future works will have the following main objectives:

1. Include a risk-based strategy approach into the calculation model, with the aim of quantifying the impact of predictive and condition-based maintenance strategies;
2. Extend the impact assessment to understand the effect of the distance to harbour on the duration of tow-in operations and weather windows;
3. Continuously improve the data and the assumptions of the O&M strategy including market-based costs, reliability parameters, process durations and technological progress;
4. Improve assumptions for operational weather limits, for example, for the floating-to-floating major component exchange by including additional effects in the time-domain simulation model, such as wind and current loads, hydrodynamic multi-body interaction between crane vessel and FOWT, closed-loop control for the DP system of the crane vessel and direct modelling of motion compensation equipment.

Disclaimer

The authors cannot make any representations or warranties of any kind, express, or implied about the completeness, accuracy or reliability of the information and related graphics. Any reliance placed on this information is at own risk and in no event shall the authors be held liable for any loss, damage including without limitation indirect or consequential damage or any loss or damage whatsoever arising from reliance on same.

The outlined input parameters for the O&M cost model shall not be used as a basis for a specific commercial project, as they will vary from case to case. The information is not intended to serve as an exhaustive list of all relevant parameters for a specific project. The report is based on a comprehensive assessment and the authors do not recommend or promote any technology, software or methodology above one another.

9 References

- [1] J. Verma, J. I. Rapha, J. L. Domínguez and V. Ferreira, "COREWIND, D6.1 General frame of the analysis and description of the new FOW assessment app," 2020.
- [2] F. Vígara, L. Cerdán, R. Durán, S. Muñoz, M. Lynch, S. Doole, C. Molins, P. Trubat and R. Guanche, "COREWIND, Deliverable D1.2 Design Basis," 2020.
- [3] "Shoreline," Shoreline AS, [Online]. Available: <https://www.shoreline.no/>. [Accessed 26 08 2021].
- [4] "Shoreline Design Support," Shoreline AS, [Online]. Available: <https://design.support.shoreline.no/support/solutions>. [Accessed 26 08 2021].
- [5] J. Carroll, A. McDonald and D. McMillan, "Failure rate, repair time and unscheduled O&M cost analysis of offshore wind turbines," *Wind Energy* v19, pp. 1107-1119, 2015.
- [6] *Reliability focused research on optimizing Wind Energy systems design, operation and maintenance: tools, proof of concepts, guidelines & methodologies for a new generation*, GH, ReliaWind, 2007.
- [7] T. Gintautas and J. D. Sørensen, "Deliverable D1.34 - Integrated system reliability analysis," *Aalborg University, Denmark*, 2017.
- [8] J. Carroll, A. McDonald, I. Dinwoodie, D. McMillan, M. Revie and I. Lazaki, *Availability, operation and maintenance costs of offshore wind turbines with different drive train configurations*, *Wind Energy*, 2016.
- [9] J. Walgern, *Impact of Wind Farm Control Technologies on Wind Turbine Reliability*, Hamburg: Uppsala Universitet, 2019.
- [10] K. Moore, "Industry report: Offshore wind needs more installation vessels ASAP," *Work Boat*, 5 May 2021. [Online]. Available: <https://www.workboat.com/wind/industry-report-offshore-wind-needs-more-installation-vessels-asap>. [Accessed 26 08 2021].
- [11] F. Vígara, L. Cerdán, R. Durán, S. Muñoz, M. Lynch, S. Doole, C. Molins, P. Trubat and R. Guanche, "COREWIND, Deliverable D1.2, Design basis," 2020.
- [12] M.-A. Schwarzkopf, F. Borisade, D. Matha, M. D. Kallinger, M. Y. Mahfouz, R. D. Vicente and S. Muñoz, "COREWIND, Deliverable D4.1, Identification of floating-wind-specific O&M requirements and monitoring technologies," 2020.
- [13] M. Y. Mahfouz, M. Salari, S. Hernández, F. Vígara, C. Molins, P. Trubat, H. Bredmose and A. Pegalajar-Jurado, "COREWIND, Deliverable D1.3, Public design and FAST models of the two 15MW floater-turbine concepts," 2020.
- [14] Saipem, "Saipem 7000 - Brochure," Saipem, [Online]. Available: https://www.saipem.com/sites/default/files/2018-12/1019spm_S7000re_L03_.pdf. [Accessed 05 May 2021].

- [15] D. Jürgens, M. Palm and A. Brandner, “Comparative Investigation on Influence of the Positioning Time of Azimuth Thrusters on the Accuracy of DP,” in *MTS Dynamic Positioning Conference*, Houston, TX, USA, 2012.
- [16] A. Shankar Verma, Z. Jiang, Z. Ren, Z. Gao and N. Petter Vedvik, “Response-Based Assessment of Operational Limits for Mating Blades on Monopile-Type Offshore Wind Turbines,” *Energies*, vol. 12, no. 10, p. 1867, 2019.
- [17] E. Gaertner, J. Rinker, L. Sethuraman, F. Zahle, B. Anderson, G. E. Barter, N. J. Abbas, F. Meng, P. Bortolotti, W. Skrzypinski, G. N. Scott, R. Feil, H. Bredmose, K. Dykes, M. Shields, C. Allen and A. Viselli, “IEA Wind TCP Task 37: Definition of the IEA 15-Megawatt Offshore Reference Wind Turbine,” Golden, CO (United States), 2020.
- [18] N. Mansfield, *Human Response to Vibration*, New York: CRC Press, 2005.
- [19] M. McCauley, J. W. Royal, C. D. Wylie, J. F. O’Hanlon and R. E. Mackie, “Motion sickness incidence: Exploratory studies of habituation, pitch and roll, and the refinement of a mathematical model,” *Office of naval research department of the navy*, 1976.
- [20] M. Griffin, “*Handbook of Human Vibration.*,” London, Academic Press Limited, 1990.
- [21] M.-A. Schwarzkopf, M. N. Scheu, O. Altay and A. Kolios, “Whole body vibration on offshore structures: An evaluation of existing guidelines for assessing low-frequency motions,” *ISOPE Conference*, Sapporo, 2018.
- [22] Nordforsk, “Assessment of Ship Performance in a Seaway: The Nordic Co-operative Project: Seakeeping Performance of Ships,” Nordic Co-operative Organization for Applied Research, 1987.
- [23] D. W. Boggs and C. P. Petersen, “Acceleration Indexes for Human Comfort in Tall Buildings—Peak or RMS?,” *Council on Tall Buildings and Urban Habitat (CTBUH) Monograph*, 1995.
- [24] “ISO 2631-1:1997. Mechanical vibration and shock - Evaluation of human exposure to whole-body vibration - Part 1: General requirements,” 1997.
- [25] “BS EN 12299:2009. Railway applications - Ride comfort for passengers - Measurement and evaluation.,” 2009.
- [26] M. N. Scheu, D. Matha, M.-A. Schwarzkopf and A. Kolios, “Human exposure to motion during maintenance on floating offshore wind turbines,” *Ocean Engineering*, vol. 165, p. 293–306, 2018.
- [27] J. Caicedo, F. Catbas, A. Cunha, V. Racic, P. Reynolds and K. Salyards, “Topics on the Dynamics of Civil Structures, Volume 1,” in *30th IMAC, A Conference and Exposition on Structural Dynamics*, 2012.
- [28] M. Almat, “Concept design of a crew transfer vessel, M.Sc. thesis,” Delft University of Technology, Delft, 2015.
- [29] “Guide to an Offshore Wind Farm - Wind Farm Costs,” *Catapult Offshore Renewable Energy*, [Online]. Available: <https://guidetoanoffshorewindfarm.com/wind-farm-costs>. [Accessed 04 08 2021].

- [30] M. Martini, A. Jurado, R. Guanche and I. J. Losada, "Evaluation of Walk-to-Work Accessibility for a Floating Wind Turbine," *Ocean Engineering*, vol. 116, pp. 216-225, 2016.
- [31] "4C-OFFSHORE: An Introduction to Crew Transfer Vessels.," 4C-Offshore, [Online]. Available: <https://www.4coffshore.com/support/an-introduction-to-crew-transfer-vessels-aid2.html>. [Accessed 17 07 2020].
- [32] J. Van der Tempel, F. Gerner, D. Cerda and A. Gobel, "A Vessel, a Motion Platform, Control System, a Method for Compensating Motions of a Vessel and a Computer Program Product," United States Patent and Trademark Office, 2013.
- [33] "G9 Offshore Wind Health and Safety : Good Practice Guideline working at height in the Offshore Wind Industry," Energy Institute, London, 2014.
- [34] DNV-GL, "DNVGL-ST-0119: Floating wind turbine structures," 2018.
- [35] ABSG Consulting Inc., "Study on Mooring System Integrity management for Floating Structures," Bureau of Safety and Environmental Enforcement (BSEE), Arlington, 2015.
- [36] ISO, *ISO 17359:2018 Condition monitoring and diagnostics of machines — General guidelines*, ISO, 2018.
- [37] J. O'Hanlon and M. McCauley, "Motion Sickness Incidence as a Function of the Frequency and Acceleration of Vertical Sinusoidal Motion," *Aerospace Magazine*, 1974.
- [38] "VDI 2057 - Part 1: Human Exposure to mechanical vibrations. Whole-body vibration.," Verein Deutscher Ingenieure, 2015.
- [39] M.-A. Schwarzkopf, "Accessibility and Maintainability of Floating Offshore Wind Turbines," RWTH Aachen University, Aachen, 2018.
- [40] "Shoreline Design: Production-based availability - O&M output," Shoreline Design, [Online]. Available: <https://design.support.shoreline.no/support/solutions/articles/80000517801-production-based-availability-o-m-output>. [Accessed 04 08 2021].
- [41] "Shoreline Design: Time-based availability - O&M output," Shoreline Design, [Online]. Available: <https://design.support.shoreline.no/support/solutions/articles/80000517800-time-based-availability-o-m-output>. [Accessed 04 08 2021].
- [42] "Shoreline Design: General costs - yearly," Shoreline Design, [Online]. Available: <https://design.support.shoreline.no/support/solutions/articles/80000517880-general-costs-yearly>. [Accessed 04 08 2021].
- [43] "Shoreline Design: Maintenance costs - yearly," Shoreline Design, [Online]. Available: <https://design.support.shoreline.no/support/solutions/articles/80000517883-maintenance-costs-yearly>. [Accessed 04 08 2021].

- [44] J. Verma, J. I. Rapha, J. L. Domínguez and V. Ferreira, “COREWIND, Deliverable D6.1, General frame of the analysis and description of the new FOW assessment app,” 2020.
- [45] ISO, “ISO 6897:1984. Guidelines for the evaluation of the response of occupants of fixed structures, especially buildings and off-shore structures, to low-frequency horizontal motion (0,063 to 1 Hz),” 1984.